

# Lawrence Berkeley National Laboratory

## LBL Publications

### Title

Simulation of Unsaturated Flow and Nonreactive Solute Transport in a Heterogeneous Soil at the Field Scale

### Permalink

<https://escholarship.org/uc/item/61r5b1df>

### Author

Rockhold, M L

### Publication Date

1993-02-01

REC'D FOR BLDG. 90 LIBRARY  
B90P

MAY 18 1993

(NOT TO BE RETURNED TO THE  
BLDG. 50 LIBRARY)

NUREG/CR-5998  
PNL-8496

---

---

# Simulation of Unsaturated Flow and Nonreactive Solute Transport in a Heterogeneous Soil at the Field Scale

---

---

Prepared by  
M. L. Rockhold

**Pacific Northwest Laboratory**  
Operated by  
Battelle Memorial Institute

Prepared for  
U.S. Nuclear Regulatory Commission

1 LOAN COPY 1  
1 Circulates 1  
1 for 4 weeks 1  
Bldg. 90 Library.  
Copy 1

NUREG/CR-5998

## AVAILABILITY NOTICE

### Availability of Reference Materials Cited in NRC Publications

Most documents cited in NRC publications will be available from one of the following sources:

1. The NRC Public Document Room, 2120 L Street, NW., Lower Level, Washington, DC 20555
2. The Superintendent of Documents, U.S. Government Printing Office, P.O. Box 37082, Washington, DC 20013-7082
3. The National Technical Information Service, Springfield, VA 22161

Although the listing that follows represents the majority of documents cited in NRC publications, it is not intended to be exhaustive.

Referenced documents available for inspection and copying for a fee from the NRC Public Document Room include NRC correspondence and internal NRC memoranda; NRC bulletins, circulars, information notices, inspection and investigation notices; licensee event reports; vendor reports and correspondence; Commission papers; and applicant and licensee documents and correspondence.

The following documents in the NUREG series are available for purchase from the GPO Sales Program: formal NRC staff and contractor reports, NRC-sponsored conference proceedings, international agreement reports, grant publications, and NRC booklets and brochures. Also available are regulatory guides, NRC regulations in the *Code of Federal Regulations*, and *Nuclear Regulatory Commission Issuances*.

Documents available from the National Technical Information Service include NUREG-series reports and technical reports prepared by other Federal agencies and reports prepared by the Atomic Energy Commission, forerunner agency to the Nuclear Regulatory Commission.

Documents available from public and special technical libraries include all open literature items, such as books, journal articles, and transactions. *Federal Register* notices, Federal and State legislation, and congressional reports can usually be obtained from these libraries.

Documents such as theses, dissertations, foreign reports and translations, and non-NRC conference proceedings are available for purchase from the organization sponsoring the publication cited.

Single copies of NRC draft reports are available free, to the extent of supply, upon written request to the Office of Administration, Distribution and Mail Services Section, U.S. Nuclear Regulatory Commission, Washington, DC 20555.

Copies of industry codes and standards used in a substantive manner in the NRC regulatory process are maintained at the NRC Library, 7920 Norfolk Avenue, Bethesda, Maryland, for use by the public. Codes and standards are usually copyrighted and may be purchased from the originating organization or, if they are American National Standards, from the American National Standards Institute, 1430 Broadway, New York, NY 10018.

## DISCLAIMER NOTICE

This report was prepared as an account of work sponsored by an agency of the United States Government. Neither the United States Government nor any agency thereof, or any of their employees, makes any warranty, expressed or implied, or assumes any legal liability of responsibility for any third party's use, or the results of such use, of any information, apparatus, product or process disclosed in this report, or represents that its use by such third party would not infringe privately owned rights.

## DISCLAIMER

This document was prepared as an account of work sponsored by the United States Government. While this document is believed to contain correct information, neither the United States Government nor any agency thereof, nor the Regents of the University of California, nor any of their employees, makes any warranty, express or implied, or assumes any legal responsibility for the accuracy, completeness, or usefulness of any information, apparatus, product, or process disclosed, or represents that its use would not infringe privately owned rights. Reference herein to any specific commercial product, process, or service by its trade name, trademark, manufacturer, or otherwise, does not necessarily constitute or imply its endorsement, recommendation, or favoring by the United States Government or any agency thereof, or the Regents of the University of California. The views and opinions of authors expressed herein do not necessarily state or reflect those of the United States Government or any agency thereof or the Regents of the University of California.

# Simulation of Unsaturated Flow and Nonreactive Solute Transport in a Heterogeneous Soil at the Field Scale

---

---

Manuscript Completed: January 1993  
Date Published: February 1993

Prepared by  
M. L. Rockhold

T. J. Nicholson, NRC Project Manager

Pacific Northwest Laboratory  
Richland, WA 99352

Prepared for  
Division of Regulatory Applications  
Office of Nuclear Regulatory Research  
U.S. Nuclear Regulatory Commission  
Washington, DC 20555  
NRC FIN L1007

## Abstract

A field-scale, unsaturated flow and solute transport experiment at the Las Cruces trench site in New Mexico was simulated as part of a "blind" modeling exercise to demonstrate the ability or inability of uncalibrated models to predict unsaturated flow and solute transport in spatially variable porous media. Simulations were conducted using a recently developed multiphase flow and transport simulator. Uniform and heterogeneous soil models were tested, and data

from a previous experiment at the site were used with an inverse procedure to estimate water retention parameters. A spatial moment analysis was used to provide a quantitative basis for comparing the mean observed and simulated flow and transport behavior. The results of this study suggest that defensible predictions of waste migration and fate at low-level waste sites will ultimately require site-specific data for model calibration.

# Contents

	Page
Abstract .....	iii
Summary .....	ix
Acknowledgments .....	xi
1 Introduction .....	1
2 Methods .....	3
2.1 The Las Cruces Trench Experiments .....	3
2.1.1 Site Description .....	3
2.1.2 Experiment 1 .....	4
2.1.3 Experiment 2A .....	5
2.1.4 Experiment 2B .....	5
2.2 Numerical Modeling .....	6
2.2.1 Flow and Transport Simulator .....	6
2.2.2 Parameter Estimation .....	8
2.2.2.1 Flow Parameters .....	8
2.2.2.2 Transport Parameters .....	11
2.2.2.3 Inverse Methods .....	11
2.2.3 Spatial Variability .....	12
2.2.3.1 Semivariogram Analyses .....	12
2.2.3.2 Stochastic Methods .....	14
2.2.3.3 Scaling .....	15
2.2.3.4 Random Field Generation .....	15
2.2.3.5 Conditional Simulation .....	16
2.2.4 Modeling Scenarios .....	17
2.2.5 Initial and Boundary Conditions .....	21
2.3 Model Evaluation .....	24
3 Results and Discussion .....	25
3.1 One-Dimensional Inverse Parameter Estimation .....	25
3.2 Two-Dimensional Flow and Transport Modeling .....	25
3.2.1 Flow Simulations .....	25
3.2.2 Transport Simulations .....	36
4 Conclusions .....	43
5 References .....	45
6 Glossary .....	51

## Figures

1	Observed Morphological Horizons at the Las Cruces Trench Site .....	3
2	Plan View of the Las Cruces Trench Site .....	4
3	Locations of Tensiometers and Solute Samplers in the Face of the Trench for Experiment 2B .....	5
4	Histograms of Log-Transformed In Situ ( $K_{fs}$ ) and Laboratory ( $K_s$ ) Measurements of Saturated Hydraulic Conductivity .....	9
5	Histograms of Log-Transformed Saturated ( $\theta_s$ ) and 15 Bar ( $\theta_{15}$ ) Water Content Data .....	10
6	Histograms of Log-Transformed van Genuchten (1980) Model $\alpha$ and $n$ Parameters .....	10
7	Horizontal and Vertical Sample and Theoretical Exponential Semivariograms Determined Using Log-Transformed $K_{fs}$ Data (after Jacobson 1990) .....	13
8	Kriging Map of $\ln(K_{fs})$ and Gaussian Simulation of $\ln(K_{fs})$ Generated Using FFT Method .....	18
9	Directional Covariance as a Function of Separation Distance for Theoretical Exponential Covariance Model and Single Realization Generated Using FFT Method .....	19
10	Water Retention and Hydraulic Conductivity Curves for Simulation Cases 1, 2, and 3 .....	20
11	Modeled Cross Section and Assignment of Boundary Conditions .....	21
12	Initial Water Content Distributions for Neutron Probe Transects 1 ( $y = 2$ m), 2 ( $y = 6$ m), and 3 ( $y = 10$ m) .....	22
13	Initial Normalized Tritium Concentrations for Solute Sample Transects 1 ( $y = 0.5$ m), 2 ( $y = 5$ m), and 3 ( $y = 9$ m) .....	23
14	Observed and Simulated Water Content Profiles for Experiment 1 .....	26
15	Observed Water Content Distributions from Neutron Probe Transects 1, 2, and 3 for Day 70 .....	27
16	Simulated Water Content Distributions for Cases 1 and 2 and Observed Water Content Distribution from Neutron Probe Transect 1 for Day 70 .....	28
17	Simulated Water Content Distributions for Cases 3 and 4 and Observed Water Content Distribution from Neutron Probe Transect 1 for Day 70 .....	30
18	Observed Water Content Distributions from Neutron Probe Transects 1, 2, and 3 for Day 310 .....	31
19	Simulated Water Content Distributions for Cases 1 and 2 and Observed Water Content Distribution from Neutron Probe Transect 1 for Day 310 .....	32



20	Simulated Water Content Distributions for Cases 3 and 4 and Observed Water Content Distribution from Neutron Probe Transect 1 for Day 310 .....	33
21	First Spatial Moments (Center of Mass) of Observed and Simulated Water Plumes .....	34
22	Second Spatial Moments (Spread About Center of Mass) of Observed and Simulated Water Plumes .....	34
23	Observed Normalized Tritium Distributions for Transects 1 ( $y = 0.5$ m), 2 ( $y = 5$ m), and 3 ( $y = 9$ m) for Day 310 .....	37
24	Simulated Tritium Distributions for Cases 1 and 2 and Observed Tritium Distribution from Solution Samplers for Day 310 .....	38
25	Simulated Tritium Distributions for Cases 3 and 4 and Observed Tritium Distribution from Solution Samplers for Day 310 .....	39
26	First Spatial Moments (Center of Mass) of Observed and Simulated Tritium Plumes .....	40
27	Second Spatial Moments (Spread About Center of Mass) of Observed and Simulated Tritium Plumes .....	40

## Tables

1	Flow and Transport Parameters Used in MSTs Simulations .....	20
2	Normalized Spatial Moments of Observed and Simulated Water Plumes for Day 310 .....	35
3	Normalized Spatial Moments of Observed and Simulated Tritium Plumes for Day 310 .....	41

## Summary

This document describes the results of modeling studies conducted by the Pacific Northwest Laboratory (PNL) for the U.S. Nuclear Regulatory Commission. The objectives of this work were 1) to evaluate datasets generated from the Las Cruces trench experiments for testing deterministic and probabilistic flow and transport models, 2) to assess several parameter estimation methods and a recently developed multiphase flow and transport simulator for potential use as performance assessment tools for application to low-level waste disposal sites, and 3) to document PNL's contributions to the unsaturated zone working group of the INTRAVAL project and its Las Cruces test case.

The INTRAVAL project is the third in a series of three international cooperative studies that are concerned with the evaluation of conceptual and mathematical models for groundwater flow and radionuclide transport. The INTRAVAL project was initiated in 1987 by the Swedish Nuclear Power Inspectorate, in Stockholm. The objective of this project is to use the results from laboratory and field experiments, as well as natural analog studies, to systematically study the model validation process. Twenty-four organizations from 14 countries currently participate in the INTRAVAL project.

As a result of the Low Level Waste Act of 1986, requirements for the licensing of near surface low-level waste disposal sites in the United States state that such sites "shall be capable of being characterized, modeled, analyzed, and monitored" (Subpart D, Section 10, Part 61, Code of Federal Regulations). The type and quantity of data required to provide adequate characterization so that defensible predictions of potential waste migration and fate can be made have not been strictly defined. This results partly from the lack of detailed data from field-scale unsaturated flow and transport experiments.

As part of a comprehensive study designed to provide validation data sets for testing stochastic and deterministic models of unsaturated flow and solute transport, the U.S. Nuclear Regulatory Commission has funded a series of field experiments at a trench on the New Mexico State University College Ranch, northeast of Las Cruces, New Mexico. The research facility and experiments were designed by researchers from the University of Arizona, New Mexico State University (NMSU), Massachusetts Institute of Technology (MIT), and PNL. The experiments conducted at the Las Cruces trench site provide detailed data on hydraulic properties and water and chemical movement through initially dry, spatially variable soils.

The most recent flow and transport experiment that was conducted at the Las Cruces trench site is a test case for the unsaturated zone working group of the INTRAVAL project. This experiment is referred to as Las Cruces trench experiment 2B. The experiment consisted of a pulse application of water with several tracers on an irrigated strip of initially dry soil. Water and solute movements were monitored in the subsurface using a neutron probe, solution samplers, and by destructive soil sampling. The experiment was then simulated by researchers from NMSU, MIT, Southwest Research Institute, and PNL before the actual data were released, as part of a "blind" modeling exercise.

The objectives of this blind modeling exercise were 1) to demonstrate the ability or inability of uncalibrated models to predict unsaturated flow and solute transport in spatially variable porous media, and 2) to develop a quantitative model validation methodology that can be used to assess the performance of various conceptual and mathematical models with consideration given to data and parameter uncertainties. Only the first of these two objectives is addressed in this document. All simulation results that are reported in this document were generated before the actual data from experiment 2B were released. Therefore, these results are blind in the sense that no data from the experiment were used for direct model calibration.

Characterization data from the Las Cruces trench site were used to independently estimate model parameters for two-dimensional, deterministic simulations of water flow and tritium transport. An inverse parameter estimation procedure was also used, in conjunction with data from one of the previous flow and transport experiments conducted at the Las Cruces trench site, to estimate water retention parameters. Simulations were conducted using uniform, homogeneous, isotropic and anisotropic soil models, as well as fully heterogeneous soil models. Geostatistical methods and a fast Fourier transform method for generating spatially correlated random fields were also used to generate single stochastic realizations that were conditioned on the saturated hydraulic conductivity data from the trench. A spatial moment analysis was used to provide a quantitative basis for comparing the mean simulated and observed flow and transport behavior.

The conditional simulation results qualitatively matched the observed water content data from experiment 2B better than any of the results from the uniform soil models during the infiltration phase of the experiment. However, the conditional simulation poorly predicted water and tritium

movement during the redistribution phase of the experiment. This suggests that single stochastic realizations are probably inappropriate for predicting unsaturated flow and solute transport behavior in spatially variable porous media.

A uniform soil model, with water retention parameters determined from a one-dimensional inverse solution and infiltration data from one of the previous trench experiments, reproduced the observed vertical water movement during the infiltration phase of the experiment better than any of the other models. However, this model also poorly predicted water and tritium movement during the redistribution phase of the experiment. Nevertheless, the inverse method appears to be a promising means for obtaining effective flow parameters using water content and pressure head data collected during infiltration and/or drainage experiments.

Comparisons of the spatial moments of the simulated and observed water content and tritium distributions indicate that the mean observed water and tritium plume dynamics were reproduced most closely by one of the uniform soil models. The model utilized average water retention parameters that were determined by simultaneously fitting the data obtained from approximately 450 core samples that were collected during excavation of the trench. The dry end of the water retention and relative permeability curves for this case were modified to provide a more accurate representation of the initial conditions of the experiment, relative to the original fitted parameters from the Las Cruces trench database.

Nine individual soil horizons were identified based on observed morphological characteristics from the exposed face of the trench. Soil core samples were collected along sampling transects from the approximate center of each horizon. Geostatistical analyses of the soil hydraulic properties determined from the core samples and in situ measurements of saturated hydraulic conductivity suggest that these nine horizons could be grouped into three horizons based on similar means and variances and spatial proximity of the soil horizons. However, observed water content data from the trench experiments reveal a distinct soil horizon with significantly lower water contents that was not evident from the site characterization data or the geostatistical analyses. This demonstrates the difficulties with site characterization and possible effects of aliasing from undersampling, and suggests that initial water content data may be the best indicator of the dominant soil layering in the unsaturated zone.

Some of the simulation cases reproduced the observed flow behavior reasonably well during the infiltration phase of the experiment, but none of the simulation cases reproduced the observed flow behavior particularly well during the redistribution phase of the experiment. This may be the result of neglecting certain phenomena such as hysteresis, or from not accurately parameterizing the models to account for the different soil horizons. Whatever the cause for these differences, the results of this study suggest that defensible predictions of waste migration and fate will ultimately require site-specific data for model calibration.

## Acknowledgments

The work described in this document was conducted for the U.S. Nuclear Regulatory Commission under contract account number TD 2766, FIN L1007, entitled Unsaturated Zone Field Studies for Validation of Transport Models. The continued support of Tom Nicholson and Ralph Cady is gratefully acknowledged.

Thanks are expressed to Jan Kool of HydroGeoLogic, Inc. for providing a copy of the SFIT code, to Mark White of

the Pacific Northwest Laboratory for providing a description of the MSTs code, and to Philip Meyer and Glendon Gee of the Pacific Northwest Laboratory for reviewing this document. Richard Hills of New Mexico State University, Peter Wierenga of the University of Arizona, and all the graduate students and staff who have contributed to the Las Cruces trench experiments are also gratefully acknowledged for generating these unique, high-quality data sets.

geostatistical techniques and a fast Fourier transform method were used to generate conditional simulations.

Observed and simulated flow and transport results are compared using a spatial moment analysis.

The first report and HYDROCOIN (1984-1990) were prepared with this document is organized as follows: Descriptions of the Las Cruces trench site, the experiments that have been

conducted there, and the methods that were used for flow and transport modeling are provided in Section 2. Observed and simulated flow and transport results are compared in Section 3. Conclusions are presented in Section 4, and cited references are listed in Section 5.

The most recent experiment that has been conducted at the Las Cruces trench site is referred to as Las Cruces trench experiment 2B. The experiment consisted of a pulse application of water with several tracers on an irrigated strip of initially dry soil. Water and solute

movements were monitored in the subsurface using a neutron probe, solution samplers, and by destructive soil sampling. The experiment was simulated by researchers from Southwest Research Institute, NMSU, MIT, and PNL before the experimental data were released, as part of a "blind" modeling exercise.

The objectives of this blind modeling exercise were (1) to demonstrate the ability or inability of unsaturated models to predict unsaturated flow and solute transport in spatially variable porous media, and (2) to develop a quantitative model validation methodology that can be used to assess the performance of various conceptual and mathematical models with consideration given to data and parameter uncertainties.

Only the first of these two objectives is addressed in this document. All simulation results that are reported in this document were generated before the actual data from experiment 2B were released. Therefore, these results are blind in the sense that no data from the experiment were used for direct model calibration.

Data on the physical and hydraulic properties of the soils from the trench site were used to estimate model parameters for two-dimensional simulations of water flow and tritium transport. Simulations were conducted using the recently developed multiphase flow and transport simulator, MST2 (White et al. 1992). Uniform isotropic and anisotropic models and fully heterogeneous models were used. An inverse parameter estimation method was tested, and

numerical models to forecast the potential migration and fate of contaminants introduced into the subsurface. The complex, spatially variable nature of the subsurface and its hydrologic, geochemical, and biological interactions make accurate and realistic predictions of field-scale contaminant migration difficult. The complexity of the processes controlling subsurface flow and transport is nowhere more evident than in the unsaturated zone.

As a result of the Low Level Waste Act of 1980, requirements for the licensing of near surface low-level waste (LLW) disposal sites state that they "shall be capable of being characterized, modeled, analyzed, and monitored" (Subpart D, Section 10, Part 61, Code of Federal Regulations). To forecast the potential migration and fate of contaminants from LLW sites, information is needed regarding the physical, chemical, and hydraulic properties of the porous media, the chemical characteristics of the waste form, geocorries of the natural and engineered parts of the waste isolation system, and the appropriate initial and boundary conditions. The type and quantity of data required to provide adequate characterization so that defensible predictions of potential waste migration and fate can be made have not been strictly defined. This is partly caused by a lack of detailed data from field-scale unsaturated flow and transport experiments.

As part of a comprehensive study designed to provide validation data sets for testing stochastic and deterministic models of unsaturated flow and transport, the U.S. Nuclear Regulatory Commission (NRC) has funded a series of field experiments at the New Mexico State University College Research Center, Las Cruces, New Mexico. The research facility and experiments were designed by researchers from the University of Arizona, New Mexico State University (NMSU), Massachusetts Institute of Technology (MIT), and the Pacific Northwest Laboratory (PNL). The experiments conducted at the Las Cruces trench site provide detailed data on hydraulic properties and water and chemical movement through initially dry, spatially variable soils.

The most recent experiment that has been conducted at the Las Cruces trench site is a test case for an international project called INTRAVAL. This project is the third in a series of three international cooperative studies that are concerned with the evaluation of conceptual and

Pacific Northwest Laboratory is operated for the U.S. Department of Energy by Battelle Memorial Institute.

## 2 Methods

The Las Cruces trench site and the field experiments that have been conducted there are described in the following section. This is followed by descriptions of the methods used for simulating unsaturated flow and solute transport for Las Cruces trench experiment 2B. Summaries are also given of hydraulic and transport parameter estimates, and spatial variability studies that have been conducted using data from the Las Cruces trench site. The different modeling scenarios, the initial and boundary conditions that were used for model simulations, and the criteria that were used for model evaluation are also described.

### 2.1 The Las Cruces Trench Experiments

#### 2.1.1 Site Description

The experimental site is located approximately 40 km northeast of Las Cruces, New Mexico. According to Wierenga (1988), the climate, geology, geomorphology, soil, and vegetation in the vicinity of the field site are similar to many arid and semiarid areas of the southwestern United States. The average annual precipitation is 23 cm, with 52% occurring between July and the end of September. The average Class A pan evaporation rate is 239 cm/yr.

A 26.4-m-long by 4.8-m-wide by 6.0-m-deep trench was excavated in undisturbed soil to provide samples for hydraulic property characterization and horizontal access to irrigated areas through the trench face. Nine soil horizons were identified, based on observed morphological characteristics on the north trench wall (Wierenga et al. 1989). Core samples were taken along 1-m-wide, 25-m-long strips from each of the nine horizons during construction of the trench. Fifty soil samples were taken from each horizon at 0.5-m-intervals in a row parallel to and approximately 0.6 m from the trench wall. The 6-m-deep soil profile and the approximate depths at which samples were collected from each horizon are shown in Figure 1.

Approximately 50 bore holes were also excavated in each horizon, at 0.5-m-intervals, in a line parallel to and 0.3 m from the trench wall, for in situ determination of saturated hydraulic conductivity using a bore hole permeameter (Reynolds and Elrick 1985). In addition, disturbed soil samples were taken next to the core locations after completion of the saturated hydraulic conductivity measurements. In layer 3, the saturated hydraulic conductivity measurements were made at 0.25-m-intervals along the trench wall.

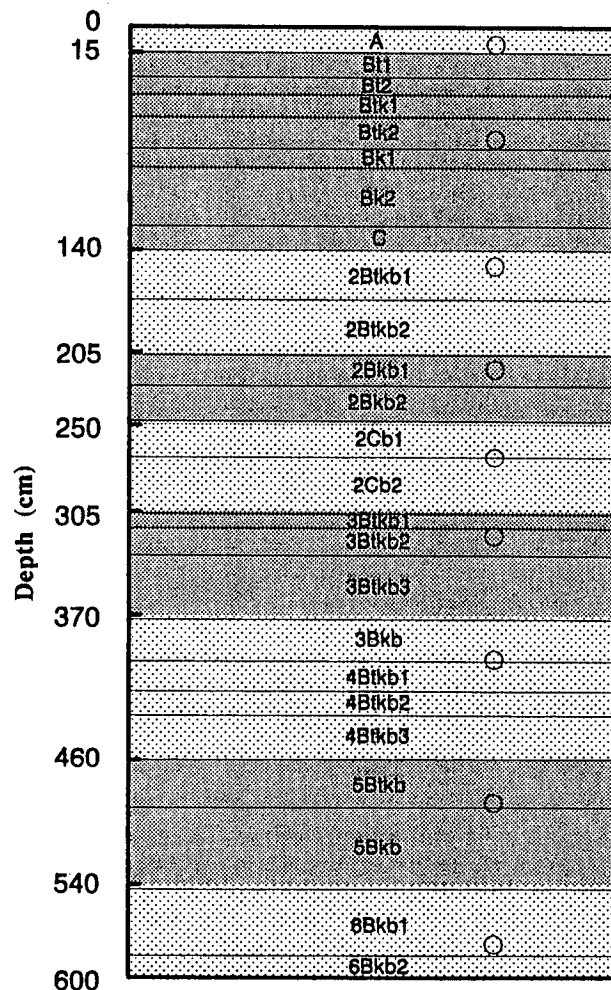


Figure 1. Observed Morphological Horizons at the Las Cruces Trench Site (from Hills and Wierenga 1991) (Circles indicate the approximate depths from which core samples were taken.)

Bulk and core samples, as well as saturated hydraulic conductivity measurements, were also taken from three vertical transects located 3.25 m, 12.75 m, and 20.75 m from the northwest corner of the trench. Samples were taken at 0.13-m-depth intervals along these transects, from depths of approximately 0.1 m to 6.2 m (Wierenga et al. 1989).

The soil core samples were taken to the laboratory for determination of bulk density, particle-size distribution, saturated hydraulic conductivity, and water retention

characteristics. Textural classifications of the nine soil horizons, based on particle-size analyses (Gee and Bauder 1986), range from sand to sandy loam (Wierenga et al. 1989). The predominant soil type is sandy loam. The average bulk densities of the soil horizons range from 1.66 to 1.74 g/cm<sup>3</sup> (Wierenga et al. 1989).

Two experimental plots were instrumented with neutron probe access tubes, tensiometers, and solution samplers for transient unsaturated flow and solute transport experiments. A plan view of the trench and irrigated experimental plots, designated Plots 1 and 2, is shown in Figure 2.

### 2.1.2 Experiment 1

The first Las Cruces trench experiment was conducted over the area labeled as Plot 1 in Figure 2. During experiment 1, water was applied to the surface of the 4 by 9-m plot area by drip emitters, four times per day, for 17 min per application period. This resulted in an average surface water flux of 1.82 cm/d. Water was applied during the first 86 days of the experiment, with tritium added to the water during the first 10 days. Both the trench and the experimental plot were covered to eliminate evaporation and infiltration of natural precipitation during the experiment.

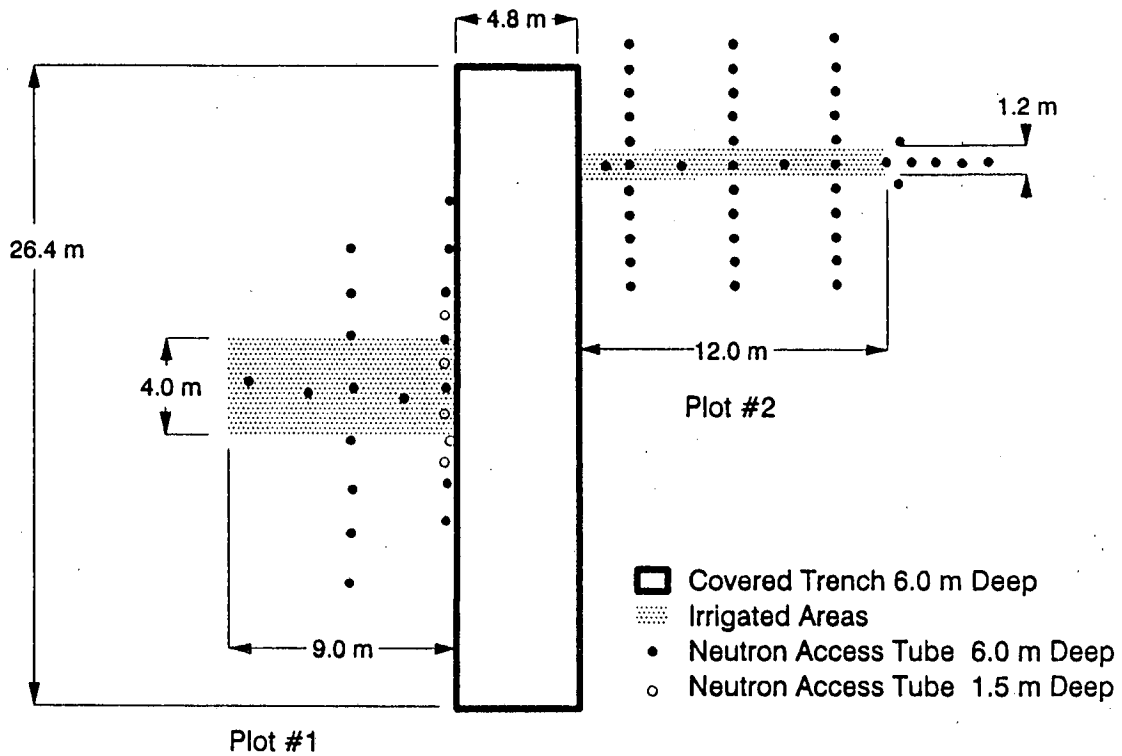


Figure 2. Plan View of the Las Cruces Trench Experimental Site (from Wierenga et al. 1989)

Water and solute movements were monitored in the subsoil during infiltration and redistribution by the use of a neutron probe and solution samplers. Neutron probe measurements were taken at 0.25-m intervals down to the 6.0-m depth. Characterization data, experimental results, and one-dimensional flow predictions for experiment 1 are described in detail by Wierenga et al. (1991).

### 2.1.3 Experiment 2A

Experiment 2A was conducted over the area labeled as Plot 2 in Figure 2. This experiment consisted of a pulse application of water and solute (tritium and bromide), applied by trickle irrigation over the 1.22- by 12-m plot area. Water containing tritium and bromide was applied at a constant and uniformly distributed rate of 0.43 cm/d during the first 11.5 days of the experiment. Irrigation was continued, without solute, for an additional 64 days. The trench and the plot were covered to eliminate evaporation and infiltration of natural precipitation during the experiment.

Water and solute movements were again monitored in the subsoil during infiltration and redistribution using a neutron probe and solution samplers. Neutron probe measurements were taken at 0.25-m intervals down to the 6.0-m depth. The solution samplers and tensiometers extend 0.5 m into the soil profile from the face of the trench. The first, second, and third rows of neutron probe access tubes (hereinafter referred to as neutron probe transects 1, 2, and 3) are located 2 m, 6 m, and 9 m from the face of the trench, respectively.

The long, narrow irrigation strip on plot 2 was used in an attempt to establish a two-dimensional (x- and z-directions) flow regime, with negligible flow in the third dimension (i.e., perpendicular to the trench face). Two-dimensional flow and transport simulation results for experiment 2A have been reported by Hills et al. (1991), Kool and Wu (1991), Rockhold and Wurstner (1991), and others.

### 2.1.4 Experiment 2B

Following the first two experiments, suggestions were made by several modeling groups regarding improvements that could be made in the experimental design for any subsequent experiments. One of these suggestions was to increase the spatial resolution of the solute concentration measurements. For experiment 2B, additional solute samplers were added to the trench face. The locations of the solution samplers and tensiometers in the face of the trench for experiment 2B are shown in Figure 3.

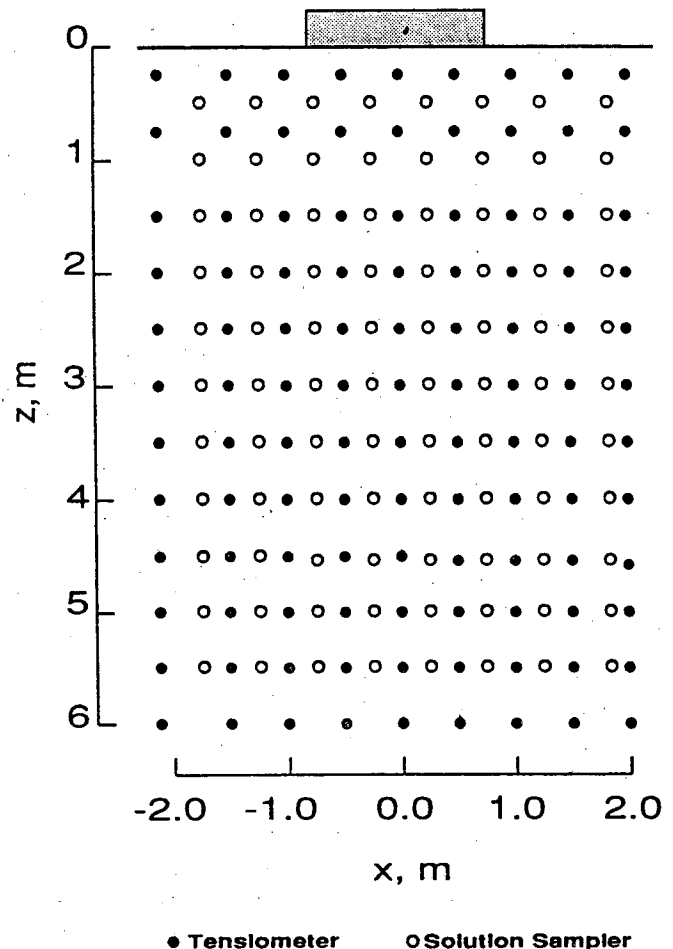


Figure 3. Locations of Tensiometers and Solute Samplers in the Face of the Trench for Experiment 2B (from Hills and Wierenga 1991)

Experiment 2B used the same plot area and irrigation system as that for experiment 2A. Water was applied uniformly at a rate of 1.82 cm/d to the 1.22- by 12-m plot area for the first 70 days of the experiment. Boron, chromium, and pentafluorobenzoic acid (PFBA) were applied with the irrigation water during the first 15 days of the experiment. Tritium, bromide, and 2,6-difluorobenzoic acid (DFBA) were applied with the irrigation water during days 29 through 44 of the experiment. The trench and the experimental plot were covered to eliminate evaporation and infiltration of natural precipitation during the experiment.



The applied relative concentration of tritium was 0.622, compared to the relative concentration of tritium of 1.0 that was applied during experiment 2A. The application of the tritium and bromide was delayed so that the existing tritium and bromide from experiment 2A could be moved deeper into the soil profile.

Destructive samples were collected prior to the start of experiment 2B and during the later stages of the experiment to determine tritium and bromide concentrations in the third dimension (y-direction). These samples were collected 63 days and 21 days before the start of infiltration for experiment 2B from two sampling planes parallel to and 1 m away from the second and third neutron probe transects, at distances of 5 and 9 m from the trench face. These samples were used in addition to data from the solute samplers to determine initial tritium and bromide distributions for the experiment. Destructive samples were also collected from these planes between days 292 and 331 of the experiment. The solute concentrations determined from these later measurements were assumed to be representative of the solute concentrations on day 310, so that they could be used in conjunction with water content measurements taken on day 310.

A detailed description of experiment 2B is given by Hills and Wierenga (1991). The characterization data and experimental results from all three of the Las Cruces trench experiments are available as ASCII files in a database, accessible through FTP on Internet (Hills and Wierenga 1991).

## 2.2 Numerical Modeling

### 2.2.1 Flow and Transport Simulator

This section describes the MSTS code (or Multiphase Sub-surface Transport Simulator) that was used for unsaturated flow and solute transport modeling. MSTS is a general purpose flow and transport simulator that was developed by Pacific Northwest Laboratory in support of the preliminary total system performance assessment of the proposed high-level nuclear-waste repository at Yucca Mountain, Nevada (White et al. 1992). All symbols and notation that are used here in reference to MSTS are defined in the nomenclature section at the end of this document.

MSTS models isothermal or non-isothermal fluid flow and solute transport through variably saturated porous media, in one-, two-, or three-dimensions, with two phases (liquid and gas), and two components (water and air). MSTS uses the integrated finite-difference method to solve the non-linear system of equations. These equations represent expressions

for the conservation of water mass, air mass, thermal energy, and species mass.

The water and air mass conservation equations are shown in Equations 1 and 2, respectively, which are written to include Darcy flow for both phases and binary diffusion of water vapor and gaseous air for the gas phase. Molecular diffusion of dissolved air in the liquid phase is ignored.

$$\begin{aligned} \frac{\partial}{\partial t} [n_d y_w \rho_l s_l + n_d x_w \rho_g s_g] = & \\ & \nabla \left[ \frac{y_w \tilde{k} k_{rl} \rho_l}{\mu_l} (\nabla P_l + \rho_l g \hat{z}) \right] \\ & + \nabla \left[ \frac{y_w \tilde{k} k_{rg} \rho_g}{\mu_g} (\nabla P_g + \rho_g g \hat{z}) \right] \\ & + \tau_g n_d \rho_g s_g D_{aw} \nabla x_w ] + \dot{m}_w \end{aligned} \quad (1)$$

$$\begin{aligned} \frac{\partial}{\partial t} [n_d y_a \rho_l s_l + n_d x_a \rho_g s_g] = & \\ & \nabla \left[ \frac{y_a \tilde{k} k_{rl} \rho_l}{\mu_l} (\nabla P_l + \rho_l g \hat{z}) \right] \\ & + \nabla \left[ \frac{y_a \tilde{k} k_{rg} \rho_g}{\mu_g} (\nabla P_g + \rho_g g \hat{z}) \right] \\ & + \tau_g n_d \rho_g s_g D_{aw} \nabla x_w ] + \dot{m}_a \end{aligned} \quad (2)$$

The thermal energy conservation equation is shown in Equation 3. This equation includes heat transfer by advection of fluids for both phases and heat transfer by conduction through the solid and liquid phases. Heat transfer by

$$\begin{aligned} \frac{\partial}{\partial t} [(1 - n_l) \rho_s u_s + n_d \rho_l u_l + n_d s_g \rho_g \mu_g] & \\ & + \nabla [\rho_l h_l V_l + \rho_g h_g V_g] = \\ & \nabla [\tilde{k}_e \nabla T] + \dot{q} + h_w \dot{m}_w + h_a \dot{m}_a \end{aligned} \quad (3)$$

conduction in the gas phase and heat transfer by binary diffusion within the gas phase are ignored. A mechanical dispersion coefficient may be included to model the phenomena of kinematic dispersion.

The solute transport equation that is used by MSTS is shown in Equation 4. This equation includes solute transport by advection and diffusion for both phases. As with the thermal energy conservation equation, a mechanical dispersion coefficient may be specified to model kinematic dispersion of the solute. Radioactive decay may be modeled; however, no decay products are tracked in the current version

of the code. Tortuosities are computed from porosity and phase saturation, using the saturation dependent formulation developed by Millington and Quirk (1961).

$$\frac{\partial C}{\partial t} + \nabla [y_c CV_l + x_c CV_g] = \nabla [\tau_l s_l n_d \dot{D}_{cl} \nabla (y_c C) + \tau_g s_g n_d \dot{D}_{cg} \nabla (x_c C)] + \dot{s}_c - \dot{R}_c C \quad (4)$$

The solute transport equation combines the advection and diffusion terms with a Peclet number dependent power law scheme (Patankar 1980) formulated for two phase flow. This scheme is shown in Equations 5 through 7 for a single dimension; where  $a_e$  represents the transport coefficient for the neighboring cell at the upper node index,  $a_w$  represents transport coefficient for the neighboring cell at the lower node index, and  $a_p$  represents the transport coefficient for the local cell.

$$a_e = D_{le} \left[ \left[ 0, \left( 1 - \frac{0.1 |F_{le}|}{D_{le}} \right)^5 \right] \right] + \left[ [0, -F_{le}] \right] + D_{ge} \left[ \left[ 0, \left( 1 - \frac{0.1 |F_{ge}|}{D_{ge}} \right)^5 \right] \right] + \left[ [0, -F_{ge}] \right] \quad (5)$$

$$a_w = D_{lw} \left[ \left[ 0, \left( 1 - \frac{0.1 |F_{lw}|}{D_{lw}} \right)^5 \right] \right] + \left[ [0, -F_{lw}] \right] + D_{gw} \left[ \left[ 0, \left( 1 - \frac{0.1 |F_{gw}|}{D_{gw}} \right)^5 \right] \right] + \left[ [0, -F_{gw}] \right] \quad (6)$$

$$a_p = a_e + a_w + F_{le} + F_{ge} - F_{lw} - F_{gw} \quad (7)$$

This power law scheme has been shown to be more accurate for a wide range of peclet numbers relative to the more commonly used hybrid or upwind weighing schemes (Patankar 1980).

The dilute concentration assumption associated with the solute transport equation implies that the solute responds as a passive scalar with respect to the other governing equations. Thus the physical and transport properties of the other governing equations are independent of solute concentrations. This assumption allows the solute transport equation to be decoupled and solved independently from the other governing equations. The computed gas- and liquid-phase flow fields, from a converged solution for the coupled mass

and heat transport equations, are applied to the solution of the solute transport equation. For single-phase, non-isothermal flow problems, only the water mass and thermal energy transport equations are solved, in coupled form. For single-phase, isothermal flow problems, only the water mass transport equation is solved.

The primary dependent variables for the water mass, air mass, thermal energy, and solute transport conservation equations are, respectively, liquid pressure, gas pressure, temperature, and solute concentration. The primary dependent variables are linked to the secondary variables, which appear as coefficients in the governing conservation equations, by constitutive relations for both the physical and hydraulic properties.

The physical properties include density, viscosity, internal energy, enthalpy, saturation pressures, and component mass fractions for both phases. Water physical properties are computed from ASME steam table functions (ASME 1967). Air physical properties are computed from empirical functions and the ideal gas law. Gas phase properties are computed by combining air and water vapor physical properties through either Dalton's partial pressure ideal gas laws, or from the relationships for the kinetic theory of gas mixtures.

The constitutive relations for the hydraulic and thermal properties link the primary dependent variables to hydraulic and thermal characteristic and transport properties such as the liquid and gas saturations, the phase relative permeabilities, and the effective thermal conductivities. A variety of options are available for describing the constitutive relations between liquid saturations, pressures, and relative permeabilities. These include the van Genuchten (1980) and Mualem (1976) models, which were used for the majority of the simulations that are reported in this document.

Interface conductances, such as hydraulic and thermal conductivities, may be specified using arithmetic, geometric, or harmonic means or an upwind weighing scheme. The water and air mass conservation equations use upwind weighing for the diffused densities. The advection terms of the thermal energy conservation equation are formulated with an upwind weighing scheme for the advected properties.

The governing equations are solved by discretizing their partial differential forms with an integrated finite-difference method. The integrated finite-difference method has also been referred to as the control-volume formulation by Patankar (1980). Spatial discretization is currently limited to multi-dimensional, regular and irregular, Cartesian or cylindrical grid systems. Temporal discretization is fully implicit (i.e., forward time-differenced).

The dependencies of the secondary variables on the primary dependent variables yield non-linearities in the finite-difference based algebraic expressions of the governing conservation equations. The nonlinear finite-difference equations are converted to linear form and solved using an iterative Newton-Raphson technique. Although the Newton-Raphson technique requires more computational effort per iteration, it has been found to provide improved convergence relative to Picard iteration, and is necessary for solving strongly heat-driven problems. The linear systems of equations are solved using either a direct banded matrix solver (Dongarra et al. 1980) or a preconditioned conjugate gradient solver (Oppe et al. 1988).

The non-isothermal, multiphase capabilities of the MSTS code were not required and therefore were not used for simulations of the Las Cruces trench experiments that are reported in this document. The governing equations used by the code for these problems were essentially reduced to the familiar Richards equation and the one-component convection-dispersion equation.

Nonisothermal, multiphase capabilities may be required for some applications associated with the performance assessment of low- and high-level waste sites. White et al. (1992) describe an application of the MSTS code for modeling nonisothermal, two-phase carbon-14 transport from the proposed high-level radioactive waste repository at Yucca Mountain, Nevada.

## 2.2.2 Parameter Estimation

### 2.2.2.1 Flow Parameters

In this study, the pressure-saturation-permeability relationships of the soils at the trench site were described by van Genuchten (1980)

$$\theta = \begin{cases} \theta_s & h \geq 0 \\ \theta_r + (\theta_s - \theta_r) [1 + (-\alpha h)^n]^{-m} & h < 0 \end{cases} \quad (8)$$

$$k_r(S_e) = S_e^{1/2} [1 - (1 - S_e^{1/m})^m]^2 \quad (9)$$

where  $\theta_s$  = saturated water content  
 $\theta_r$  = residual water content  
 $h$  = pressure head (a.k.a. matric potential)  
 $\alpha, n$  = curve-fitting parameters  
 $m = 1 - 1/n$   
 $k_r$  = relative permeability  
 $S_e = (\theta - \theta_r) / (\theta_s - \theta_r)$

Estimates of the parameters in the van Genuchten water retention function for the individual core samples that were collected during the excavation of the trench are available in the Las Cruces trench database in file VGPARM.DAT. This file also contains the laboratory measurements of saturated hydraulic conductivity ( $K_s$ ). The water retention parameters in this file were determined by fitting the van Genuchten model to the water retention data using a non-linear, least-squares curve-fitting algorithm. Only the van Genuchten  $\alpha$  and  $n$  parameters were actually estimated during the curve-fitting process. The residual water content values for each core sample were fixed at the water contents corresponding to a matric potential of 15 bars (15,300 cm), which were determined using a pressure plate extraction apparatus in the laboratory (Klute 1986). The saturated water contents were fixed at their measured values.

By fixing the residual water content values at the water contents corresponding to a matric potential of 15 bars, the residual water content values are higher than the initial water contents that were measured in parts of the soil profile. Hills et al. (1991) report simulation results for experiment 2A in which they simply increased the initial water content values that were used in their numerical model so that all the modeled initial water contents were greater than the residual (or 15 bar) water content values. However, this is inconsistent with the measured initial water content data.

An alternative to fixing the residual water contents at the 15 bar water content values is to use a constrained least-squares curve-fitting procedure for parameter estimation. The fitted residual water content values can then be constrained to values less than the lowest measured initial water content values in the soil profile. Kool and Wu (1991) report van Genuchten model parameters for the core samples from the nine horizontal transects that were estimated by constraining the residual water content values to values less than the minimum observed water content for each soil horizon.

In situ estimates of saturated hydraulic conductivity ( $K_{fs}$ ) that were determined using a bore hole permeameter during excavation of the trench are also available in the Las Cruces trench database in file KFIELD.DAT. The laboratory measurements of saturated hydraulic conductivity represent vertical measurements because of the vertical orientation of the core samples. The in situ hydraulic conductivity data are more representative of three-dimensional averages because water flows radially out from the borehole during these measurements, creating a saturated "bulb" of soil (Reynolds and Elrick 1985).

Hills and Wierenga (1991) report average water retention parameters and saturated hydraulic conductivity values for the nine identified soil horizons. These averages were determined from laboratory measurements using the data from each of the nine horizontal sampling transects, which each contain approximately 50 samples. The average water retention parameters and the average saturated hydraulic conductivity for the entire soil profile were also determined from the laboratory measurements by combining the data from all nine horizons (approximately 450 sets of data points). Simulation results generated using this set of average "uniform" soil model parameters are compared to observed water flow and tritium transport data from experiment 2A by Hills et al. (1991).

Hills and Wierenga (1991) also generated histograms and normal probability plots for the log-transformed and untransformed  $K_s$  and  $K_{fs}$  data from the nine horizontal transects. In addition, Kolmogorov-Smirnov tests were performed using both the log-transformed and untransformed  $K_s$  and  $K_{fs}$  data to evaluate the goodness of fit of the sample populations to normal and log-normal distributions. These tests and the histograms suggest that the  $K_s$  data are neither normally nor lognormally distributed, but the  $K_{fs}$  data are log-normally distributed.

As noted previously, data were also collected in 0.25-m horizontal intervals in horizon 3 and from three vertical transects at 0.13-m-depth intervals. These additional data were combined with the approximately 450 sets of data from the horizontal transects to generate sample statistics and histograms for the log-transformed water retention parameters and  $K_s$  and  $K_{fs}$  data. These statistics and histograms are shown in Figures 4, 5, and 6.

The solid curves shown in these figures represent the fits of Gaussian curves to the histogram data. The sample statistics shown in Figures 4, 5, and 6 vary from those reported by Hills and Wierenga (1991) because they represent the entire two-dimensional data set rather than just the nine horizontal transects. It should be noted that some of the sample locations for the horizontal and vertical transects are the same. The data and parameter estimates from these sample locations are repeated, but with different sample numbers in files VGPARM.DAT and KFIELD.DAT. Therefore, the data were screened to ensure that no data from the same sample locations were used twice when the sample statistics that appear in Figures 4, 5, and 6 were generated.

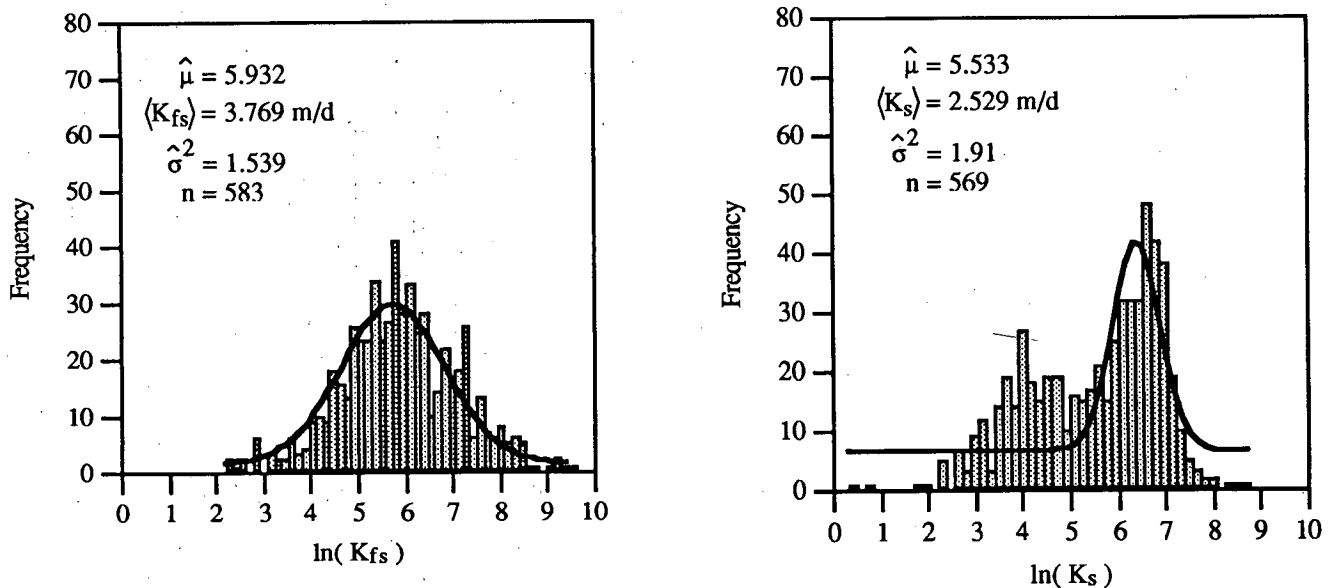


Figure 4. Histograms of Log-Transformed In Situ ( $K_{fs}$ ) and Laboratory ( $K_s$ ) Measurements of Saturated Hydraulic Conductivity

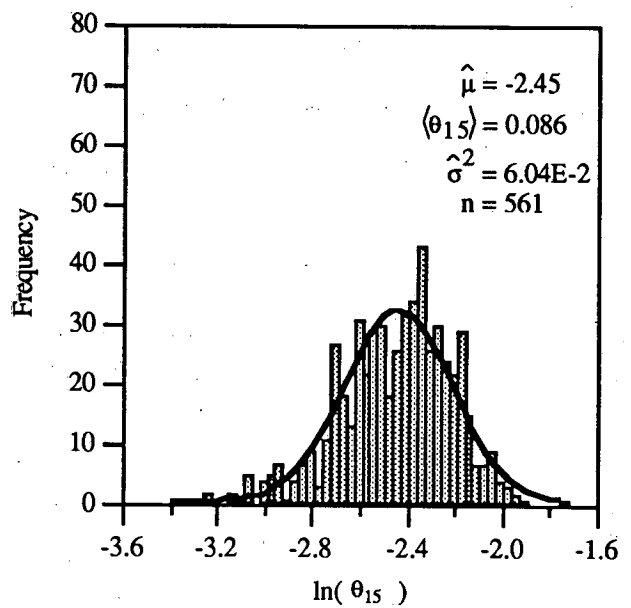
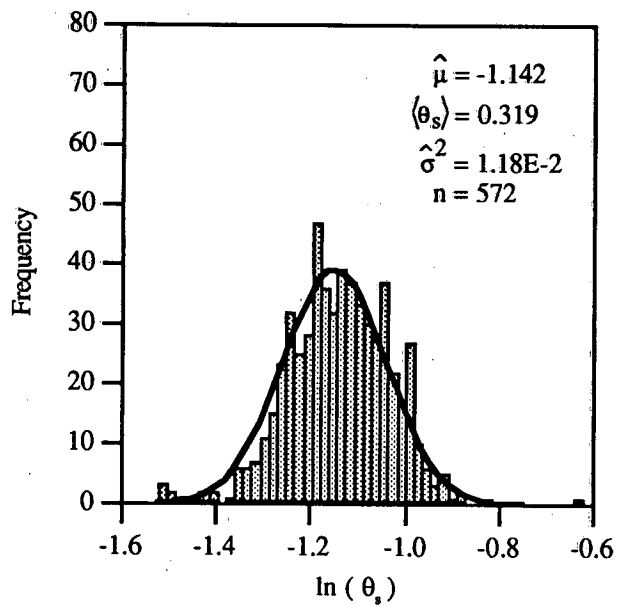


Figure 5. Histograms of Log-Transformed Saturated ( $\theta_s$ ) and 15 Bar ( $\theta_{15}$ ) Water Content Data

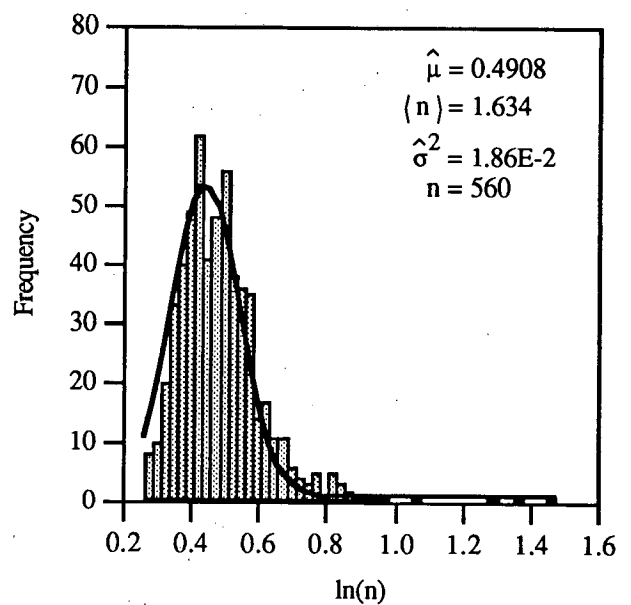
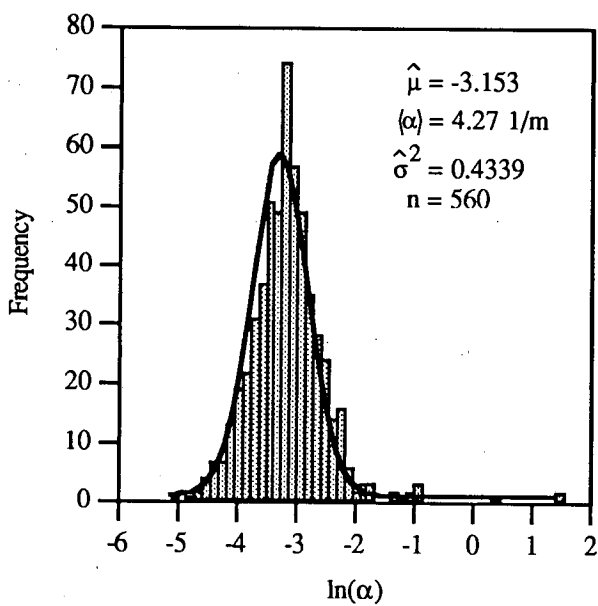


Figure 6. Histograms of Log-Transformed van Genuchten (1980) Model  $\alpha$  and  $n$  Parameters

### 2.2.2.2 Transport Parameters

To model the transport of conservative, nonreactive solutes such as tritium, estimates of the coefficient of molecular diffusion and dispersivities are also required. If dispersivities are assumed to be isotropic, the dispersion coefficient,  $D$ , can be defined as

$$D = D_m + \epsilon |q| \quad (10)$$

where  $D_m$  = coefficient of molecular diffusion ( $L^2 T^{-1}$ )

$\epsilon$  = dispersivity (L)

$q$  = magnitude of Darcian flux

Transport parameters have been estimated from tracer studies conducted in lysimeters adjacent to the Las Cruces trench by Porro (1989). The soils filling the lysimeters were taken from an area near the trench, so they are texturally similar. Estimates of the pore water velocities during these lysimeter experiments, which were conducted using a surface water flux of 1.84 cm/d, range from 10.85 to 18.37 cm/d. Estimates of dispersivity from these lysimeter experiments range from 2.15 to 7.7 cm for tritium. The transport parameters that were determined from these studies for tritium, bromide, and chromium are summarized by Hills and Wierenga (1991). Field transport parameters for tritium have also been estimated using the convection-dispersion equation and data from Las Cruces trench experiment 1 by Elabd et al. (1988).

### 2.2.2.3 Inverse Methods

For the characterization and modeling of LLW sites, it is of practical interest to estimate effective unsaturated flow parameters with as few data as possible. Because of the spatial variability of soil hydraulic properties, in situ measurements are often preferred over laboratory measurements. However, both field and laboratory data are probably necessary to adequately characterize and model unsaturated water flow and solute transport processes at LLW sites.

Although the parameter estimates in the Las Cruces trench site database provide useful information about the spatial variability at the site, they do not necessarily allow one to estimate effective flow parameters for simple uniform or layered model representations of the site. An alternative to using these parameter estimates is to solve an inverse problem with appropriate initial and boundary conditions using matric potential and/or water content data collected during transient infiltration and/or drainage from a field plot.

To solve the inverse problem for transient unsaturated flow, a parametric model for the soil hydraulic properties must

first be selected. After selecting a parametric model, such as the van Genuchten (1980) model, and initial parameter estimates, the flow equation is solved for the appropriate initial and boundary conditions. The value of some objective function is then evaluated and minimized using Newton's method or some modification of it such as the Levenberg-Marquardt method.

The parameter estimation problem can be formulated as a weighted least-squares minimization problem:

$$\min O(b) = 0.5 [q^* - q(b)]^T W [q^* - q(b)] + 0.5 (b^* - b)^T V (b^* - b) \quad (11)$$

where  $O(b)$  = objective function

$b$  = model parameter vector

$q^*$  = observation vector containing measured tensions or water contents

$q(b)$  = predicted response for a given parameter vector  $b$

$b^*$  = direct estimates or measurements of the parameters  $b$

$W$  and  $V$  = symmetric weighing matrices that contain information about measurement accuracy, parameter correlations, etc.

The coefficient 0.5 is used for notational convenience after Kool et al. (1987). If no additional information is available except for the observations,  $q^*$ ,  $W$  can be set equal to 1 (the identity matrix) and  $V$  can be set equal to zero to obtain an ordinary least-squares objective function

$$\min O(b) = 0.5 [q^* - q(b)]^T [q^* - q(b)] \quad (12)$$

Ordinary least-squares formulations are commonly used for parameter estimation problems because of their simplicity and because they require a minimum amount of information (Kool et al. 1987).

Inverse techniques have been used for estimating parameters for one-dimensional unsaturated flow by Zachman et al. (1981, 1982), Kool et al. (1985), Kool and Parker (1988), Toorman et al. (1992), and others. Mishra and Parker (1989) also used inverse techniques to estimate parameters for one-dimensional, coupled unsaturated flow and solute transport. Most of these studies have used hypothetical data sets or laboratory data from one-step outflow experiments. However, Dane and Hruska (1983) and Kool et al. (1987) have also used inverse parameter estimation techniques to determine unsaturated flow parameters using water content, tension, and drainage data from field lysimeters.

In this study, the inverse method described by Kool and Parker (1988) was used with water content data obtained during the infiltration phase of Las Cruces trench experiment 1 to estimate effective van Genuchten water retention parameters for a uniform soil model. The problem was formulated as a one-dimensional, vertical, 6-m-long column of uniform soil with a surface boundary flux equal to 1.82 cm/d, and a unit gradient lower boundary condition. This surface boundary flux corresponds to the irrigation rate that was applied to the surface of the plot during experiment 1. Initial conditions were determined from the average of the neutron probe measurements from the three access tubes located in the center of plot 1 (tube numbers 250, 350, and 450), and the initial tensions reported by Wierenga et al. (1990) for experiment 1.

The three center neutron probe access tubes were used to minimize the influence of edge effects. The irrigated area of the plot was wide enough (4 m) so that the assumption of primarily one-dimensional, vertical flow was thought to be reasonable. Wierenga et al. (1991) have also obtained good comparisons between one-dimensional flow predictions and data from the center access tubes for experiment 1.

To ensure that unique parameter estimates were obtained, only the van Genuchten model  $\alpha$  and  $n$  parameters were estimated. The value of  $\theta_r$  was fixed at 0.04, which is slightly less than lowest field-measured water content prior to the start of experiment 1. The value of  $\theta_s$  was fixed at 0.32, which is the geometric mean of the measured  $\theta_s$  values for the entire two-dimensional data set from the trench. The value of  $K_{fs}$  was fixed at 3.76 m/d, which is approximately equal to geometric mean of the field-measured values from the full two-dimensional data set.

The direct problem was solved using a fully implicit, mass-lumped, Galerkin-type, linear finite element code with variable time step and uniform node spacing of 5 cm. The problem was also simulated using uniform 2.5-cm node spacing to evaluate possible truncation errors in the numerical solution caused by inadequate spatial discretization. Nearly identical results were obtained using 2.5-cm and 5-cm node spacings.

The inverse problem was formulated as an ordinary least-squares problem with water content data from days 10, 19, 27, and 35 used in the objective function to optimize the van Genuchten model  $\alpha$  and  $n$  parameters. The non-linear least-squares problem for the two parameters ( $\alpha$  and  $n$ ) was solved using the Levenberg-Marquardt method. The inverse problem was run several times with different initial parameter estimates to ensure that the same solution was obtained.

This confirmed that the solution had converged to a global rather than a local minimum. The inverse problem was also solved using perturbations of both  $K_s$  and  $\theta_s$ . These simulations resulted in larger root-mean-squared errors, which suggests that the geometric mean values of  $K_s$  and  $\theta_s$  are relatively good estimates of the effective values of these parameters. The simulation results for the inverse problem are summarized in Section 3 of this report.

The finite element flow code that was used is a modified version of the model described by van Genuchten (1982) that uses the mass-conservative time-stepping procedure proposed by Milly (1985). The flow code and inverse parameter estimation procedure are combined into the SFIT code, which is described in detail by Kool and Parker (1988).

### 2.2.3 Spatial Variability

The spatial variability of soils with respect to their hydraulic properties has been studied by numerous researchers (Nielsen et al. 1973; Warrick et al. 1977; Simmons et al. 1979; Sisson and Wierenga 1981; and others).

#### 2.2.3.1 Semivariogram Analyses

The spatial structure and variability of data can be modeled using a geostatistical tool known as the semivariogram (Journel and Huijbregts 1978). Nicholson et al. (1989) and Jacobson (1990) used directional semivariograms to estimate spatial correlation lengths for the soil hydraulic properties at the Las Cruces trench site using the two-dimensional set of the  $\ln(K_{fs})$  data. Directional sample semivariograms (a.k.a. variograms) can be represented by the following equation

$$\gamma(\vec{\xi}) = \frac{1}{2N} \sum_{i=1}^N [Z(x_i) - Z(x_i + \vec{\xi})]^2 \quad (13)$$

where  $N$  = number of data pairs,  $[Z(x_i) - Z(x_i + \vec{\xi})]$  separated by the displacement or separation vector  $\vec{\xi}$  (Journel and Huijbregts 1978).

Analyses of directional sample semivariograms generated using the  $\ln(K_{fs})$  data from the trench site indicate that the principal directions of anisotropy correspond to the horizontal and vertical directions (Nicholson et al. 1989). From the sample semivariograms, Nicholson et al. (1989) determined that the spatial correlation of the  $\ln(K_{fs})$  data could be described using a two-dimensional, exponential semivariogram model. The theoretical semivariogram model can be expressed as

$$\vec{\xi} = \begin{cases} C_0 & \text{if } \left| \frac{\vec{\xi}}{\xi} \right| = 0 \\ C_0 + C_1 [1 - \exp\{- (r)^{0.5}\}] & \text{if } \left| \frac{\vec{\xi}}{\xi} \right| > 0 \end{cases} \quad (14)$$

where  $C_0 + C_1 = \text{sill}$

$C_0 = \text{nugget}$

$$r = \left( \frac{\xi_x}{\lambda_x} \right)^2 + \left( \frac{\xi_z}{\lambda_z} \right)^2$$

$\lambda_x = \text{horizontal correlation length}$

$\lambda_z = \text{vertical correlation length}$

The sill is defined as the true variance and is found when the semivariogram reaches a constant value. The nugget represents a variance that may be caused by measurement errors and/or spatial variations on a scale smaller than the sampling interval (Nicholson et al. 1989). The fitted exponential semivariogram model reported by Nicholson et al. (1989) indicated a nugget effect, equal to 0.4, and horizontal and vertical correlation lengths of 2.0 and 0.2 m, respectively. The sill was assumed to be equal to the sample variance of 1.54.

Jacobson (1990) used a two-dimensional data set of 584 values of  $\ln(K_{fs})$  data to estimate correlation lengths for the hydraulic properties at the trench site using the exponential semivariogram model. Sample semivariograms were calculated for four directions (0, 45, 90, and 135 degrees), using a window of 20 degrees, and a distance lag of 0.5 m. The variograms for 0 and 90 degrees correspond to the horizontal and vertical directions, respectively. When the entire two-dimensional data set was used, the fitted exponential variogram model indicated a nugget effect of 0.4, horizontal and vertical correlation lengths of 2.5 and 0.5 m, respectively, and a sill of 1.54. The theoretical and sample semivariograms determined from this analysis are shown in Figure 7.

Jacobson (1990) also grouped data from each of the horizontal transects based on similar means and variances, and spatial proximity, to estimate variances and correlation lengths. The sampling depths for the horizontal transects correspond to the observed morphological horizons as depicted in Figure 1. When data from horizons 1 and 2 were combined, the exponential semivariogram analyses indicated a nugget effect, equal to 0.27, with no distinct sill or correlation length in either the vertical or horizontal direction.

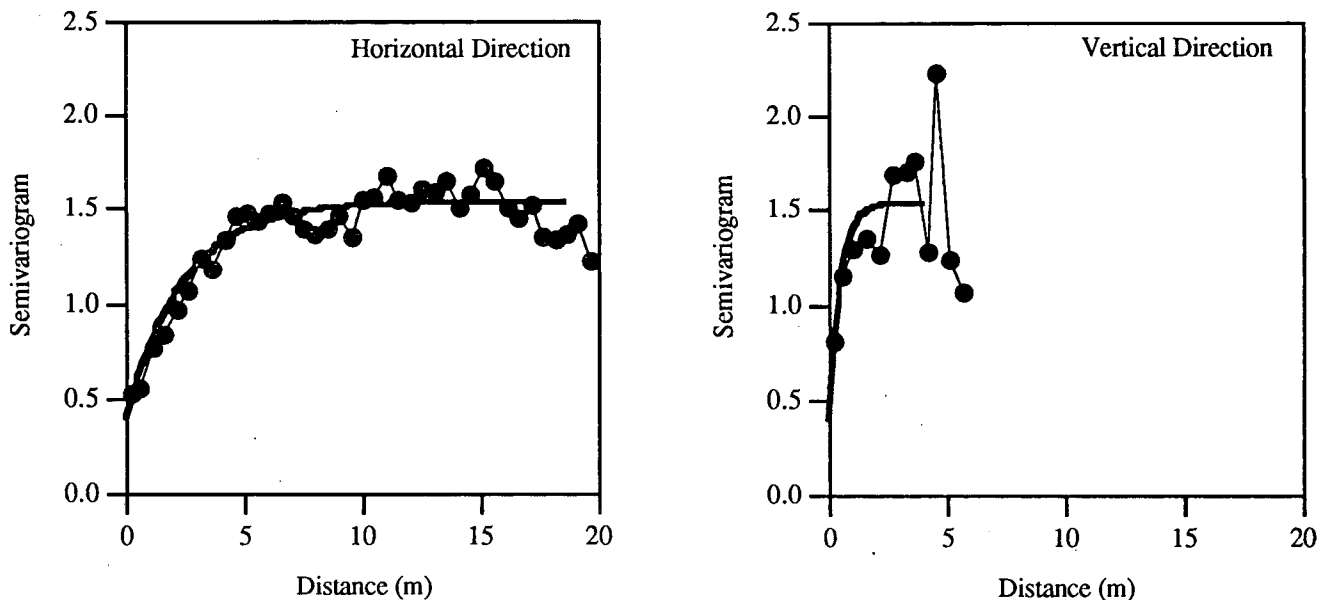


Figure 7. Horizontal and Vertical Sample and Theoretical Exponential Semivariograms Determined Using Log-Transformed  $K_{fs}$  Data (after Jacobson 1990)



When data from horizons 3 through 6 were combined, the fitted exponential semivariogram indicated a sill of 1.98, a horizontal correlation length of 2.0 m, no apparent correlation in the vertical direction and no nugget effect. When data from horizons 7 through 9 were combined, a nugget effect equal to 1.03 was determined with no apparent correlation in either the vertical or horizontal directions. When data from all nine horizons were combined, without the data from the vertical transects, a pure nugget effect, equal to 1.55 was determined. Data from the three vertical transects were also combined and the fitted exponential variogram yielded a sill of 1.06, a vertical correlation length of 0.15 m, and no nugget effect.

In the geostatistics literature, the term "practical range" is commonly used when referring to distances over which samples are correlated (Journel and Huijbregts 1978). It should be noted that the correlation length that is referred to here for the exponential semivariogram model is not the same as the practical range. The practical range is defined as the distance at which the variogram value is 95% of the sill (Journel and Huijbregts 1978). The correlation length is defined as the distance at which the variogram value is  $1-e^{-1}$  or approximately 63% of the sill, excluding the nugget (Jacobson 1990). For the exponential semivariogram model, the tangent at the origin reaches the sill at about one fifth of the practical range (Isaaks and Srivastava 1989).

The horizontal correlation lengths that were estimated from these previous analyses, with an exponential semivariogram model, range from 2 to 2.5 m. Estimates of the vertical correlation lengths range from 0.15 to 0.5 m. Estimates of the correlation lengths can be sensitive to the sample support size and spacing and to the directional tolerance that is specified during the calculation of the semivariograms. The accuracy of the estimate of the vertical correlation length is particularly important because the degree of anisotropy in effective hydraulic conductivities that is predicted by some stochastic flow theories is highly sensitive to the vertical correlation length (Mantoglou and Gelhar 1987a, b, c; Jacobson 1990).

### 2.2.3.2 Stochastic Methods

The recognition that the spatial variability of soil hydraulic properties can have a significant effect on flow and transport through the unsaturated zone has led to the development of stochastic methods for unsaturated flow and transport modeling (Yeh et al. 1985a, b, c; Mantoglou and Gelhar 1987a, b, c; Polmann et al. 1988; and others). The application of these stochastic methods requires a knowledge of the means

and variances of the flow parameters, any correlations between parameters, and the spatial covariance of hydraulic properties.

The stochastic methods described by Yeh et al. (1987a, b, c), Mantoglou and Gelhar (1987a, b, c), and Polmann et al. (1988) for modeling large-scale unsaturated flow assume that the unsaturated hydraulic conductivity of the soil can be represented by

$$\ln(K) = \ln(K_s) - \beta h \quad (15)$$

where  $K$  = unsaturated hydraulic conductivity  
 $K_s$  = saturated hydraulic conductivity  
 $\beta$  = soil parameter

The hydraulic parameters  $\ln(K_s)$  and  $\beta$  are represented as two- or three-dimensional, statistically anisotropic, homogeneous, random fields with prescribed covariance functions.

The parameters such as  $\ln(K_s)$  will have a covariance function of the form

$$R(\vec{\xi}) = E[f(\vec{x} + \vec{\xi}) f(\vec{x})] \quad (16)$$

where  $f = \ln(K_s) - E[\ln(K_s)]$

$\vec{x}$  = position vector (Nicholson et al. 1989)

The function,  $f$ , represents the perturbation of  $\ln(K_s)$ . Two-dimensional, exponential covariances corresponding to the semivariogram function shown previously in Equation 14 can be calculated using the following function

$$R(\vec{\xi}) = \begin{cases} C_0 + C_1 & \text{if } |\vec{\xi}| = 0 \\ C_1 \exp \left[ - \left\{ \left( \frac{\xi_x}{\lambda_x} \right)^2 + \left( \frac{\xi_z}{\lambda_z} \right)^2 \right\}^{0.5} \right] & \text{if } |\vec{\xi}| > 0 \end{cases} \quad (17)$$

where all parameters have already been defined.

The random variables,  $\ln(K_s)$  and  $\beta$  are substituted into the Richards equation (Richards 1931) and solved using a perturbation approach with spectral representation techniques (Polmann et al. 1988). Additional details about these perturbation techniques are described by Yeh et al. (1987a, b, c) and Mantoglou and Gelhar (1987a, b, c) for steady-state and unsteady flow, respectively.

The Monte Carlo method is an alternative to the perturbation approach for obtaining stochastic predictions of unsaturated flow and solute transport. In the Monte Carlo method, the flow (and/or transport) problem is solved repeatedly after sampling from the probability distribution or cumulative distribution function that describes the random variable(s). The perturbation approach and the Monte Carlo approach for stochastic simulation of unsaturated flow and transport both require estimates of the covariance function for the random variable(s). Both approaches result in estimates of mean flow behavior (and/or transport behavior if solute transport is modeled) and the variances about the mean under conditions of parameter uncertainty.

Smith and Freeze (1979a) note that the perturbation approach is efficient but may not be appropriate for some problems in which the input variables have a large variance. Monte Carlo methods provide an effective alternative for large input variances but may require excessive computational resources. However, with recent improvements in computer hardware, such as massively parallel computers (Dougherty 1991) and the development of fast, accurate algorithms for solving the Richards equation (Kirkland et al. 1992), Monte Carlo simulation of large-scale, multi-dimensional, transient unsaturated flow and solute transport problems is becoming more practical.

Zimmerman et al. (1990) review other techniques for propagating data and parameter uncertainties into performance assessment models. Zimmerman et al. (1991) also compare parameter estimation and sensitivity analysis techniques and their effects on the uncertainty in ground water flow model predictions. Many of these techniques can also be readily applied to unsaturated flow and transport problems.

### 2.2.3.3 Scaling

Numerous researchers have attempted to determine correlations and scaling relationships between water retention parameters and saturated hydraulic conductivity to reduce the number of parameters that are required to describe the spatial variability of soil hydraulic properties (Carsel and Parrish 1988; Hopmans 1987; Warrick et al. 1977; Warrick 1990). Most of the scaling approaches that have been described in the literature are based on the concept of geometric similitude and the classical work by Miller and Miller (1956).

This approach relies on the definition of a single characteristic length scale that reflects the sizes of soil particles and pore dimensions in particular geometric arrangements. This length scale has been used to develop physical scaling relationships that relate soil hydraulic properties that have

been measured at different scales and/or at different spatial locations to each other.

Hills et al. (1989c) used relative saturation values that were determined during the soil sampling at the Las Cruces trench site to estimate local values of the van Genuchten  $\alpha$  and  $n$  parameters. These parameters were estimated by fixing  $\alpha$  or  $n$  and fitting the other parameter while minimizing the residual sum of squares on relative saturation using an iterative numerical procedure. Correlation coefficients were determined for various parameter combinations by regressing each parameter against the others. The strongest correlation of any parameter combination was found between the  $\ln(\alpha)$  and  $\ln(K_s)$ , using a constant value of  $n$ , equal to 1.53 (Hills et al. 1989c; Warrick 1990). The correlation coefficient for this case was 0.541 (Hills et al. 1989c). The spatial variability of the soil hydraulic properties at the trench site could be described almost as well using a constant value on  $n$  with variable  $\alpha$  as it could using variable  $n$  and  $\alpha$  parameters (Hills et al. 1989). The procedure used by Hills et al. (1989) is analogous to the scaling procedure used by Hopmans (1987) and Warrick et al. (1977). For a soil that is "Miller similar" (Sposito and Jury 1990), the correlation between  $\ln(\alpha)$  and  $\ln(K_s)$  should be approximately equal to 1 (Hills et al. 1989).

Attempts to characterize the spatial variability of soil hydraulic properties with a single scaling factor have met with varying degrees of success (Warrick et al. 1977; Russo and Bresler 1982; Jury et al. 1987). Jury et al. (1987) analyzed several comprehensive field data sets and concluded that the quantification of the spatial variability of soil hydraulic properties requires at least three scaling parameters. These scaling parameters can be thought of as being realizations of spatial stochastic functions and scale the matrix potential,  $h$ , the hydraulic conductivity,  $K$ , and  $\ln(h)$  in terms of  $\ln(K)$ . The generalized scaling analysis outlined by Jury et al. (1987) is also described by Sposito and Jury (1990). No attempts were made to conduct this type of generalized scaling analysis with the Las Cruces trench data, but the analyses by Jury et al. (1987) suggest that a generalized scaling procedure, such as that described by Sposito and Jury (1990), may be necessary to fully characterize the spatial variability of soil hydraulic properties.

### 2.2.3.4 Random Field Generation

To incorporate information about the spatial variability of porous media into flow and transport simulations, methods for generating random fields with the desired statistical and spatial characteristics must be used. Several methods have

been developed for generating random fields that have been applied to hydrology problems. These include the nearest neighbor method (Smith and Freeze 1979a,b), matrix decomposition methods (Clifton and Neuman 1982), the turning-bands method (Matheron 1973; Delhomme 1978; Mantoglou and Wilson 1982; Tompson et al. 1989), and the fast Fourier transform (FFT) method (Gutjahr 1989). With the exception of the nearest neighbor method, these techniques can all be used to generate unconditional simulations or realizations of spatially correlated, Gaussian (or normally distributed) random fields with prescribed covariance functions. Unconditional simulation refers to the generation of random fields that maintain the mean (or expectation) and variance, with a prescribed covariance behavior, but do not preserve the values of the observed data at their measurement locations.

Each of these methods for generating spatially correlated random fields has certain advantages and disadvantages. The nearest neighbor methods are intuitively simple, but may not generate statistically homogeneous (or stationary) random fields. In addition, the form of the covariance function cannot be specified a priori. The matrix decomposition methods can be relatively fast for small problems, but require the decomposition and diagonalization of a matrix, which can be computationally expensive for large fields. The turning-bands method has traditionally been one of the most popular methods for generating random fields for hydrology applications. This method can be very fast, especially if FFT methods are used for generating the line processes (Tompson et al. 1989). However, the turning-bands method has been criticized for introducing artificial features into the generated fields (Tompson et al. 1989; Gutjahr 1989; Zimmerman and Wilson 1990). The FFT method is very fast and is claimed to be one of the best procedures available for generating two-dimensional random fields (Gutjahr 1989). However, this method may be less practical than the turning-bands method for generating large three-dimensional fields because it requires additional storage so that fields that are larger than what is actually needed can be generated to compensate for the periodicity of the Fourier series (Gutjahr 1989; Press et al. 1992). Tompson et al. (1989) suggested that the FFT method may be the most efficient method for generating random fields for problems of small to moderate size, while the turning-bands method may be more efficient for larger three-dimensional problems ( $10^5$  points or more).

Several other methods have been popular for generating random fields for mining and petroleum applications. These include sequential Gaussian simulation (Journel 1980), sequential indicator simulation (Journel and Alabert 1989), and simulated annealing (Deutsch 1992; Farmer 1991).

These methods and matrix decomposition methods have been used for conditional simulation, which refers to the generation of random fields that maintain the mean and variance with a prescribed covariance behavior and preserve the values of the observed data at their measurement locations.

Unlike some of the previously mentioned methods, indicator simulation and simulated annealing are not limited to the generation of multigaussian fields with a single covariance model. Therefore they are more flexible than some of the other methods, but they can also be more computationally expensive. Indicator simulation has been praised for its ability to preserve the spatial connectivity of extreme-valued permeabilities, which tend to be blurred by Gaussian simulation approaches (Journel and Alabert 1989). At larger scales, this spatial connectivity of extreme-valued permeabilities may be the most important feature controlling flow and transport processes.

The two-dimensional set of  $\ln(K_{fs})$  data from the Las Cruces trench site are normally distributed. Therefore, most of the aforementioned methods are applicable for generating spatially correlated random fields of  $\ln(K_s)$  for this study. However, due to its speed, a FFT method was used for generating two-dimensional, unconditioned random fields of  $\ln(K_{fs})$ . The unconditioned random fields were then conditioned on the measured data from the trench using the procedure described below. Additional details about FFT methods for generating random fields are discussed by Borgman et al. (1984) and Gutjahr (1989).

#### 2.2.3.5 Conditional Simulation

As stated previously, conditional simulation refers to the generation of random fields that maintain the mean and variance of a random variable such as  $\ln(K_s)$  with a prescribed covariance behavior, and preserve the values of the observed data at their measurement locations. A conditional simulation procedure was employed in this study that uses the geostatistical method for spatial estimation known as kriging. The theory and motivation for kriging and conditional simulation are described in detail by Journel and Huijbregts (1978).

The core samples and in situ measurements of  $K_{fs}$  that were collected at the Las Cruces trench site were collected from the area of the trench as it was being excavated. Because no measurements of the soil hydraulic properties were made in the area of experimental plot 2, conditional simulation is not directly applicable. However, if it is assumed that the spatial distribution of hydraulic properties in the plane of the trench is representative of the distribution in any given

vertical plane parallel to the trench that passes through the experimental plot area, then conditional simulation can be used to generate realizations of the hydraulic properties.

As described by Isaaks and Srivastava (1989), the acronym BLUE is often associated with ordinary kriging, which stands for "best linear unbiased estimator." Ordinary kriging estimates are linear combinations of the available data that are unbiased because the kriging procedure attempts to make the mean residual or error equal to zero and minimizes the error variance. The minimization of the error variance results in a smoothing of the true data dispersion (Journel and Huijbregts 1978). Like ordinary kriging, conditional simulation maintains the mean and covariance, as well as the histogram, but the simulated value at each point in a generated field is not the best possible estimator. It can be shown that the variance of estimation of a conditionally simulated value is exactly twice the kriging variance (Journel and Huijbregts 1978). Kriging estimates are, on average, closer to the real data, but conditionally simulated values generally provide a better reproduction of the fluctuations in the real data (Journel and Huijbregts 1978).

The following procedure was used to generate conditional simulations of random hydraulic conductivity fields for this study. Ordinary point kriging was first used to generate kriged estimates of  $\ln(K_s)$  at the nodal coordinates of the grid used for flow and transport simulations. A FFT method was then used to generate unconditioned, spatially correlated random fields of  $\ln(K_s)$  values at the coordinates of the model grid. A kriged map of  $\ln(K_{fs})$  generated from the trench data is shown in Figure 8 with a single, unconditioned realization of  $\ln(K_{fs})$  that was generated using a FFT method. The exponential semivariogram parameters determined by Jacobson (1990) for the full two-dimensional set of  $\ln(K_{fs})$  data from the trench were used for kriging and for generating the unconditioned random field. The directional covariances computed from the single realization of  $\ln(K_{fs})$  are compared with the directional covariances for the theoretical (or target) model in Figure 9. Values from the unconditioned random field were interpolated to the  $K_{fs}$  measurement locations, and ordinary point kriging was again used to estimate values at the coordinates of the model grid from these interpolated values of the unconditioned random field. The conditioned field of  $\ln(K_{fs})$  was then generated using the following equation

$$Z^*_{SC}(x) = Z^*_{OK}(x) + [Z_S(x) - Z^*_{SK}(x)] \quad (18)$$

where  $Z^*_{OK}$  = kriged values

$Z_S$  = values of unconditioned random field

$Z^*_{SK}$  = kriged values generated from the unconditioned values of the random field sampled at the measurement locations.

Gutjahr (1989) also discusses a method for kriging and conditioning in the spectral domain that could potentially be much more efficient than the procedure described above.

#### 2.2.4 Modeling Scenarios

Four different sets of two-dimensional simulations were generated to demonstrate the effects of different parameter estimates and heterogeneity on predicted water flow and tritium transport for experiment 2B. Case 1 represents a uniform, isotropic soil model. The hydraulic properties used for case 1 represent a modification of the average best-fit water retention parameters and saturated hydraulic conductivity from laboratory measurements for all nine soil horizons that are reported by Hills and Wierenga (1991). As noted previously, the estimates of the residual water content values that are reported in the Las Cruces trench database are greater than the initial water contents that were observed in parts of the soil profile. The dry end of the water retention and hydraulic conductivity curves that were used for case 1 were modified so that the low initial water contents that were observed in parts of the soil profile could be more accurately represented.

The modification to the water retention curve that was used for the case 1 simulation essentially consisted of splicing a second van Genuchten curve onto the original water retention curve. The composite curve is represented by two sets of parameters for the van Genuchten (1980) model. No data were used to fit the composite curve at the dry end; however, this could easily be done if data were available.

Ross et al. (1991) recently suggested a method for extending water retention curves to dryness in which a suction or tension of 1000 MPa (or 1.E+5 m) was used to approximate oven dryness. Gee et al. (1992) also report data generated using a water activity meter showing that as water potentials approach 1000 MPa, water content is essentially reduced to 0.0. The modified water retention curve used for the case 1 simulation also reaches a water content of 0.0 at a matric potential of approximately 1000 MPa.

Simulation case 2 represents a uniform, anisotropic soil model. The hydraulic properties used for case 2 correspond to properties that were used previously by Kool and Wu (1991) for simulation of Las Cruces trench experiment 2A. The water retention parameters for this case are the average best-fit water retention parameters determined using data from the nine soil horizons. The residual water content

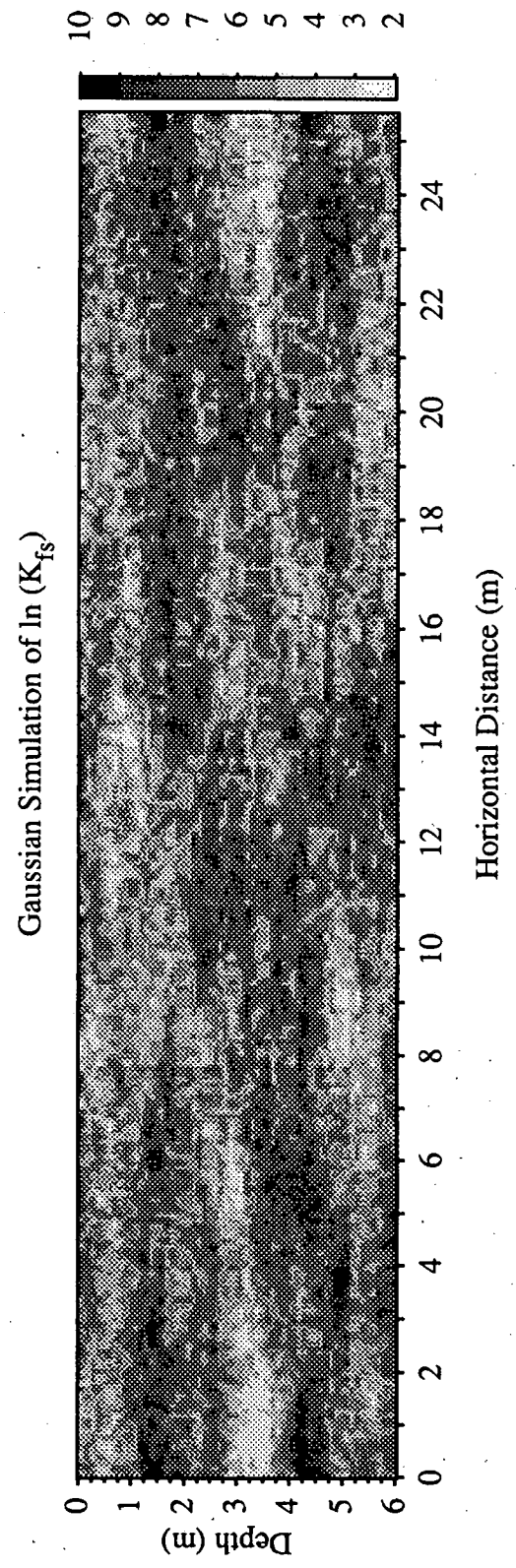
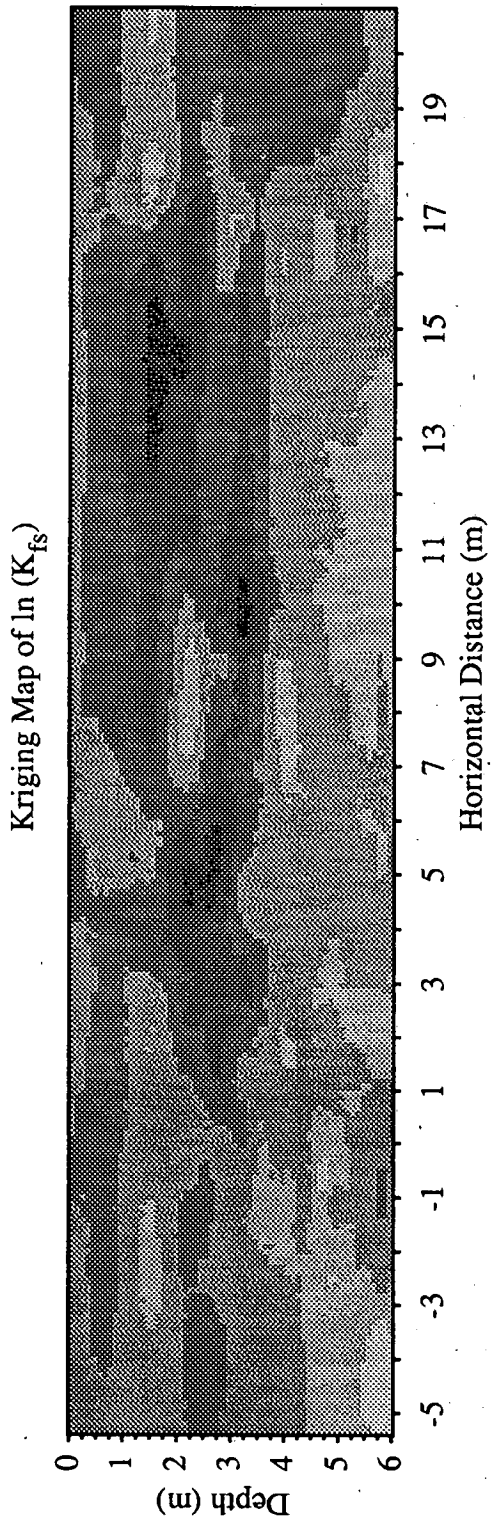
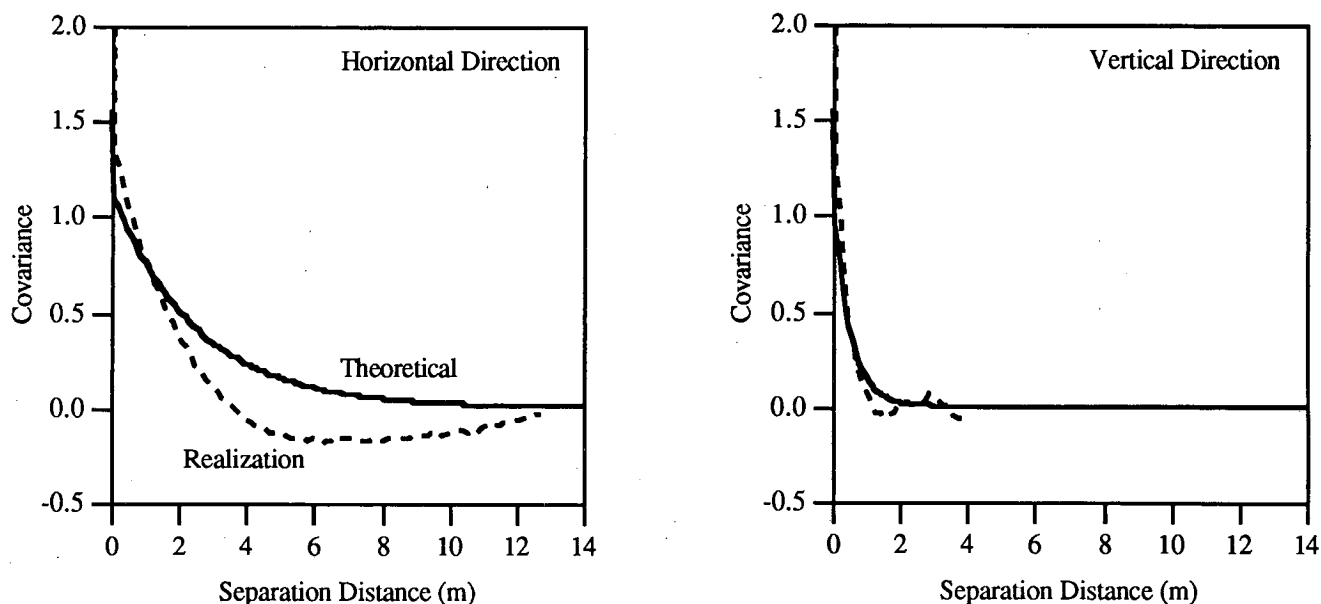


Figure 8. Kriging Map of  $\ln(K_{fs})$  and Gaussian Simulation of  $\ln(K_{fs})$  Generated Using FFT Method



**Figure 9. Directional Covariance as a Function of Separation Distance for Theoretical Exponential Covariance Model and Single Realization Generated Using FFT Method**

values were constrained during the curve-fitting process to values less than the lowest measured initial water content in each horizon. The saturated hydraulic conductivity in the vertical direction ( $K_{zz}$ ) was computed from the individual laboratory measurements, assuming a lognormal distribution (Kool and Wu 1991). The saturated hydraulic conductivity in the horizontal direction ( $K_{xx}$ ) was assigned a value twice as large as the vertical direction in an attempt to better reproduce the observed spread of the water plume for experiment 2A.

Simulation case 3 represents a uniform, isotropic soil model. The van Genuchten model  $\alpha$  and  $n$  parameters that were used for case 3 correspond to the parameters that were estimated from a one-dimensional inverse solution described previously in Section 2.2.4 and water content data obtained during the first 35 days of infiltration for experiment 1. The saturated water content and hydraulic conductivity values that were used for case 3 are geometric mean values calculated from the full two-dimensional set of laboratory water retention and  $K_{fs}$  data, respectively. The water retention and hydraulic conductivity curves corresponding to simulation cases 1, 2, and 3 are shown in Figure 10.

Simulation case 4 represents a fully heterogeneous model. The water retention parameters that were used for this case

correspond to kriged estimates based on the fitted parameters reported by Kool and Wu (1991). The kriged estimates were generated based on the fitted parameters for samples collected between the x-coordinates of -3.78 and 5.22 in the Plot coordinate system. The saturated hydraulic conductivities that were used for case 4 correspond to a spatially correlated random field that was conditioned on the  $K_{fs}$  data from the trench, as described previously. All kriged parameter fields were generated assuming an exponential covariance model with horizontal and vertical correlation lengths of 2.5 and 0.5 m, respectively, based on the semivariogram analyses by Jacobson (1991).

For simulating the transport of tritium, dispersivities were assumed to be homogeneous and isotropic, and the tritium was assumed to be nonreactive. A molecular diffusion coefficient,  $D_m$ , equal to  $1.0E-4$  m<sup>2</sup>/d was assumed for all simulation cases. For the first three simulation cases, which represent uniform soil models, the dispersivity,  $\epsilon$ , was assumed to be equal to 0.05 m. For the fourth simulation case, which represents a fully heterogeneous model, the dispersivity was assumed to be equal to 0.0 m. The radioactive decay of tritium was modeled, assuming a half-life for tritium of 12.26 years. The flow and transport parameters that were used for model simulations are summarized in Table 1.

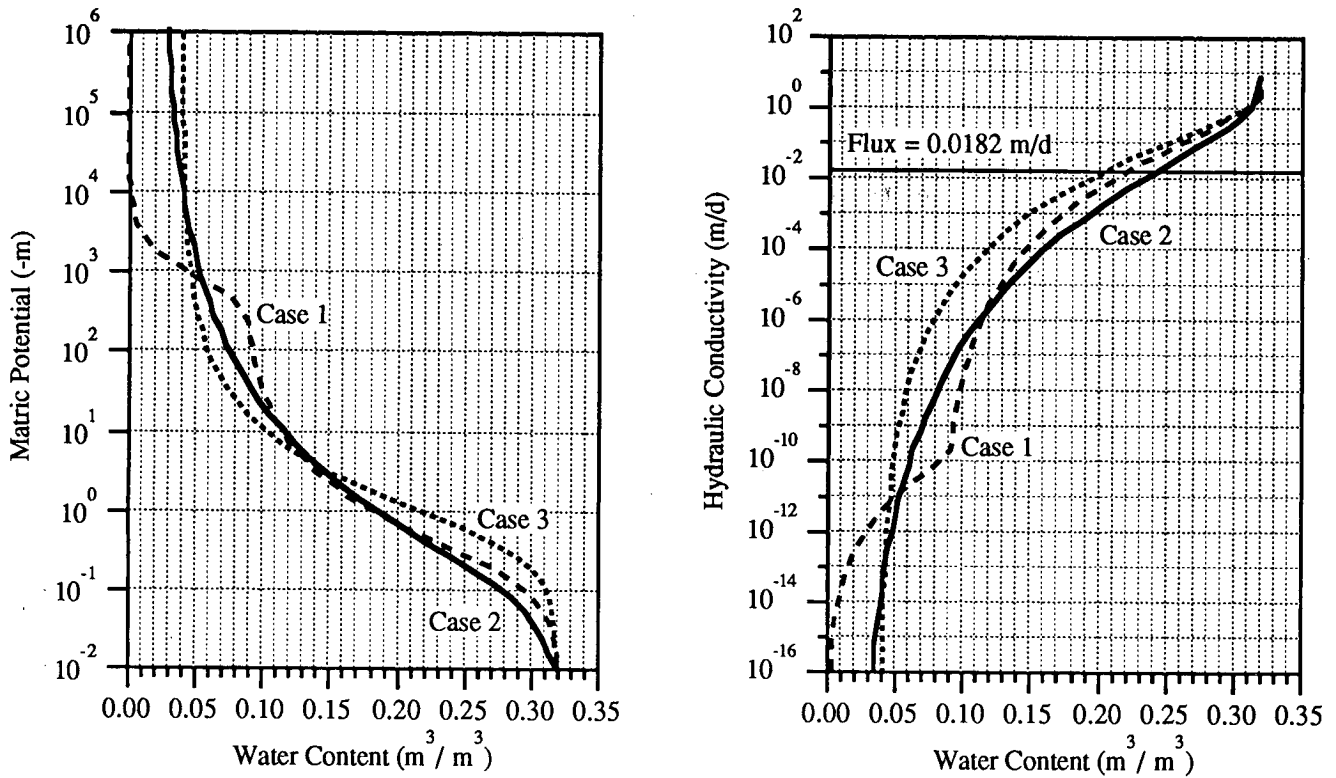


Figure 10. Water Retention and Hydraulic Conductivity Curves for Simulation Cases 1, 2, and 3

Table 1. Flow and Transport Parameters Used in MSTs Simulations

	Simulation Case			
	1(a)	2	3	4
<u>Hydraulic Parameters</u>				
$K_{xx}; K_{zz}$ (m/d)	2.701; 2.701	13.1; 6.55	3.76; 3.76	Individually
$\theta_s$	0.3209	0.32	0.32	Assigned To
$\theta_r$	0.0828	0.025	0.04	Every Node
$\alpha$ (1/m)	5.501	11.2	2.176	in the Model
$n$	1.5093	1.253	1.4956	Domain
<u>Transport Parameters</u>				
$\epsilon_{xx}; \epsilon_{zz}$ (m)	0.05; 0.05	0.05; 0.05	0.05; 0.05	0.0; 0.0
$D_m$ (m <sup>2</sup> /d)	0.0001	0.0001	0.0001	0.0001

(a) Hydraulic parameters used for dry end of curves are  $K_{xx} = K_{zz} = 1.E-10$  (m/d),  $\theta_s = 0.092$ ,  $\theta_r = 0.0$ ,  $\alpha = 0.0015$  (1/m), and  $n = 2.5$ .

## 2.2.5 Initial and Boundary Conditions

Initial water content values were measured in all of the neutron probe access tubes in plot 2, on day 0, prior to the start of infiltration for experiment 2B. Transects 1, 2, and 3 are located 2 m, 6 m, and 10 m from the face of the trench, respectively. The initial water content distribution from transect 1 was used for all two-dimensional model simulations that are reported in this document.

Initial normalized tritium concentrations were determined on day 0 from solute samples collected from the solution samplers. The solution samplers extend 0.5 m into the soil profile from the face of the trench. Soil samples were also collected from sampling planes located 5 and 9 m from the face of the trench on days -63 and -21 for determination of initial solute concentrations in the third dimension (y-direction). The initial tritium concentrations determined on day 0 from the solution samplers were used for all two-dimensional model simulations.

Although the neutron probe and solute measurement transects are offset by 1 to 1.5 m, the water content and normalized tritium concentration data from adjacent measurement transects were paired to provide initial conditions for flow and transport simulations. Bilinear interpolation was used to interpolate between the measurement locations to the coordinates of nodes in the model grid for the initial conditions.

The modeled domain used for all simulations represents an 11-m-wide by 7-m-deep cross section. These dimensions were sufficient to maintain the simulated water contents near the boundaries of the domain at or near their initial values. Uniform 0.1-m node spacing was used in both the horizontal and vertical directions. This spatial discretization results in a total of 7700 nodes.

A Neumann or flux boundary condition of 0.0182 m/d was prescribed as the surface boundary condition that corresponded to the irrigated strip source for the first 70 days of the experiment. After day 70, this boundary was specified as a zero-flux boundary. A Dirichlet boundary condition with a normalized tritium concentration of 0.622 was specified for the strip source during days 29 through 44 of the experiment. As mentioned previously, this normalized tritium concentration is relative to the concentration of tritium that was applied during experiment 2A. This strip source boundary was specified as a zero-concentration boundary prior to day 29 and after day 44. Zero-flux and zero-concentration gradient boundary conditions were imposed on the remainder of the upper boundary and on the side boundaries. Unit hydraulic gradient and zero-concentration gradient boundary conditions were specified for the lower boundary of the modeled domain for the entire duration of the simulations. The modeled cross section and assignment of boundary conditions are shown in Figure 11. The initial water content and tritium distributions are shown in Figures 12 and 13, respectively.

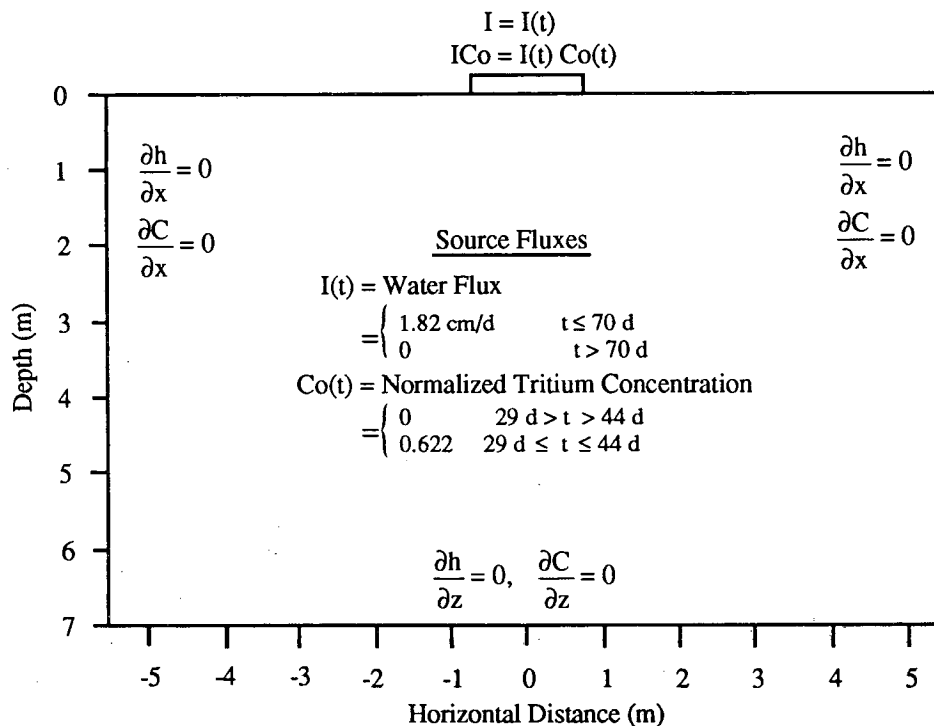


Figure 11. Modeled Cross Section and Assignment of Boundary Conditions



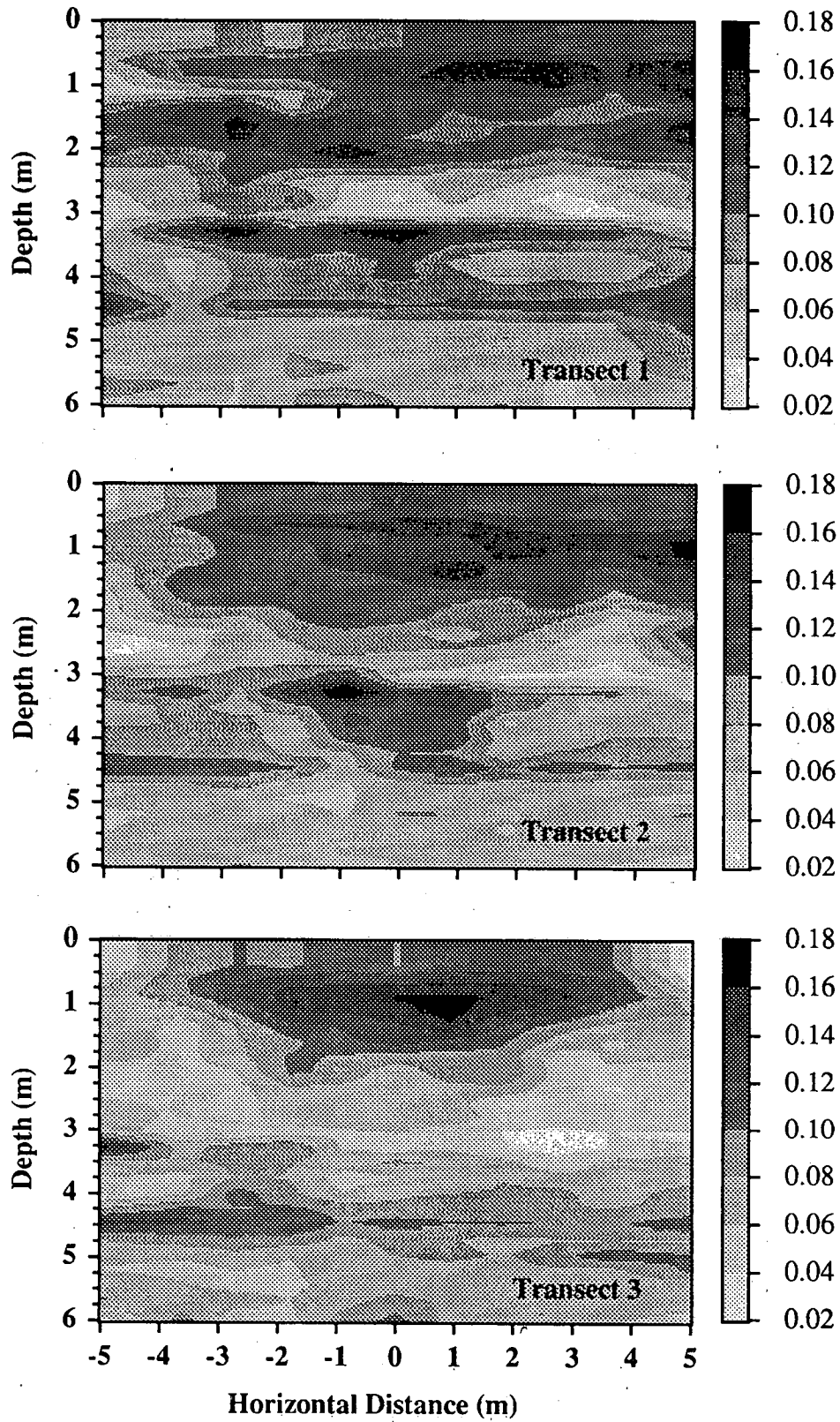


Figure 12. Initial Water Content Distributions for Neutron Probe Transects 1 ( $y = 2$  m), 2 ( $y = 6$  m), and 3 ( $y = 10$  m)

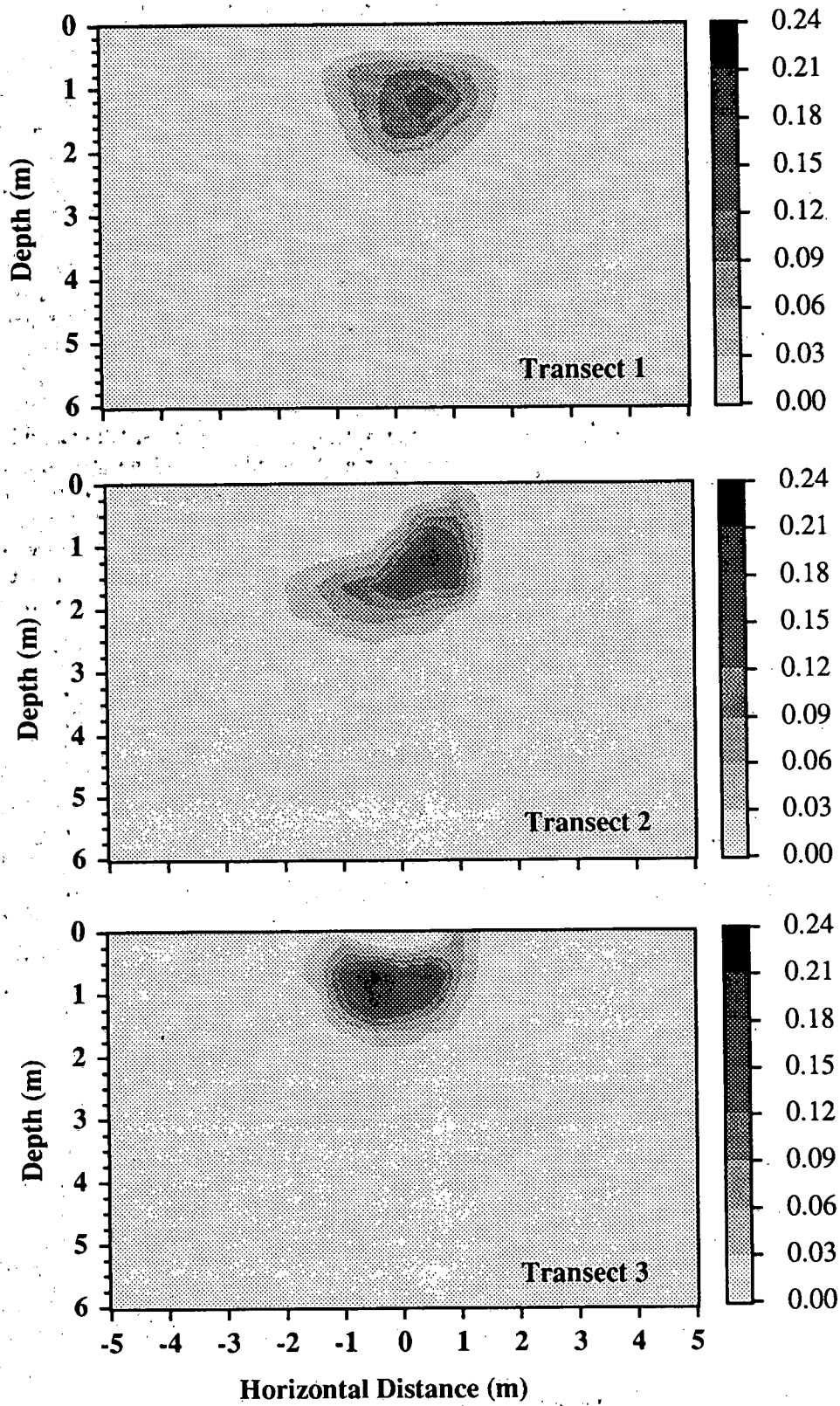


Figure 13. Initial Normalized Tritium Concentrations for Solute Sample  
 Transects 1 ( $y = 0.5$  m), 2 ( $y = 5$  m), and 3 ( $y = 9$  m)

## 2.3 Model Evaluation

Contour plots of water content and normalized tritium concentration distributions were used for qualitative comparisons of the observed and simulated flow and transport results. In addition, a spatial moment analysis was used to provide a quantitative basis for comparing the mean simulated and observed flow and transport behavior.

Spatial moments provide an integral measure of multi-dimensional mass transport processes. The  $ij$ -th moment,  $M$ , of a water content or concentration distribution in space is defined as

$$M_{ij}^A(t) = \int_{-\infty}^{\infty} \int_{-\infty}^{\infty} A(x,z,t) x^i z^j dx dz \quad (19)$$

where  $A(x,z,t)$  is used here to represent either the water content change from the initial condition, or the normalized tritium concentration times the volumetric water content. The integral of Equation 19 is defined over all two-dimensional space. However the integrand will be nonzero only over regions where the concentrations or water content changes are nonzero. Therefore the spatial moment,  $M$ , is an integrated measure of the concentration field or water content distribution only over the extent of the solute or water plume.

The zero-th moment is equal to the total mass or activity of tracer in solution or the change in total mass of water in the system. The first moment, normalized by the total mass, defines the location of the center (denoted by subscript  $c$ ) of solute or water mass (Freyberg 1986).

$$x_c = M_{10} / M_{00} \quad (20a)$$

$$z_c = M_{01} / M_{00} \quad (20b)$$

The second moment about the center of mass defines a spatial covariance tensor,

$$\sigma = \begin{bmatrix} \sigma_{xx} & \sigma_{xz} \\ \sigma_{zx} & \sigma_{zz} \end{bmatrix} \quad (21)$$

$$\text{where } \sigma_{xx} = M_{20} / M_{00} - x_c^2$$

$$\sigma_{zz} = M_{02} / M_{00} - z_c^2$$

$$\sigma_{xz} = \sigma_{zx} = M_{11} / M_{00} - x_c z_c$$

The components of this covariance tensor are physically related to the spread of the water or solute plume about its center of mass (Freyberg 1986).

The neutron probe and solution sample measurement grids for Las Cruces trench experiment 2B were much coarser than the computational grid used for numerical simulations. Therefore, all simulation results were interpolated to the measurement locations using bilinear interpolation. The interpolated simulation results were then used for spatial moment calculations. Freyberg (1986) suggests that the estimated values of the coordinates of the center of mass and of the components of the covariance tensor are relatively insensitive to grid spacing and interpolation technique. However, alternate spatial moment estimation methods and techniques for reducing possible bias introduced by the grid spacing and weighing used for interpolation are discussed by Barry and Sposito (1990).

Other quantitative measures such as relative-root-mean-squared-errors and fluxes through specified horizontal planes as a function of time could also have been used to evaluate the different simulation results. Although no emphasis has been placed in this study on any particular performance objective, travel time is an additional measure that is commonly used as a performance objective criteria for LLW sites.

## 3 Results and Discussion

### 3.1 One-Dimensional Inverse Parameter Estimation

Simulated and observed water content profiles for experiment 1 are shown in Figure 14. As noted previously, water was applied to the surface of the 4-m by 9-m plot for the first 86 days of the experiment. Water content data from the three center neutron probe access tubes (tube numbers 250, 350, and 450), for days 10, 19, 27, and 35 were used in the inverse procedure to estimate the van Genuchten model  $\alpha$  and  $n$  parameters.

As shown in Figure 14, a distinct zone of lower water content is evident from the water content profiles for days 27 and 35, between the 2- and 3-m depths. This zone roughly corresponds with the fourth and fifth (or 2Bkb and 2Cb) soil horizons that were identified based on morphological characteristics as depicted in Figure 1. Figure 12 also indicates lower initial water content values in these horizons for all three neutron probe measurement transects. No particularly distinguishing features are evident from the characterization data for these horizons; however, the lower water content values suggest a slightly coarser texture for this zone. The actual sampling depths from which characterization data were obtained in the fourth and fifth soil horizons are 2.16 and 2.71 m, respectively.

Attempts were made to simultaneously estimate the van Genuchten model  $\alpha$  and  $n$  parameters for a three-layer soil model, with a distinct layer between the 2- and 3-m depths, using only water content data obtained during the infiltration phase of experiment 1. Unique parameter estimates could not be obtained for this number of parameters using only the water content data. Attempts were also made to simultaneously estimate  $K_s$ ,  $\theta_s$ ,  $\alpha$ , and  $n$  for a uniform soil model using only the water content data. However, unique parameter estimates could not be obtained in this case either.

Kool et al. (1987) demonstrated that the van Genuchten model  $\alpha$  and  $n$  parameters could be uniquely estimated using only water content profiles during drainage in a field lysimeter. However, they determined that the simultaneous estimation of three or more parameters required additional information such as the measured pressure head at one depth. Similarly, Toorman et al. (1992) showed that parameter estimation sensitivity can be improved during one-step outflow experiments by including the measurement of pressure head at some distance away from the outflow boundary. Kool et al. (1987) also noted that  $K_s$  is an

ill-determined parameter if no observations at saturated or near-saturated conditions are available.

In an attempt to improve the parameter estimation sensitivity for the inverse solutions with both the uniform (four parameter) and layered (six parameter) soil models, the matric potential data from the tensiometers located 0.5 m from the face of the trench were used as auxiliary variables with the average water content data from the three center neutron probe access tubes. Unique parameter estimates could still not be obtained for this number of parameters in either case, even with these additional data. The inability to obtain unique parameter estimates using these additional data may be the result of the tensiometers not being located very close to the center neutron probe access tubes and the fact that field data are relatively noisy. Nevertheless, the inverse method appears to be a promising means of obtaining effective flow and/or transport parameters for unsaturated flow modeling and certainly warrants further study. Two-dimensional simulation results that were obtained using the parameters from the one-dimensional inverse solution depicted in Figure 14 are described in the following section.

### 3.2 Two-Dimensional Flow and Transport Modeling

The results from the four different sets of two-dimensional flow and transport simulations are compared with observed water content and tritium concentration data using contour plots and a spatial moment analysis in this section. The observed and simulated water content distributions are compared first, followed by the transport results.

#### 3.2.1 Flow Simulations

The observed water content distributions from neutron probe transects 1, 2, and 3 for day 70 are shown in Figure 15. Day 70 was the final day of infiltration for experiment 2B. The water content distributions from all three transects are similar, and all show a distinct zone of lower water content between the 2- and 3-m depths.

Simulated water content distributions for cases 1 and 2 are compared with the observed water content distribution from neutron probe transect 1 for day 70 in Figure 16. The depth of water infiltration for case 1 is much closer to the observed data than case 2. However, the lateral spreading of the wetting front appears to be predicted better by case 2. As noted previously, the anisotropic hydraulic conductivities that were used for case 2 were selected in an attempt to match the

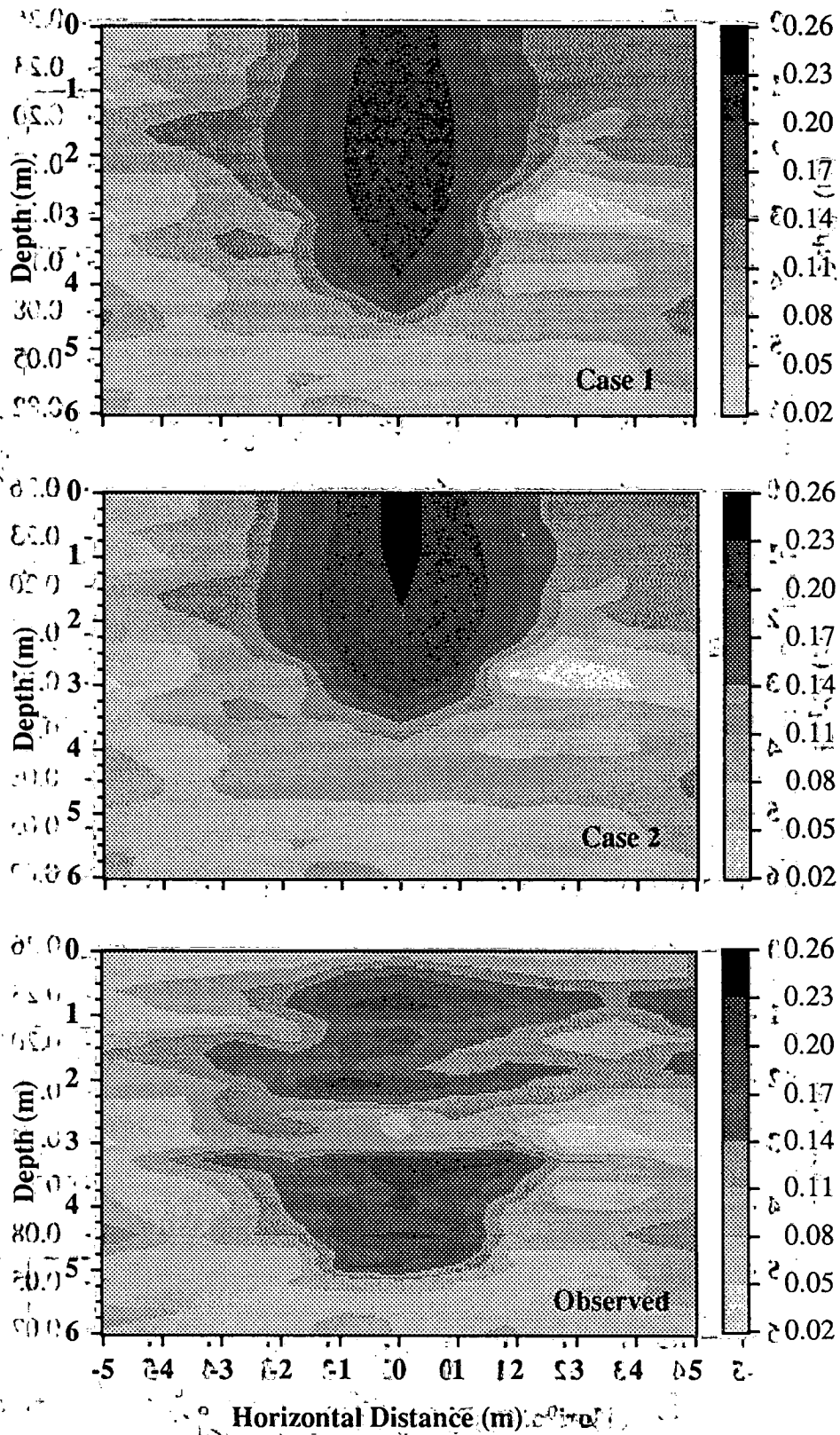


Figure 16. Simulated Water Content Distributions for Cases 1 and 2 and Observed Water Content Distribution from Neutron Probe Transect 1 for Day 70

observed spreading of the water plume for experiment 2A by Kool and Wu (1991).

The simulated water content distributions for cases 3 and 4 are compared with the observed water content distribution from transect 1 for day 70 in Figure 17. The water retention parameters obtained from the one-dimensional inverse solution and data from experiment 1 were used for simulation case 3. Case 4 represents kriged water retention parameter estimates and a single stochastic realization of a random hydraulic conductivity field that was conditioned on the data from the trench.

The simulated water plume for case 3 matches both the vertical penetration and lateral spreading of the observed water plume relatively well. However, the simulated plume is slightly more dispersed than the observed plume. The simulated water plume for case 4 qualitatively matches the observed water plume on day 70 better than any of the other simulation cases, but the vertical penetration of the simulated plume for case 4 is not quite as great as the observed plume. In addition, the simulated plume for case 4 drifts to the left of the center of the plot.

The observed water content distributions from neutron probe transects 1, 2, and 3 for day 310 are shown in Figure 18. The water content distributions from all three transects are similar. No data were logged for the neutron probe access tube located at  $x = 4$  m in transect 3 on day 310, so the water plume appears to exhibit less lateral spreading for this transect. The distinct zone of lower water content between the 2- and 3-m depths persists throughout the infiltration and redistribution phase of the experiment in all three transects.

The simulated water content distributions for cases 1 and 2 are compared with the observed water content distribution from transect 1 for day 310 in Figure 19. The vertical position of the observed water plume is still better represented by case 1, and the horizontal spread of the observed plume is more closely matched by simulation case 2. On day 310, the water content distribution above the 3 m depth is nearly the same as the initial water content distribution prior to the start of the experiment.

Figure 20 shows the simulated water content distributions for cases 3 and 4 and the observed water content distribution from transect 1 on day 310. The simulated water content distribution for case 3 is much too dispersed relative to the observed data. The lateral spreading of the simulated plume is also overpredicted by simulation case 4, relative to the

observed data. The simulated plume for case 4 has also continued to drift too far to the left of center.

The first spatial moments of the simulated water plumes and the observed water plume from transect 1 are plotted in Figure 21. The normalized X moments, or x-coordinates of the centers of mass, are approximately the same for all simulation cases with the exception of case 4, which drifts to the left. The normalized Z moments, or z-coordinates of the centers of mass, vary considerably between the different simulation cases. The normalized Z moments for case 4 match the Z moments of the observed water plume more closely than any of the other simulation cases up through about day 150. The normalized Z moment for case 3 is almost identical to the Z moment of the observed plume on day 310.

The second spatial moments of the simulated water plumes and the observed water plume from transect 1 are plotted in Figure 22. The normalized XX moments of the observed plume, which are a measure of the horizontal spread of the plume about its center of mass, are most closely matched over all times by simulation case 2, which uses a horizontal to vertical hydraulic conductivity anisotropy ratio of 2:1. Simulation case 3 predicts the observed spread of the water plume quite well up through about day 70, but overpredicts the spread of the plume during the redistribution phase of the experiment. Case 4 overpredicts the horizontal spread of the water plume after about day 26.

The normalized ZZ moments, which are a measure of the vertical spread of the plume about its center of mass, indicate that case 3 matches the observed vertical spread of the water plume most closely up through about day 150, but simulation case 1 matches the observed vertical spread of the plume better at later times. Simulation case 4 matches the vertical spread of the observed water plume reasonably well up through day 70. After day 70, the simulated water plume appears to have found a zone of higher conductivity that has channeled the flow in the horizontal direction, to the left of the center line of the field plot. The spatial moments of the observed and simulated water plumes for day 310 are summarized in Table 2.

On day 70, the simulated water plumes for all four simulation cases arguably match the observed water content data from transect 1 reasonably well. However on day 310, none of the simulation results appear to match the observed data very well. Thus it appears as though water flow during infiltration is more easily predicted than during redistribution.



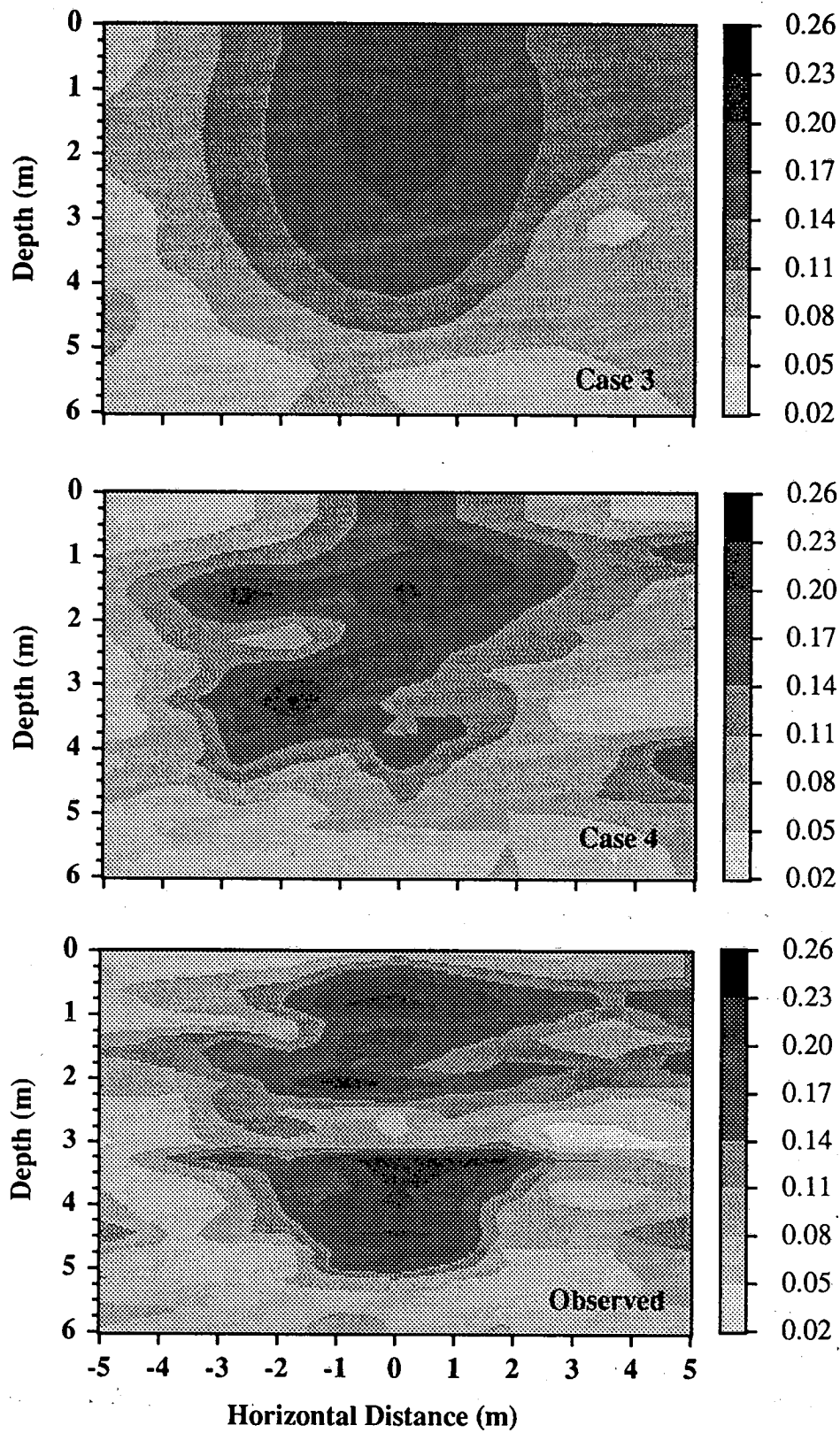


Figure 17. Simulated Water Content Distributions for Cases 3 and 4 and Observed Water Content Distribution from Neutron Probe Transect 1 for Day 70

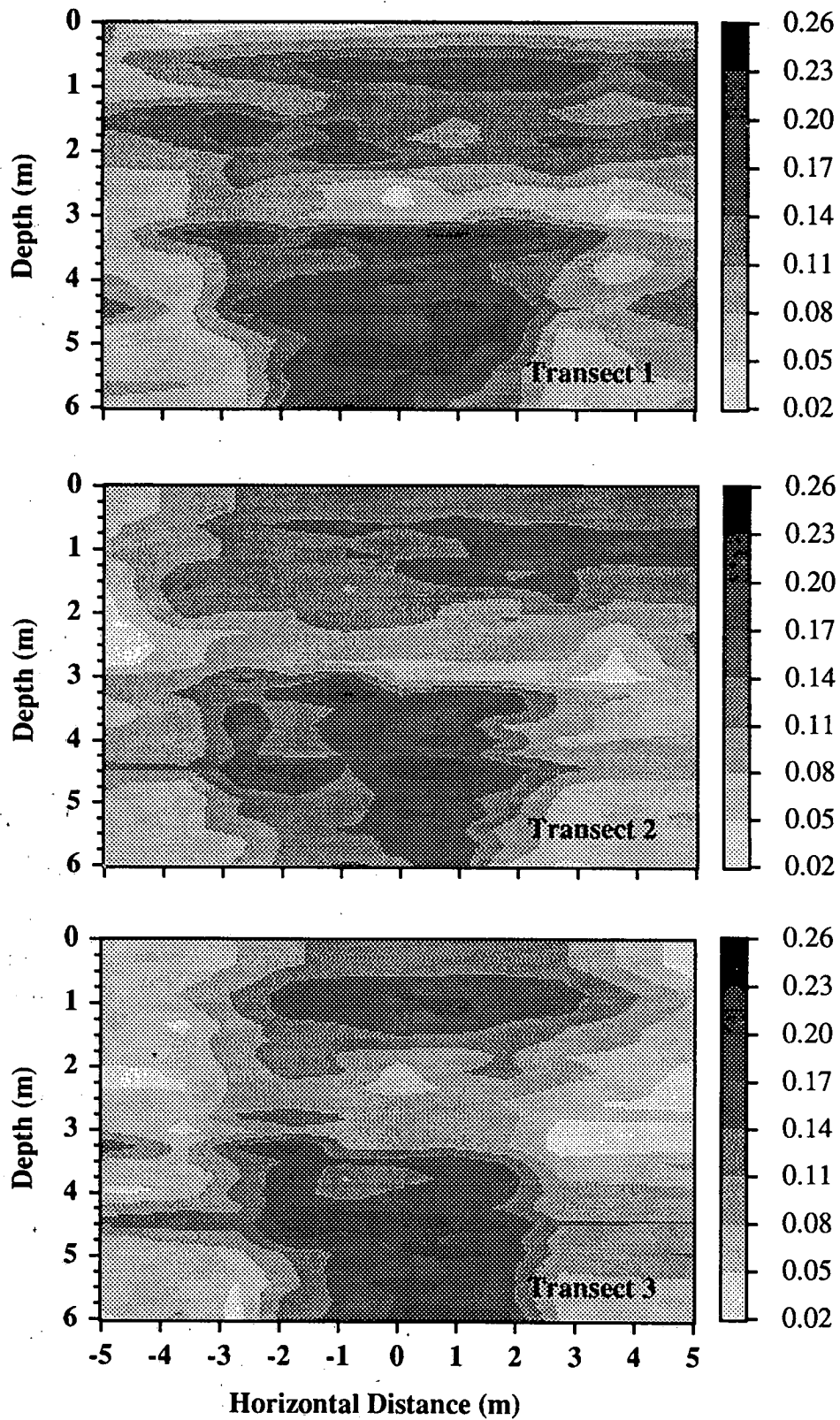


Figure 18. Observed Water Content Distributions from Neutron Probe Transects 1, 2, and 3 for Day 310



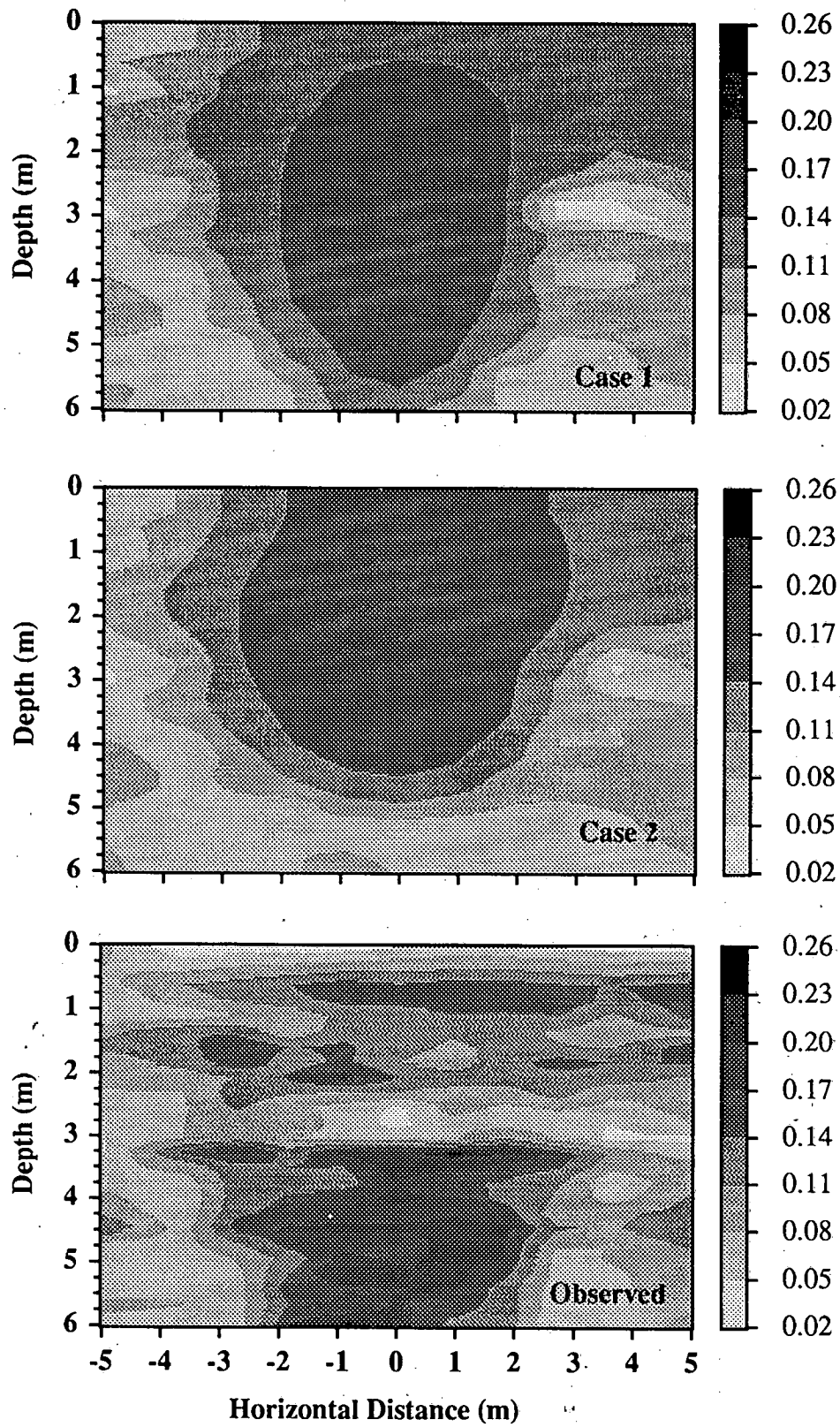


Figure 19. Simulated Water Content Distributions for Cases-1 and 2 and Observed Water Content Distribution from Neutron Probe Transect 1 for Day 310

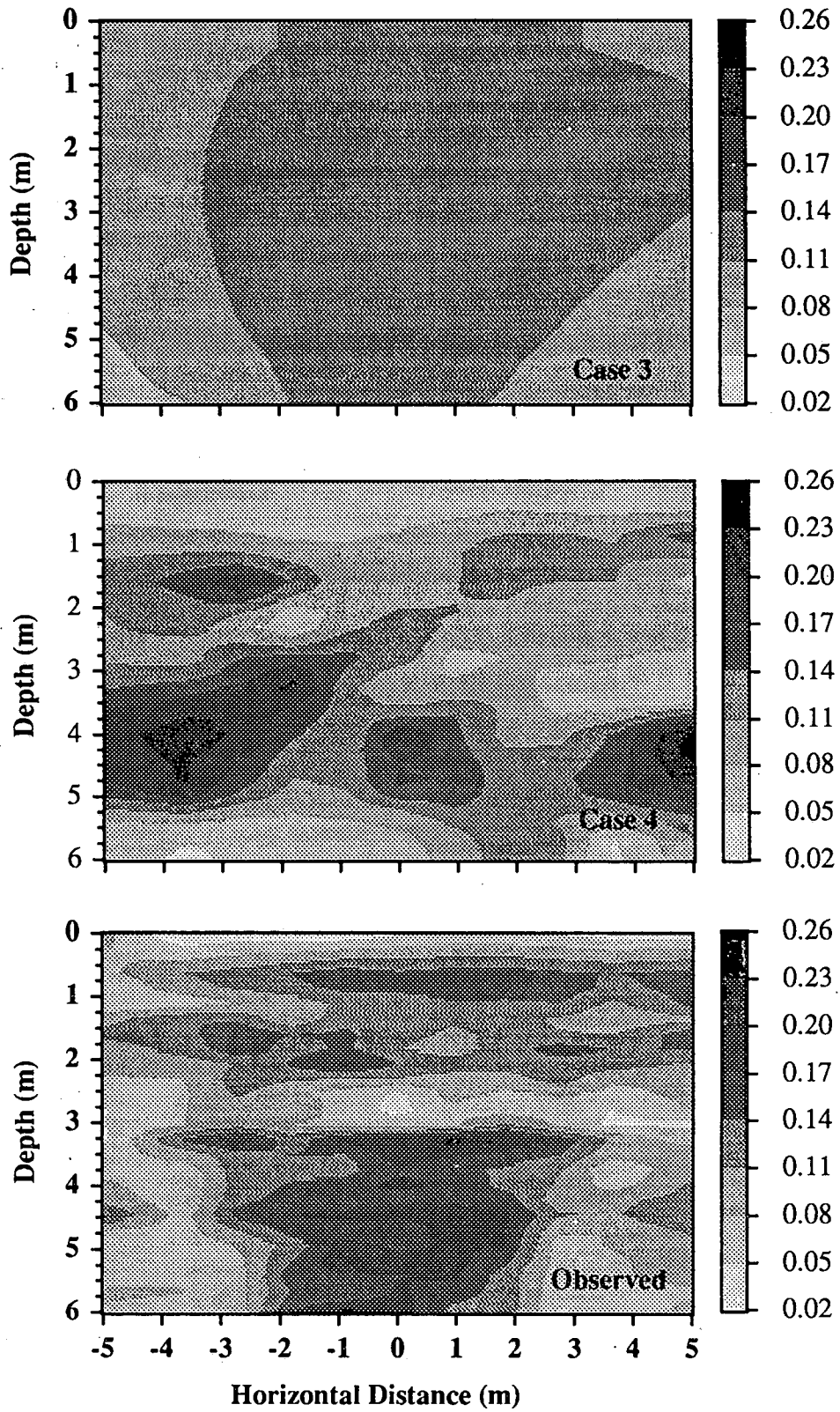


Figure 20. Simulated Water Content Distributions for Cases 3 and 4 and Observed Water Content Distribution from Neutron Probe Transect 1 for Day 310

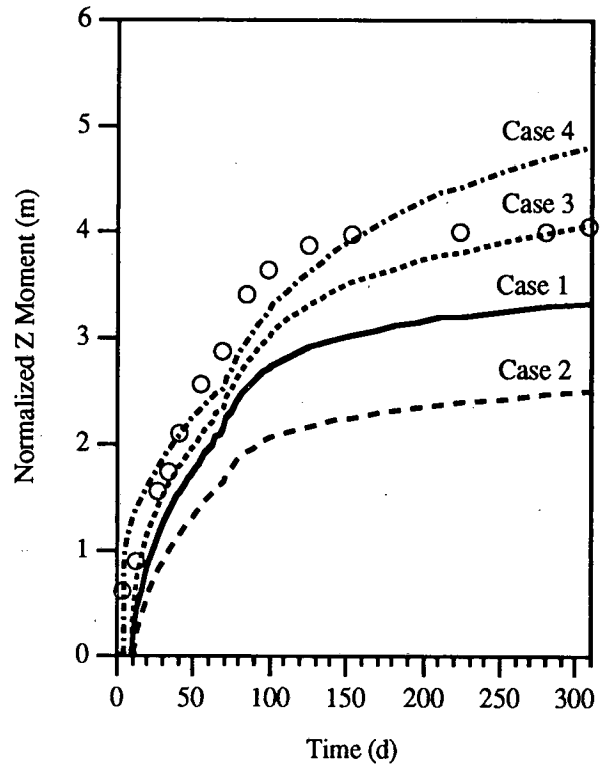
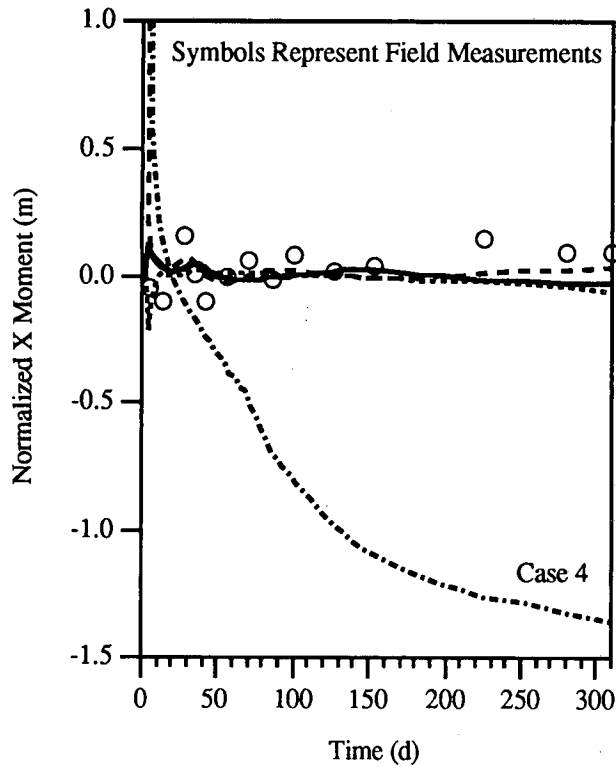


Figure 21. First Spatial Moments (Center of Mass) of Observed and Simulated Water Plumes

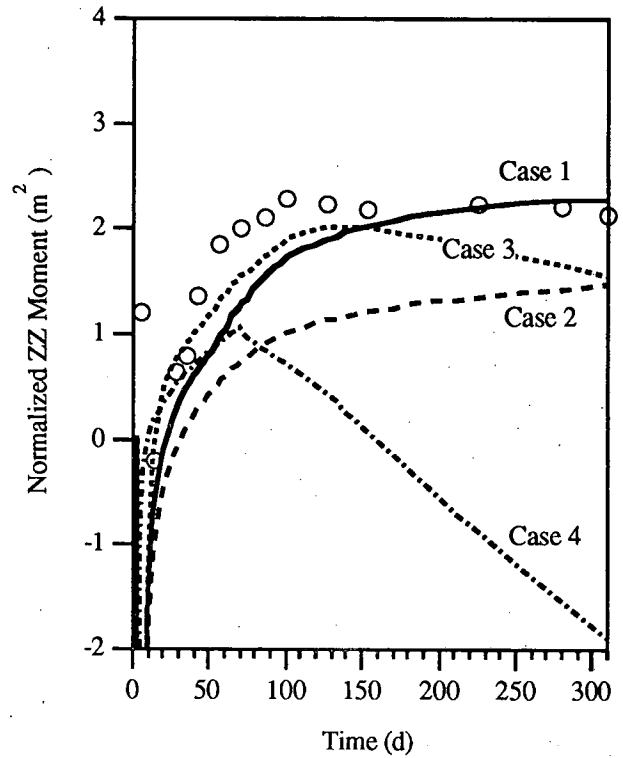
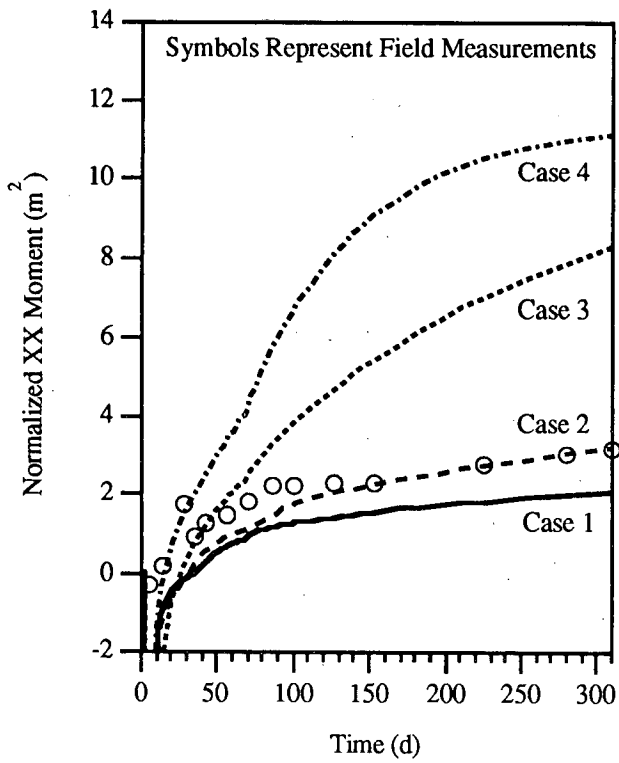


Figure 22. Second Spatial Moments (Spread About Center of Mass) of Observed and Simulated Water Plumes

Table 2. Normalized Spatial Moments of Observed and Simulated Water Plumes for Day 310

Spatial Moments	Observed Water Plumes				Simulated Water Plumes			
	1	2	3	Ave	1	2	3	4
M <sub>10</sub> (m)	0.09	-0.20	-0.10	-0.07	-0.03	0.02	-0.07	-1.36
M <sub>01</sub> (m)	3.23	4.59	2.47	3.43	2.04	3.19	8.23	11.1
M <sub>20</sub> (m <sup>2</sup> )	4.01	3.90	3.77	3.89	3.32	2.49	4.04	4.79
M <sub>02</sub> (m <sup>2</sup> )	2.12	1.89	1.61	1.87	2.26	1.45	1.55	1.89

The water retention parameters for cases 1 and 2 were estimated using different least-squares curve-fitting procedures. For case 2, the values of  $\theta_r$  were constrained to values less than the lowest measured water content in each soil horizon. By constraining  $\theta_r$ , the concavity of the water retention curve is reduced, or the curve is flattened, which results in a smaller value of the fitted  $n$  parameter, relative to case 1. Since the restriction that  $m = 1 - 1/n$  was imposed, and no unsaturated hydraulic conductivity data are available, the smaller  $n$  value effectively reduces predicted unsaturated hydraulic conductivities at water contents greater than approximately 0.12, relative to case 1, as shown in Figure 10. This reduced unsaturated hydraulic conductivity results in an underprediction of the rate of water movement. The original fitted van Genuchten model parameters in the Las Cruces trench database do not appear to be well suited for representing water retention characteristics and predicting unsaturated hydraulic conductivities over the full range of water contents that were observed during experiment 2B. The simple extension of the average water retention curve that was used for case 1 enabled the full range of water contents that were observed during the experiment to be accurately represented.

The water retention parameters that were used for simulation case 3 were obtained from a one-dimensional inverse procedure using water content data collected during the infiltration phase of experiment 1. Therefore, the resulting water retention curve for case 3 could be thought of as an imbibition or wetting curve. The water retention curves used for cases 1 and 2 were fit to water retention data that were collected during drainage from core samples in the laboratory. Therefore, the water retention curves used for cases 1 and 2 represent primary drainage curves. However, the air-entry potential (or the reciprocal of the van Genuchten  $\alpha$  parameter) of the main imbibition curve or any scanning curves should be greater than (or less negative than) the air-entry potential of

the primary drainage curve. The water retention curves for cases 1, 2, and 3 show the opposite behavior.

Hysteresis in the water retention characteristics and relative permeability relations was not considered or accounted for in these simulations. However, the fact that the simulation results from case 3 match the observed data quite well during the infiltration phase of the experiment, but not during the redistribution phase, suggests that hysteresis may have an effect on the observed flow and transport behavior.

Kool and Parker (1987) have suggested that as a first approximation, the primary wetting and drying water retention curves can be described using the same set of van Genuchten parameters, but with the  $\alpha$  parameter for the wetting curve equal to two times the value of the  $\alpha$  parameter for the drying curve. Kool and Wu (1991) demonstrated that this simple approximation has the effect of reducing the lateral spreading and increasing the vertical plume penetration depth in simulations of Las Cruces trench experiment 2A. However, from these simulations they concluded that hysteresis does not have a significant effect on water movement, or its influence was masked by other opposing processes.

The hysteresis model of Kool and Parker (1987) is based on a single fluid phase for models that use the Richards equation, such as VAM2D (Huyakorn, Kool, and Wu 1991). The original hysteresis model of Kool and Parker (1987) does not account for the effects of non-wetting fluid (air) entrapment and hysteresis in the relative permeability. Modified versions of the original model that have been incorporated into the VAM2D code indirectly account for the effects of entrapped air, but still neglect hysteresis in the relative permeability. The hysteresis model proposed by Parker and Lenhard (1987) and Lenhard and Parker (1987) also accounts for hysteresis in the relative permeability. This latter model has been used successfully to simulate

experimentally observed two-phase transient hysteretic fluid flow phenomena (Lenhard et al. 1991). Lenhard (1992) has also extended this two-phase hysteresis model to three-phase systems.

Kool and Wu (1991) also investigated the use of state-dependent expressions for anisotropy in the hydraulic conductivity for simulations of experiment 2A. These expressions are an isolated result of some of the previously mentioned stochastic flow theories (Polmann et al. 1988). The use of these expressions for anisotropy resulted in the simulated lateral spreading of the water plume being severely overpredicted and the depth of plume penetration being underpredicted for experiment 2A. Kool and Wu (1991) suggest that these expressions for state-dependent anisotropy may work well under relatively wet conditions, but they did not work very well under the dry conditions of Las Cruces trench experiment 2A.

Simulation case 4 represents a fully heterogeneous model. The results that were obtained from this simulation qualitatively matched the characteristics of the observed data better than any of the other simulations during the infiltration phase of the experiment. However on day 310, the simulated water plume exhibited too much lateral spreading and not enough vertical penetration. Simulation case 4 essentially represents a single stochastic realization of a random hydraulic conductivity field that was conditioned on the  $K_{fs}$  data from the trench. If multiple realizations were generated for Monte Carlo simulations, the ensemble mean predicted flow and transport behavior would presumably match the observed flow and transport behavior better than the single realization used for case 4.

The hydraulic properties that were used for case 4 correspond to or were conditioned on measurements from the area of the trench immediately in front of plot 2. However, these measurements were collected at distances of 2.3 to 2.6 m, or approximately one correlation length away, from neutron probe transect 1. Therefore there is no reason to believe that these measurements are any more representative of the hydraulic properties in the plane of neutron probe transect 1 than measurements from some other part of the trench.

From Figure 8, it is evident that a zone of higher hydraulic conductivity exists between the x-coordinates of 1 m and 7 m, between the 2- and 3-m depths, in the plot 2 coordinate system. If the hydraulic properties from this region of the trench had been selected for simulation case 4, the simulation results might match the observed flow behavior much better. Higher hydraulic conductivities between the 2- and 3-m depths would translate into lower water content values for a given flux rate and constant water retention parameters,

which would be consistent with the observed water content data from the experiment.

### 3.2.2 Transport Simulations

The observed normalized tritium distributions for solute sampling transects 1, 2, and 3 on day 310 are shown in Figure 23. As noted previously, the measurements from transect 1 are from the solution samplers, which extend 0.5 m into the soil profile from the face of the trench. The second and third sampling transects are located 1 m away from the 2nd and 3rd neutron probe measurement transects, at distances of 5 and 9 m from the face of the trench, respectively. The observed normalized tritium distributions from each of the measurement transects are similar, but the depth of penetration of the solute plume appears to be slightly deeper for transect 3.

Simulated tritium distributions for cases 1 and 2 are compared with the observed tritium distribution for transect 1 on day 310 in Figure 24. The simulated tritium plume for case 1 matches the observed tritium plume slightly better than case 2. However both sets of simulation results appear to match the observed data reasonably well in terms of both the shapes of the plumes and the concentration distributions within the plumes.

Simulated tritium distributions for cases 3 and 4 are compared with the observed tritium distribution for transect 1 on day 310 in Figure 25. The shape of the simulated plume for case 3 is similar to the observed plume, but the simulated plume is too diffuse. The shape of the simulated plume for case 4 does not match the observed plume well at all. The simulated plume is much too diffuse with far too much lateral spreading.

For predicting flow through porous media, it is generally more important to accurately predict the mean flow behavior. However, for predicting contaminant transport, the tails of the distribution are often of greater importance because of concerns over whether or not the peak contaminant concentrations exceed a dose limit or the first contaminant arrival times are shorter than some travel time performance objective criteria. Therefore, it is also of interest to compare other performance measures such as the maximum observed and simulated tritium concentrations.

The first spatial moments of the simulated and observed tritium plumes are shown in Figure 26. The normalized X moments are similar to those calculated for the water plumes, which is to be expected because tritium is non-reactive. The normalized Z moments show a compression-expansion phenomena at early times, which is the result of

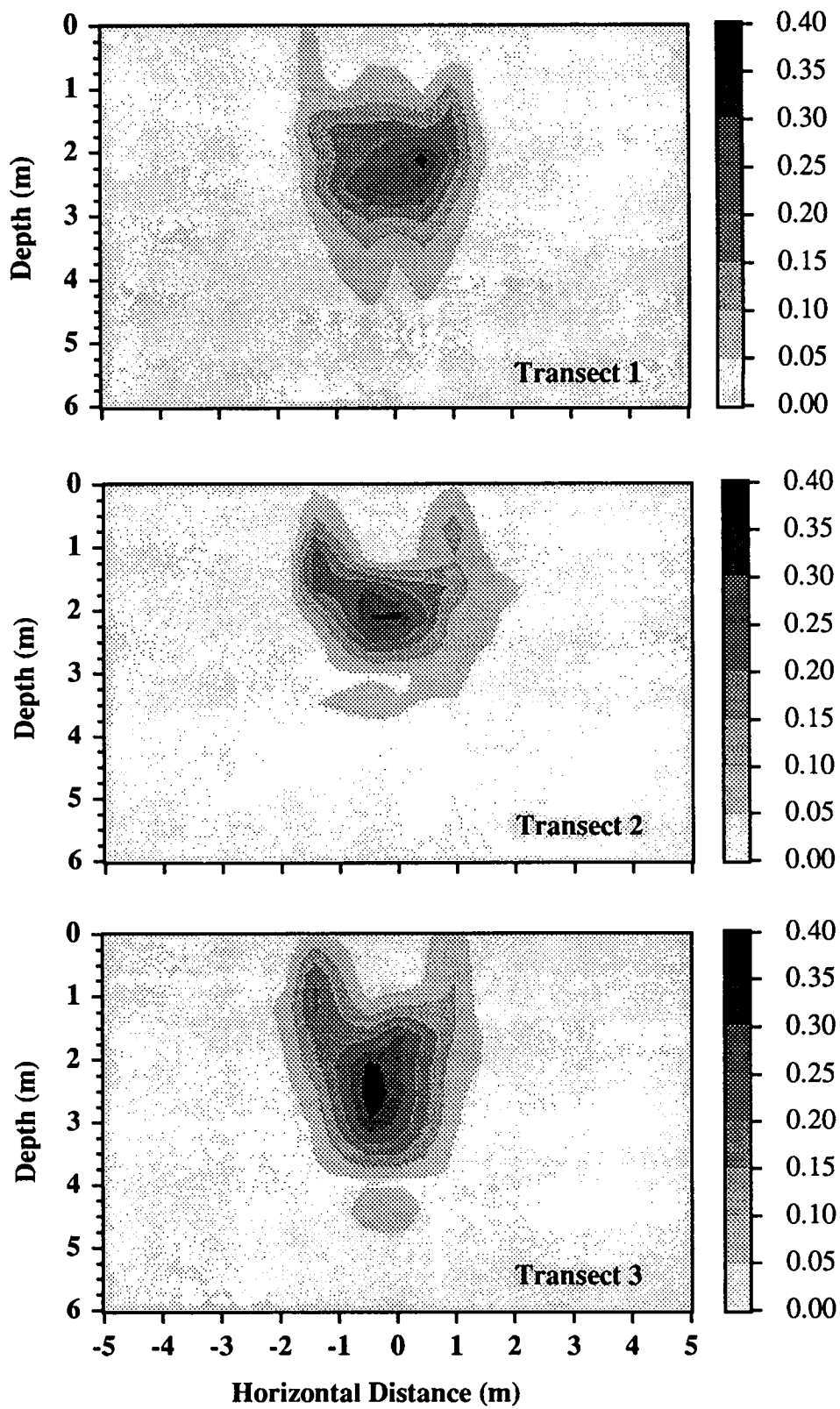


Figure 23. Observed Normalized Tritium Distributions for Transects 1 ( $y = 0.5$  m), 2 ( $y = 5$  m), and 3 ( $y = 9$  m) for Day 310

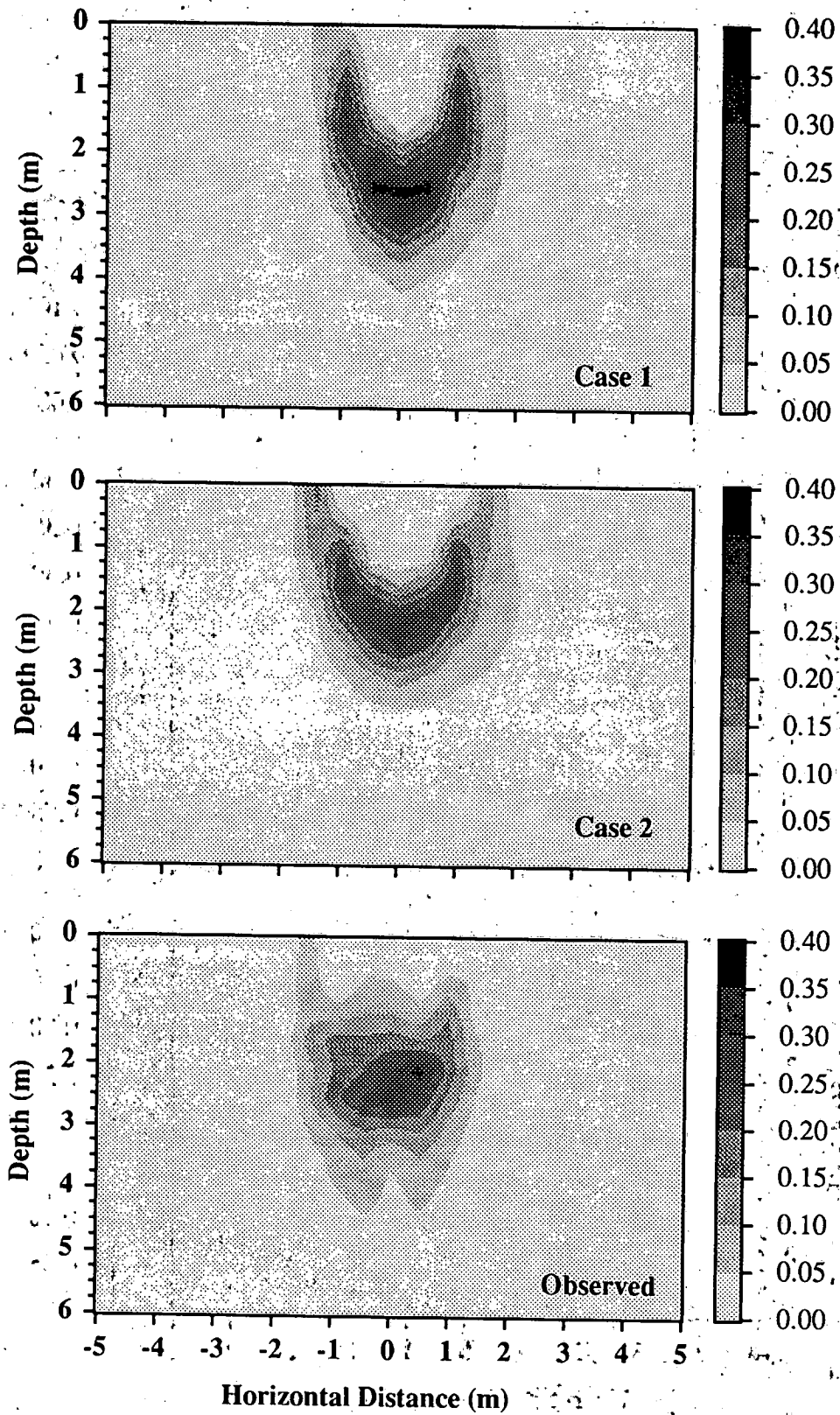


Figure 24. Simulated Tritium Distributions for Cases 1 and 2 and Observed Tritium Distribution from Solution Samplers for Day 310

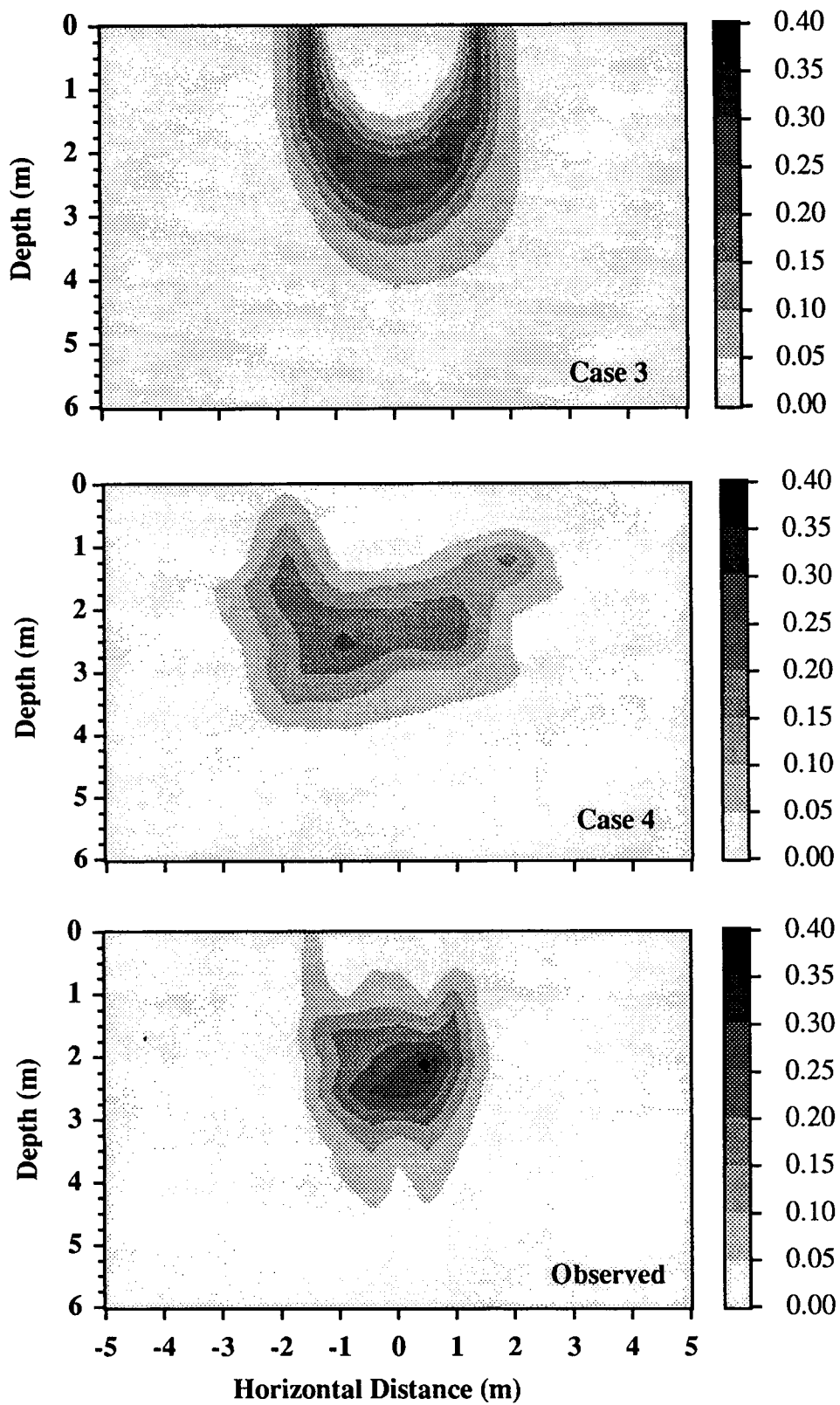


Figure 25. Simulated Tritium Distributions for Cases 3 and 4 and Observed Tritium Distribution from Solution Samplers for Day 310



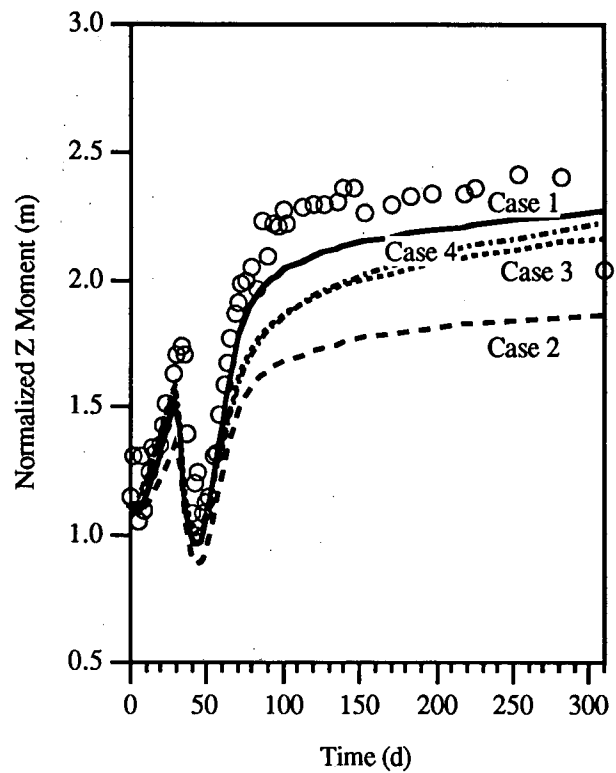
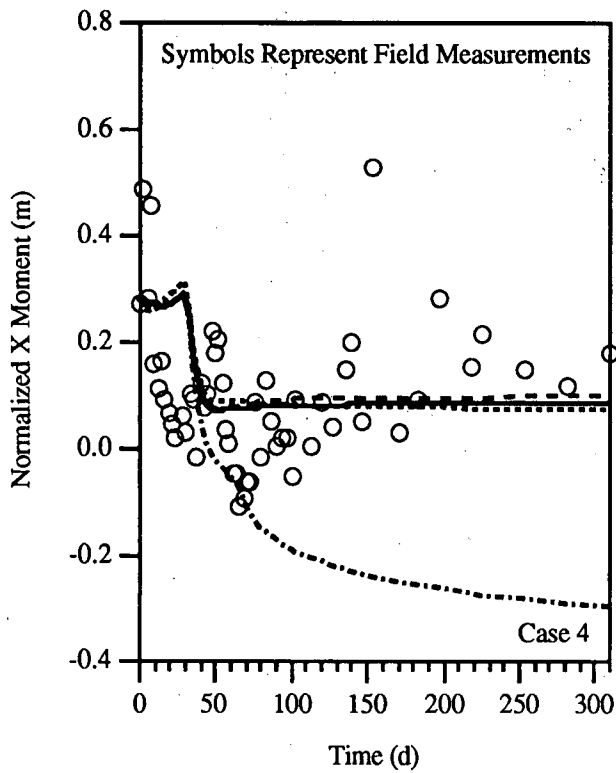


Figure 26. First Spatial Moments (Center of Mass) of Observed and Simulated Tritium Plumes

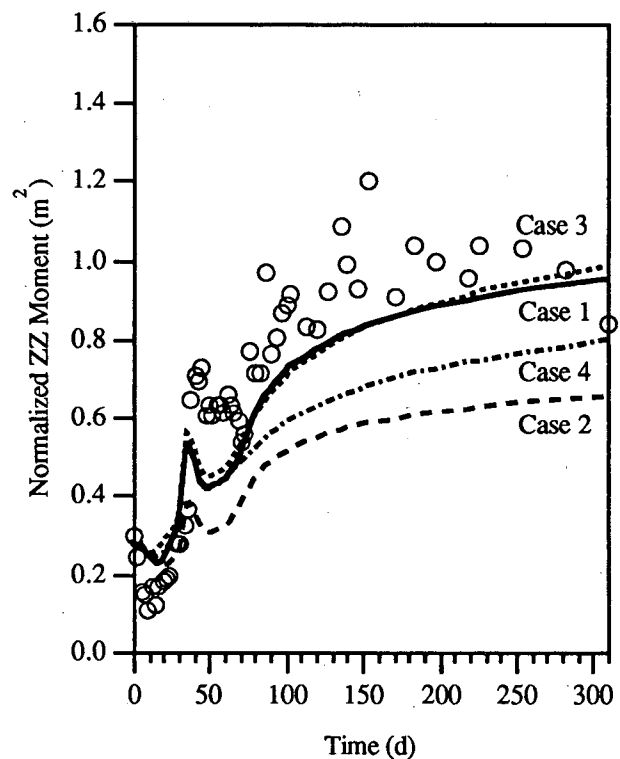
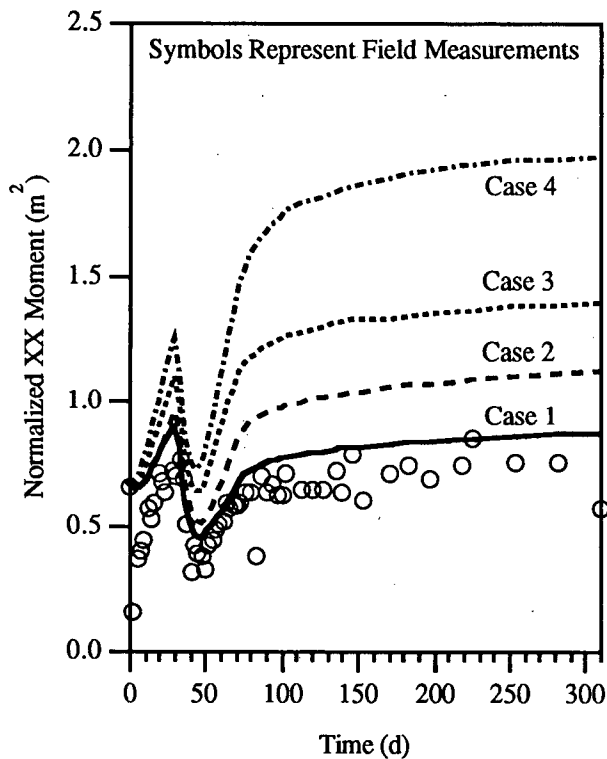


Figure 27. Second Spatial Moments (Spread About Center of Mass) of Observed and Simulated Tritium Plumes

the displacement of the initial tritium from experiment 2A. The normalized Z moments of the observed tritium plume are most closely matched by simulation case 1.

The second spatial moments of the simulated and observed tritium plumes are shown in Figure 27. The horizontal spread of the simulated tritium plumes show a similar behavior to the observed water plumes. The horizontal spread of the observed tritium plume is most closely matched by simulation case 1 and overpredicted by all of the other simulation cases. The vertical spread of the observed tritium plume is matched equally well by simulation cases 1 and 3 for all times, and underpredicted by cases 2 and 4. The spatial moments of the observed and simulated tritium plumes are summarized in Table 3 for day 310.

The maximum observed and simulated tritium concentrations for day 310 are also shown in Table 3. The maximum normalized tritium concentration that was predicted from simulation case 1 on day 310 is almost the same as the maximum observed concentration from the solution samplers on day 310. The maximum concentrations predicted by the other simulation cases are all significantly lower than the observed maximum. There appears to be a negative correlation between the horizontal spread (or lateral dispersion)

of the simulated tritium plumes and the maximum predicted concentrations. However, this apparent correlation is not evident for the observed tritium data, which show the highest observed tritium concentration in transect 2. The tritium data from transect 2 also exhibit the greatest apparent lateral dispersion. Overall, the observed water and tritium plume dynamics are matched most closely by simulation case 1.

The stochastic continuum theories presented by Gelhar and Axness (1983) and Dagan (1984) have been used to estimate macro-dispersivities for the prediction of transport under steady, saturated flow conditions based on the mean and variance of the hydraulic properties and spatial correlation lengths. Russo (1991) recently tested Dagan's (1984) model using numerical experiments for transient, unsaturated flow conditions in scale-heterogeneous (or "Miller-similar") soil. He obtained good agreement between the components of the spatial covariance and the effective dispersivity tensors that were calculated from a spatial moment analysis and those predicted from Dagan's (1984) model. No attempts were made to make this kind of comparison in this study because the travel distance of the tritium plume was not considered great enough relative to the estimated vertical correlation length of  $K_z$ .

**Table 3. Normalized Spatial Moments of Observed and Simulated Tritium Plumes for Day 310**

Spatial Moments	Observed Tritium Plumes				Simulated Tritium Plumes			
	1	2	3	Ave	1	2	3	4
$M_{10}$ (m)	0.18	0.06	-0.12	0.04	0.08	0.10	0.07	-0.30
$M_{01}$ (m)	0.58	1.12	0.89	0.86	0.87	1.12	1.39	1.97
$M_{20}$ (m <sup>2</sup> )	2.04	2.25	2.44	2.24	2.26	1.86	2.16	2.22
$M_{02}$ (m <sup>2</sup> )	0.84	1.07	1.46	1.12	0.95	0.66	0.99	0.80
Max. Conc. (C/C <sub>0</sub> )	0.3290	0.3696	0.3396		0.3244	0.2840	0.2719	0.2194

## 4 Conclusions

The objectives of this work were 1) to evaluate data sets generated from the Las Cruces trench experiments for testing deterministic and probabilistic flow and transport models, 2) to assess several parameter estimation methods and a recently developed multiphase flow and transport simulator for potential use as performance assessment tools for application to LLW disposal sites, and 3) to document PNL's contributions to the unsaturated zone working group of the INTRAVAL project and its Las Cruces test case.

The most recent flow and transport experiment (2B) that was conducted at the Las Cruces trench site in New Mexico is a test case for the INTRAVAL project and was simulated for this study as part of a "blind" modeling exercise. The objectives of this blind modeling exercise were 1) to demonstrate the ability or inability of uncalibrated models to predict unsaturated flow and solute transport in spatially variable porous media, and 2) to develop a quantitative model validation methodology that can be used to assess the performance of various conceptual and mathematical models with consideration given to data and parameter uncertainties. Only the first of these two objectives was addressed in this document.

The MSTs code was used to simulate Las Cruces trench experiment 2B using different model parameterizations. Uniform isotropic and anisotropic and fully heterogeneous models were tested. Geostatistical methods and a fast Fourier transform method for generating spatially correlated random fields were used to generate single stochastic realizations that were conditioned on the measured hydraulic conductivity data from the trench. Effective flow parameters for one of the simulation cases were also estimated using a one-dimensional inverse parameter estimation procedure and water content data obtained during the infiltration phase of Las Cruces trench experiment 1. A spatial moment analysis was used to provide a quantitative basis for comparing the mean simulated and observed flow and transport behavior.

The results from the single, conditional simulation that was presented qualitatively matched the observed water content data from experiment 2B better than any of the results from the uniform soil models during the infiltration phase of the experiment. However, the conditional simulation poorly predicted water and tritium movement during the redistribution phase of the experiment. This suggests that single stochastic realizations are probably inappropriate for predicting mean unsaturated flow and solute transport behavior in spatially variable porous media. If a Monte Carlo simulation was conducted, the ensemble mean simulated flow and transport behavior would probably match the observed data

better than any single realization. With recent developments in computer hardware and improved simulation algorithms, Monte Carlo simulation of large-scale, transient unsaturated flow and solute transport is now more practical.

A uniform soil model, with water retention parameters determined from a one-dimensional inverse solution and infiltration data from one of the previous trench experiments, reproduced the observed vertical water movement during the infiltration phase of the experiment better than any of the other models. However, this model poorly predicted water and tritium movement during the redistribution phase of the experiment. Nevertheless, the inverse method appears to be a promising means for obtaining effective flow parameters using water content and pressure head data collected during infiltration and/or drainage experiments. The motivation for testing this inverse parameter estimation approach is that it could potentially be used in conjunction with data from a simple field infiltration and/or drainage experiment at a LLW site to simultaneously obtain site characterization data, a validation data set, and a calibrated set of flow parameters.

Comparisons of the spatial moments of the simulated and observed water content and tritium distributions indicate that the mean observed water and tritium plume dynamics were reproduced most closely by one of the uniform soil models. This model utilized average water retention parameters that were determined by simultaneously fitting data obtained from approximately 450 core samples that were collected during excavation of the trench. The dry end of the water retention and relative permeability curves for this case were modified to provide a more accurate representation of the initial conditions of the experiment, relative to the original fitted parameters from the Las Cruces trench database. An accurate representation of soil hydraulic properties in the dry range is particularly important for modeling near-surface processes such as evapotranspiration.

Nine individual soil horizons were identified based on observed morphological characteristics from the exposed face of the trench. Soil core samples were collected along sampling transects from the approximate center of each horizon. Geostatistical analyses of the soil hydraulic properties determined from the core samples and in situ measurements of saturated hydraulic conductivity suggest that these nine horizons could be grouped into three horizons based on similar means and variances and spatial proximity of the soil horizons. However, observed water content data from the trench experiments reveal a distinct soil horizon with significantly lower water contents that was not evident from the site characterization data or the geostatistical analyses. This

demonstrates the difficulties in site characterization and possible effects of aliasing from undersampling, and suggests that initial water content data may be the best indicator of the dominant soil layering in the unsaturated zone.

Some of the simulation cases reproduced the observed flow behavior reasonably well during the infiltration phase of the experiment, but not during the redistribution phase of the experiment. This may be the result of neglecting certain phenomena such as hysteresis, or from not accurately parameterizing the models to account for the different soil horizons.

It should be emphasized again that the simulation results that were reported in this document were generated before the

data from experiment 2B were released. Therefore no data from the experiment were used for direct model calibration. Nevertheless, these simulations were certainly biased toward reproducing the observed flow and transport behavior because of the abundance of site characterization data and the previous experiments that have been conducted at the Las Cruces trench site. The predicted flow and transport results that were obtained in this study probably reproduced the observed field data considerably better than what can typically be expected from predictions of unsaturated flow and contaminant transport at LLW sites simply because very few data are generally available for LLW sites. This suggests that defensible predictions of waste migration and fate at LLW sites will ultimately require site-specific data for model calibration.

## 5 References

- ASME. 1967. "Thermodynamic and Transport Properties of Steam." The American Society of Mechanical Engineers, United Engineering Center, New York.
- Barry, D. A., and G. Sposito. 1990. "Three-Dimensional Statistical Moment Analysis of the Stanford/Waterloo Borden Tracer Test." Water Resour. Res. 26:1735-1747.
- Borgman L., M. Taheri, and R. Hagan. 1984. "Three-Dimensional Frequency-Domain Simulation of Geological Variables." In Geostatistics for Natural Resource Characterization, Reidel, Dordrecht, Holland.
- Carsel, R. F., and R. S. Parrish. 1988. "Developing Joint Probability Distributions of Water Retention Characteristics." Water Resour. Res. 24:755-770.
- Clifton, P. M. and S. P. Neuman. 1982. "Effects of Kriging and Inverse Modeling on Conditional Simulation of the Arva Valley Aquifer in Southern Arizona." Water Resour. Res. 18:1215-1234.
- Dagan, G. 1984. "Solute Transport in Heterogeneous Porous Formations." J. Fluid Mech. 145:151-177.
- Dane, J. H., and S. Hruska. 1983. "In Situ Determination of Soil Hydraulic Properties During Drainage." Soil Sci. Soc. Am. J. 47: 619-624.
- Delhomme, J. P. 1979. "Spatial Variability and Uncertainty in Groundwater Flow Parameters: A Geostatistical Approach." Water Resour. Res. 15(2): 269-280.
- Deutsch, C. 1992. Annealing Techniques Applied to Reservoir Modeling and the Integration of Geological and Engineering (Well Test) Data. Ph.D. Dissertation, Stanford University, Stanford, California.
- Dongarra, J. J., C. B. Moler, J. R. Bunch, and G. W. Stewart. 1980. LINPACK User's Guide. Society for Industrial and Applied Mathematics, Philadelphia, Pennsylvania.
- Dougherty, D. E. 1991. "Hydrologic Applications of the Connection Machine CM-2." Water Resour. Res. 27:3137-3147.
- Elabd, H., I. Porro, and P. J. Wierenga. 1988. "Estimation of Field Transport Parameters Using the Convection-Dispersion Equation." In Proceedings of the International Conference on Validation of Flow and Transport Models for the Unsaturated Zone, eds. P. J. Wierenga and D. Bachelet, May 22 - 25, Ruidoso, New Mexico.
- Farmer, C. 1991. "Numerical Rocks." In The Mathematical Generation of Reservoir Geology, Oxford University Press, New York, New York.
- Freyburg, D. L. 1986. "A Natural Gradient Experiment on Solute Transport in a Sand Aquifer: 2. Spatial Moments and the Advection and Dispersion of Nonreactive Tracers." Water Resour. Res. 22: 2031-2046.
- Gee, G. W., and J. W. Bauder. 1986. "Particle-Size Analysis." In Methods of Soil Analysis, Part 1. Physical and Mineralogical Methods, Second Edition, ed. A. Klute, pp.9:383-411, American Society of Agronomy, Inc. and Soil Science Society of America, Inc., Madison, Wisconsin.
- Gee, G. W., M. D. Campbell, G. S. Campbell, and J. H. Campbell. 1992. "Rapid Measurement of Low Water Potentials Using a Water Activity Meter." Soil Sci. Soc. Am. J. 56:1068-1070.
- Gelhar, L. W., and C. Axness. 1983. "Three-Dimensional Stochastic Analysis of Macrodispersion in Aquifers." Water Resour. Res. 19:161-190.
- Gutjahr, A. 1989. Fast Fourier Transforms for Random Fields. Project Report No. 4-R58-2690R for Los Alamos National Laboratory, New Mexico Institute of Mining and Technology, Socorro, New Mexico.
- Hills, R. G., I. Porro, D. B. Hudson, and P. J. Wierenga. 1989a. "Modeling One-Dimensional Infiltration into Very Dry Soils. 1. Model Development and Evaluation." Water Resour. Res. 25:1259-1269.
- Hills, R. G., D. B. Hudson, I. Porro, and P. J. Wierenga. 1989b. "Modeling One-Dimensional Infiltration into Very Dry Soils. 2. Estimation of the Soil-Water Parameters and Model Predictions." Water Resour. Res. 25:1271-1282.

- Hills, R. G., D. B. Hudson, and P. J. Wierenga. 1989c. "Spatial Variability at the Las Cruces Trench Site." In Proceedings of the Conference on Indirect Methods for Estimating the Hydraulic Properties of Unsaturated Soils, ed. M. Th. van Genuchten, Oct. 11 -13, Riverside, California.
- Hills, R. G., and P. J. Wierenga. 1991. Model Validation at the Las Cruces Trench Site. NUREG/CR-5716, U.S. Nuclear Regulatory Commission, Washington, D.C.
- Hills, R. G., P. J. Wierenga, D. B. Hudson, and M. R. Kirkland. 1991. "The Second Las Cruces Trench Experiment: Experimental Results and Two-Dimensional Flow Predictions." Water Resour. Res. 27:2707-2718.
- Hopmans, J. W. 1987. "A Comparison of Various Methods to Scale Soil Hydraulic Properties." J. Hydrology 93:241-256.
- Hopmans, J. W., H. Schukking, and P. J. J. F. Torfs. 1988. "Two-Dimensional Steady State Unsaturated Water Flow in Heterogeneous Soils With Autocorrelated Soil Hydraulic Properties." Water Res. Res. 24:2005-2017.
- Huyakorn, P. S., J. B. Kool, and Y. S. Wu. 1991. VAM2D - Variably Saturated Analysis Model in Two Dimensions, Version 5.2 With Hysteresis and Chained Decay Transport. NUREG/CR-5352, U.S. Nuclear Regulatory Commission, Washington, D.C.
- Isaaks, E., and R. Srivastava. 1989. An Introduction to Applied Geostatistics. Oxford University Press, New York, New York.
- Jacobson, E. A. 1990. "Investigation of the Spatial Correlation of Saturated Hydraulic Conductivities from the Vertical Wall of a Trench." In Proceedings of the Canadian/American Conference on Hydrogeology - Parameter Identification and Estimation for Aquifer and Reservoir Characterization, September 18 - 20, Calgary, Alberta, Canada.
- Journal, A. G. 1980. "The Lognormal Approach to Predicting Local Distributions of Selective Mining Unit Grades." Math. Geology 12:285-303.
- Journal, A. G., and F. Alabert. 1989. "Non-Gaussian Data Expansion in the Earth Sciences." Terra Nova 1:123-134.
- Journal, A. G., and Ch. J. Huijbregts. 1978. Mining Geostatistics. Academic Press, Inc., New York.
- Jury, W. A., D. Russo, and G. Sposito. 1987. "The Spatial Variability of Water and Solute Transport Properties in Unsaturated Soils, II. Analysis of Scaling Theory." Hilgardia 55:33-57.
- Kirkland, M. R., R. G. Hills, and P. J. Wierenga. 1992. "Algorithms for Solving Richards' Equation for Variably Saturated Soils." Water Resour. Res. 28:2049-2058.
- Klute, A. 1986. "Water Retention: Laboratory Methods." In Methods of Soil Analysis, Part 1 - Physical and Mineralogical Methods, ed. A. Klute, American Society of Agronomy, Madison, Wisconsin.
- Kool, J. B., and J. C. Parker. 1988. "Analysis of the Inverse Problem for Transient Unsaturated Flow." Water Resour. Res. 24:817-830.
- Kool, J. B., J. C. Parker, and M. Th. van Genuchten. 1985. "Determining Soil Hydraulic Properties from One-Step Outflow Experiments by Parameter Estimation, I. Theory and Numerical Studies." Soil Sci. Soc. Am. J. 49:1348-1354.
- Kool, J. B., J. C. Parker, and M. Th. van Genuchten. 1987. "Parameter Estimation for Unsaturated Flow and Transport Models - A Review." Water Resour. Res. 91:255-293.
- Kool, J. B., and Y. S. Wu. 1991. Validation and Testing of the VAM2D Computer Code. NUREG/CR-5795, U.S. Nuclear Regulatory Commission, Washington, D.C.
- Lenhard, R. J. 1992. "Measurement and Modeling of Three-Phase Saturation-Pressure Hysteresis." J. Contam. Hydrol. 9:243-269.
- Lenhard, R. J., and J. C. Parker. 1987. "A Model for Hysteretic Constitutive Relations Governing Multiphase Flow 2. Permeability-Saturation Relations." Water Resour. Res. 23:2197-2206.
- Lenhard, R. J., J. C. Parker, and J. J. Kaluarachchi. 1991. "Comparing Simulated and Experimental Hysteretic Two-Phase Transient Fluid Flow Phenomena." Water Resour. Res. 27:2113-2124.

- Mantoglou, A., and L. W. Gelhar. 1987a. "Stochastic Modeling of Large Scale Transient Unsaturated Flow Systems." Water Resour. Res. 23:37-46.
- Mantoglou, A., and L. W. Gelhar. 1987b. "Capillary Tension Head Variance, Mean Soil Moisture Content, and Effective Specific Moisture Capacity of Transient Unsaturated Flow in Stratified Soils." Water Resour. Res. 23:47-56.
- Mantoglou, A., and L. W. Gelhar. 1987b. "Effective Hydraulic Conductivities of Transient Unsaturated Flow in Stratified Soils." Water Resour. Res. 23:57-68.
- Mantoglou, A., and J. L. Wilson. 1982. "The Turning Bands Method for Simulation of Random Fields Using Line Generation by a Spectral Method." Water Resour. Res. 18:1379-1394.
- Matheron, G. 1973. "Intrinsic Random Functions and Their Applications." Adv. Appl. Prob. 5:439-468.
- Miller, E. E., and R. D. Miller. 1956. "Physical Theory for Capillary Flow Phenomena." J. Appl. Phys. 27:324-332.
- Millington, R. J. and J. M. Quirk. 1961. "Permeability of Porous Solids." Trans. Faraday Soc. 57:1200-1207.
- Milly, P. C. D. 1985. "A Mass-Conservative Procedure for Time Stepping in Models of Unsaturated Flow." Adv. Water Resour. 8:32-36.
- Mishra, S., and J. C. Parker. 1989. "Parameter Estimation for Coupled Unsaturated Flow and Transport." Water Resour. Res. 25:385-396.
- Mualem, Y. 1976. "A New Model for Predicting the Hydraulic Conductivity of Unsaturated Porous Media." Water Resour. Res. 12:513-522.
- Nicholson, T. J., P. J. Wierenga, G. W. Gee, E. A. Jacobson, D. J. Polmann, D. B. McLaughlin, and L. W. Gelhar. 1989. "Validation of Stochastic Flow and Transport Models for Unsaturated Soils: Field Study and Preliminary Results." In Proceedings of the Conference on Geostatistical, Sensitivity, and Uncertainty Methods for Ground-Water Flow and Radionuclide Transport Modeling, September 15 - 17, 1987, San Francisco, California, Battelle Press, Columbus, Ohio.
- Nielsen, D. R., J. W. Biggar, and K. T. Erh. 1973. "Spatial Variability of Field-Measured Soil-Water Properties." Hilgardia 42:215-260.
- Oppe, T. C., W. D. Joubert, and D. R. Kincaid. 1988. NSPCG User's Guide, Version 1.0. A Package for Solving Large Sparse Linear Systems by Various Iterative Methods. CNA-216, Center for Numerical Analysis, University of Texas, Austin, Texas.
- Parker, J. C., and R. J. Lenhard. 1987. "A Model for Hysteretic Constitutive Relations Governing Multiphase Flow 1. Saturation-Pressure Relations." Water Resour. Res. 23:2187-2196.
- Patankar, S. V. 1980. Numerical Heat Transfer and Fluid Flow. Hemisphere Publishing Corporation, New York.
- Polmann, D. J., E. G. Vomvoris, D. McLaughlin, E. M. Hammick, and L. W. Gelhar. 1988. Application of Stochastic Methods to the Simulation of Large-Scale Unsaturated Flow and Transport. NUREG/CR-5094, U.S. Nuclear Regulatory Commission, Washington, D.C.
- Porro, I. 1989. "Solute Transport Through Large Unsaturated Soil Columns." Ph.D. Dissertation, New Mexico State University, Las Cruces, New Mexico.
- Press, W. A., S. A. Teukolsky, W. T. Vetterling, and B. P. Flannery. 1992. Numerical Recipes in Fortran. The Art of Scientific Computing. Cambridge University Press, New York.
- Reynolds, W. D. and D. E. Elrick. 1985. "In Situ Measurement of Field-Saturated Hydraulic Conductivity, Sorptivity, and the  $\alpha$ -Parameter Using the Guelph Permeameter." Soil Sci. 140:292-302.
- Richards, L. A. 1931. "Capillary Conduction of Liquids Through Porous Mediums." Physics 1:318-333.
- Rockhold, M. L., and S. K. Wurster. 1991. Simulation of Unsaturated Flow and Solute Transport at the Las Cruces Trench Site using the PORFLO-3 Computer Code. PNL-7562, Pacific Northwest Laboratory, Richland, Washington.
- Ross, P. J., J. Williams, and K. L. Bristow. 1991. "Equation for Extending Water-Retention Curves to Dryness." Soil Sci. Soc. Am. J. 55:923-927.

- Russo, D. 1991. "Stochastic Analysis of Simulated Vadose Zone Solute Transport in a Vertical Cross Section of Heterogeneous Soil During Nonsteady Water Flow." Water Resour. Res. 27:267-283.
- Russo, D., and E. Bresler. 1982. "A Univariate Versus a Multivariate Parameter Distribution in a Stochastic-Conceptual Analysis of Unsaturated Flow." Water Resour. Res. 18:483-486.
- Simmons, C. S., D. R. Nielsen, and J. W. Biggar. 1979. "Scaling of Field-Measured Soil Water Properties." Hilgardia 47:77-174.
- Sisson, J. B. and P. J. Wierenga. 1981. "Spatial Variability of Steady-State Infiltration Rates as a Stochastic Process." Soil Sci. Soc. Am. J. 45:699-704.
- Smith, L. and R. A. Freeze. 1979a. "Stochastic Analysis of Steady State Groundwater Flow in a Bounded Domain 1. One-Dimensional Simulations." Water Resour. Res. 15:521-528.
- Smith, L. and R. A. Freeze. 1979b. "Stochastic Analysis of Steady State Groundwater Flow in a Bounded Domain 2. Two-Dimensional Simulations." Water Resour. Res. 15:1543-1559.
- Sposito, G. and W. A. Jury. 1990. "Miller Similitude and Generalized Scaling Analysis." In Proceedings of the Symposium on Scaling in Soil Physics: Principles and Applications, ed. D. Hillel and D. E. Elrick, pp. 13-22, October 18, 1989, Las Vegas, Nevada, Soil Sci. Soc. Am. Special Publication No. 25.
- Tompson, A. F. B., R. Ababou, and L. W. Gelhar. 1989. "Implementation of the Three-Dimensional Turning Bands Random Field Generator." Water Resour. Res. 25: 2227-2243.
- Toorman, A. F., P. J. Wierenga, and R. G. Hills. 1992. "Parameter Estimation of Hydraulic Properties from One-Step Outflow Data." Water Resour. Res. 28:3021-3028.
- van Genuchten, M. Th. 1980. "A Closed-Form Equation for Predicting the Hydraulic Conductivity of Unsaturated Soils." Soil Sci. Soc. Am. J. 44:892-898.
- van Genuchten, M. Th. 1982. "A Comparison of Numerical Solutions of the One-Dimensional Unsaturated-Saturated Flow Equation." Adv. Water Resour. 5:47-55.
- Warrick, A. W. 1990. "Application of Scaling to the Characterization of the Spatial Variability in Soils." In Proceedings of the Symposium on Scaling in Soil Physics: Principles and Applications, eds. D. Hillel and D. E. Elrick., pp. 39-51, October 18, 1989, Las Vegas, Nevada, Soil Sci. Soc. Am. Special Publication no. 25.
- Warrick, A. W., G. J. Mullen, and D. R. Nielsen. 1977. "Scaling Field-Measured Soil Hydraulic Properties Using a Similar Media Concept." Water Resour. Res. 13:355-362.
- White, M. D., M. D. Freshley, and P. W. Eslinger. 1992. "Simulation of Two-Phase Carbon-14 Transport at Yucca Mountain, Nevada." In Proceedings of the Fifth International Conference on Solving Ground Water Problems with Models, February 11 - 13, Dallas, Texas.
- Wierenga, P. J. 1988. "Validation of Flow and Transport Models at the Jornada Test Facility." In Proceedings of the International Conference on Validation of Flow and Transport Models for the Unsaturated Zone, eds. P. J. Wierenga and D. Bachelet, May 22 - 25, Ruidoso, New Mexico.
- Wierenga, P. J., R. G. Hills, and D. B. Hudson. 1991. "The Las Cruces Trench Site: Characterization, Experimental Results, and One-Dimensional Flow Predictions." Water Resour. Res. 27:2695-2705.
- Wierenga, P. J., D. B. Hudson, R. G. Hills, I. Porro, J. Vinson, and M. R. Kirkland. 1990. Flow and Transport at the Las Cruces Trench Site: Experiments 1 and 2. NUREG/CR-5607, U.S. Nuclear Regulatory Commission, Washington, D.C.
- Wierenga, P. J., A. F. Toorman, D. B. Hudson, J. Vinson, M. Nash, and R. G. Hills. 1989. Soil Physical Properties at the Las Cruces Trench Site. NUREG/CR-5441, U.S. Nuclear Regulatory Commission, Washington, D.C.
- Yeh, T.-C. J., L. W. Gelhar, and A. L. Gutjahr. 1985a. "Stochastic Analysis of Unsaturated Flow in Heterogeneous Soils. 1. Statistically Isotropic Media." Water Resour. Res. 21:447-456.
- Yeh, T.-C. J., L. W. Gelhar, and A. L. Gutjahr. 1985b. "Stochastic Analysis of Unsaturated Flow in Heterogeneous Soils. 2. Statistically Anisotropic Media." Water Resour. Res. 21:457-464.



Yeh, T.-C. J., L. W. Gelhar, and A. L. Gutjahr. 1985c. "Stochastic Analysis of Unsaturated Flow in Heterogeneous Soils. 3. Observations and Applications." Water Resour. Res. 21:465-471.

Zachmann, D. W., P. C. Duchateau, and A. Klute. 1981. "The Calibration of the Richards Flow Equation for a Draining Column by Parameter Identification." Soil Sci. Soc. Am. J. 45:1012-1015.

Zachmann, D. W., P. C. Duchateau, and A. Klute. 1982. "Simultaneous Approximation of Water Capacity and Soil Hydraulic Conductivity by Parameter Identification." Soil Sci. 134:157-163.

Zimmerman, D. A., and J. L. Wilson. 1990. Description of and User's Manual for TUBA: A Computer Code for Generating Two-Dimensional Random Fields via the Turning Bands Method. SEASOFT, Albuquerque, New Mexico.

Zimmerman, D. A., K. K. Wahl, A. L. Gutjahr, and P. A. Davis. 1990. A Review of Techniques for Propagating Data and Parameter Uncertainties in High-Level Radioactive Waste Repository Performance Assessment Models. NUREG/CR-5393, SAND89-1432, Prepared by Sandia National Laboratories for the U.S. Nuclear Regulatory Commission, Washington, D.C.

Zimmerman, D. A., R. T. Hanson, and P. A. Davis. 1991. A Comparison of Parameter Estimation and Sensitivity Analysis Techniques and Their Impact on the Uncertainty in Ground Water Flow Model Predictions. NUREG/CR-5522, SAND90-0128, Prepared by Sandia National Laboratories for the U.S. Nuclear Regulatory Commission, Washington, D.C.

## 6 Glossary of Symbols

### Roman Symbols

$C$	species concentration, (mol,ci)/m <sup>3</sup>
$C_g$	gas phase species concentration, (mol,ci)/m <sup>3</sup> gas
$C_l$	liquid phase species concentration, (mol,ci)/m <sup>3</sup> liquid
$c_l$	liquid specific heat, J/kg K
$l$	liquid mechanical dispersion coefficient, m <sup>2</sup> /s
$c_g, D_{cl}$	gas species diffusion coefficient, liquid species diffusion coefficient, m <sup>2</sup> /s
$D_{ge}, D_{le}$	gas diffusion coefficient upper face, liquid diffusion coefficient upper face, m/s
$D_{gw}, D_{lw}$	gas diffusion coefficient lower face, liquid diffusion coefficient lower face, m/s
$F_{ge}, F_{le}$	gas advection coefficient upper face, liquid advection coefficient upper face, m/s
$F_{gw}, F_{lw}$	gas advection coefficient lower face, liquid advection coefficient lower face, m/s
$g$	acceleration of gravity, m/s <sup>2</sup>
$h_a, h_w$	air enthalpy, water enthalpy, J/kg K
$h_g, h_l$	gas enthalpy, liquid enthalpy, J/kg K
$k$	intrinsic permeability,
$k_e$	equivalent thermal conductivity, W/m K
$k_{rg}, k_{rl}$	gas relative permeability, liquid relative permeability
$m_a, m_w$	air mass source, water mass source, kg/m <sup>3</sup> s
$n_d, n_e, n_t$	diffuse porosity, effective porosity, total porosity
$P_g, P_l$	gas pressure, liquid pressure, Pa

$P_{cap}, P_{sat}, P_v$	capillary pressure, saturation pressure, vapor pressure, Pa
$q$	thermal energy source, W/m <sup>3</sup>
$R_c$	specie decay rate, 1/s
$R_l$	aqueous phase gas constant, J/kg K
$s_c$	specie source, (mol,ci)/m <sup>3</sup> s
$s_g, s_l$	gas saturation, liquid saturation
$t$	time, s
$T$	temperature, C or K
$u_g, u_l, u_s$	gas internal energy, liquid internal energy, solid internal energy, J/kg K
$V_g, V_l$	gas Darcy velocity vector, liquid Darcy velocity vector, m/s
$x_a, x_w$	gas phase air mass fraction, gas phase water mass fraction
$y_a, y_w$	liquid phase air mass fraction, liquid phase water mass fraction
$z$	vertical height, m

### Greek Symbols

$\mu_g, \mu_l$	gas viscosity, liquid viscosity, s
$\rho_g, \rho_l$	gas density, liquid density, kg/m <sup>3</sup>
$\tau_g, \tau_l$	gas tortuosity, liquid tortuosity

### Mathematical Symbols

$\sim$	tensor
$\wedge$	unit vector
$\partial$	partial derivative
$\nabla$	gradient operator
$[[x, y]]$	maximum function

## Distribution

**No. of  
Copies**

**No. of  
Copies**

**OFFSITE**

5	<p>T. J. Nicholson U.S. Nuclear Regulatory Commission Office of Nuclear Regulatory Research Mail Stop NL-005 Washington, DC 20555</p> <p>U.S. Nuclear Regulatory Commission Director, Division of Regulatory Applications Office of Nuclear Regulatory Research Mail Stop NL/S-260 Washington, DC 20555</p> <p>U.S. Nuclear Regulatory Commission Chief, Waste Management Branch Division of Regulatory Applications Office of Nuclear Regulatory Research Mail Stop NL/S-260 Washington, DC 20555</p> <p>U.S. Nuclear Regulatory Commission Director, Division of Low Level Waste Management and Decommissioning Office of Nuclear Material Safety &amp; Safeguards Mail Stop 44-3 Washington, DC 20555</p> <p>U.S. Nuclear Regulatory Commission Document Control Center Division of Low Level Waste Management Office of Nuclear Material Safety &amp; Safeguards Mail Stop 44-3 Washington, DC 20555</p>	<p>P. Davis Sandia National Laboratory Division 6416 P.O. Box 5800 Albuquerque, NM 87185</p> <p>Dr. T. Hakonson Los Alamos National Laboratory Mail Stop K495 Los Alamos, NM 87547</p> <p>R. G. Hills Department of Mechanical Engineering Box 30001, Department 3450 New Mexico State University Las Cruces, NM 88003</p> <p>T. L. Jones Department of Crop and Soil Sciences Box 3Q Las Cruces, NM 88003</p> <p>W. J. Jury Department of Soils University of California Riverside, CA 92502</p> <p>K. Keller Geology Department Washington State University Pullman, WA 99164</p> <p>M. W. Kozak Sandia National Laboratory Division 6416 P.O. Box 5800 Albuquerque, NM 87185</p> <p>T. J. McCartin U.S. Nuclear Regulatory Commission Office of Nuclear Regulatory Research Mail Stop NL/S-260 Washington, DC 20555</p>
5	<p>R. Cady U.S. Nuclear Regulatory Commission Office of Nuclear Regulatory Research Mail Stop NL/S-260 Washington, DC 20555</p> <p>G. S. Campbell Agronomy Department Washington State University Pullman, WA 99164</p>	

**No. of  
Copies**

J. McCord  
Sandia National Laboratory  
Division 6416  
P.O. Box 5800  
Albuquerque, NM 87185

D. B. McLaughlin  
Ralph M. Parsons Laboratory, 48-209  
Department of Civil Engineering  
Massachusetts Institute of Technology  
Cambridge, MA 02139

S. P. Neuman  
Department of Hydrology and Water Resources  
University of Arizona  
Tucson, AZ 85721

V. Rogers  
Rogers & Associates Engineering Corp.  
P.O. Box 330  
Salt Lake City, UT 84107

B. Sagar  
Center for Nuclear Waste Regulatory Analysis  
6220 Culebra Road  
P.O. Drawer 28500  
San Antonio, TX 78284

R. K. Shulz  
University of California-Berkeley  
108 Hilgard Hall  
Berkeley, CA 84720

J. B. Sisson  
EG&G  
P.O. Box 1625, MS 2107  
Idaho Falls, ID 83415

S. W. Tyler  
Desert Research Institute  
P.O. Box 60220  
Reno, NV 89506

W. J. Waugh  
UNC GeoTech  
P.O. Box 14000  
Grand Junction, CO 81502

**No. of  
Copies**

E. P. Weeks  
U.S. Geological Survey  
Federal Center Mail Stop 413  
Denver, CO 80225

E. P. Springer  
Environmental Science Group  
HSE 12  
Health, Safety and Environment Division  
Los Alamos National Laboratory  
Los Alamos, NM 87545

J. W. Mercer  
GeoTrans, Inc.  
46050 Manekin Plaza  
Suite 100  
Sterling, VA 22170

P. J. Wierenga  
Dept. of Soil and Water Science  
429 Shantz Bldg.  
University of Arizona  
Tucson, AZ 85721

M. H. Young  
Dept. of Soil and Water Science  
429 Shantz Bldg.  
University of Arizona  
Tucson, AZ 85721

F. Ross  
U.S. Nuclear Regulatory Commission  
11555 Rockville Pike  
Rockville, MD 20852

M. Thaggard  
U.S. Nuclear Regulatory Commission  
11555 Rockville Pike  
Rockville, MD 20852

M. A. Celia  
Dept. of Civil Engineering and Operations  
Research  
Princeton University  
Princeton, NJ 08544

**No. of  
Copies**

**ONSITE**

35 Pacific Northwest Laboratory

M. P. Bergeron  
M. D. Campbell  
J. W. Cary  
C. R. Cole  
M. J. Fayer  
G. W. Gee  
M. J. Graham  
C. T. Kincaid  
R. R. Kirkham  
R. J. Lenhard  
W. E. Nichols  
J. C. Ritter  
M. L. Rockhold (10)  
R. J. Serne  
C. S. Simmons  
R. L. Skaggs  
J. L. Smoot  
G. P. Streile  
J. E. Szecsody  
Publication Coordination  
Technical Report Files (5)

Routing

R. M. Ecker  
M. J. Graham  
C. J. Hostetler  
P. M. Irving  
C. S. Sloane  
P. C. Hays (last)

**BIBLIOGRAPHIC DATA SHEET**

*(See instructions on the reverse)*

1. REPORT NUMBER  
*(Assigned by NRC. Add Vol., Supp., Rev.,  
and Addendum Numbers, if any.)*

NUREG/CR-5998  
PNL-8496

2. TITLE AND SUBTITLE

Simulation of Unsaturated Flow and Nonreactive Solute Transport  
in a Heterogeneous Soil at the Field Scale

3. DATE REPORT PUBLISHED

MONTH	YEAR
February	1993

4. FIN OR GRANT NUMBER

L1007

5. AUTHOR(S)

M.L. Rockhold

6. TYPE OF REPORT

Technical

7. PERIOD COVERED *(Inclusive Dates)*

8. PERFORMING ORGANIZATION - NAME AND ADDRESS *(If NRC, provide Division, Office or Region, U.S. Nuclear Regulatory Commission, and mailing address; if contractor, provide name and mailing address.)*

Pacific Northwest Laboratory  
Richland, WA 99352

9. SPONSORING ORGANIZATION - NAME AND ADDRESS *(If NRC, type "Same as above"; if contractor, provide NRC Division, Office or Region, U.S. Nuclear Regulatory Commission, and mailing address.)*

Division of Regulatory Applications  
Office of Nuclear Regulatory Research  
U.S. Nuclear Regulatory Commission  
Washington, DC 20555

10. SUPPLEMENTARY NOTES

11. ABSTRACT *(200 words or less)*

A field-scale, unsaturated flow and solute transport experiment at the Las Cruces trench site in New Mexico was simulated as part of a "blind" modeling exercise to demonstrate the ability or inability of uncalibrated models to predict unsaturated flow and solute transport in spatially variable porous media. Simulations were conducted using a recently developed multiphase flow and transport simulator. Uniform and heterogeneous soil models were tested, and data from a previous experiment at the site were used with an inverse procedure to estimate water retention parameters. A spatial moment analysis was used to provide a quantitative basis for comparing the mean observed and simulated flow and transport behavior. The results of this study suggest that defensible predictions of waste migration and fate at low-level waste sites will ultimately require site-specific data for model calibration.

12. KEY WORDS/DESCRIPTORS *(List words or phrases that will assist researchers in locating the report.)*

unsaturated flow, spatial variability, stochastic methods, model validation, solute transport, wasted migration

13. AVAILABILITY STATEMENT

unlimited

14. SECURITY CLASSIFICATION

*(This Page)*

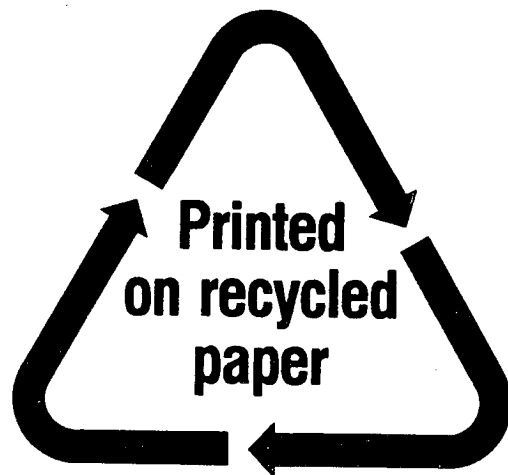
unlimited

*(This Report)*

unlimited

15. NUMBER OF PAGES

16. PRICE



Federal Recycling Program

NUREG/CR-5998

SIMULATION OF UNSATURATED FLOW AND NONREACTIVE SOLUTE  
TRANSPORT IN A HETEROGENEOUS SOIL AT THE FIELD SCALE

FEBRUARY 1993

UNITED STATES  
NUCLEAR REGULATORY COMMISSION  
WASHINGTON, D.C. 20555-0001

OFFICIAL BUSINESS  
PENALTY FOR PRIVATE USE, \$300

FIRST CLASS MAIL  
POSTAGE AND FEES PAID  
USNRC  
PERMIT NO. G-67

AAF342



LBL Libraries